Pergamon

0146-6380(95)00049-6

Org. Geochem. Vol. 23, No. 6, pp. 485–526, 1995

0146-6380/95 $9.50 + 0.00

Molecular indicators for palaeoenvironmental change in a Messinian evaporitic sequence (Vena del Gesso, Italy). II: High-resolution variations in abundances and ^{13}C contents of free and sulphur-bound carbon skeletons in a single marl bed

FABIEN KENIG[1]*, JAAP S. SINNINGHE DAMSTÉ,[1] NEIL L. FREWIN,[1]†
J. M. HAYES[2] and JAN W. DE LEEUW[1]

[1]Division of Marine Biogeochemistry, Netherlands Institute for Sea Research (NIOZ), P.O. Box 59, 1790 AB Den Burg, Texel, The Netherlands and [2]Biogeochemical Laboratories, Geology Building, Indiana University, Bloomington, IN 47405, U.S.A.

Abstract—The extractable organic matter of 10 immature samples from a marl bed of one evaporitic cycle of the Vena del Gesso sediments (Gessoso-solfifera Fm., Messinian, Italy) was analyzed quantitatively for free hydrocarbons and organic sulphur compounds. Nickel boride was used as a desulphurizing agent to recover sulphur-bound lipids from the polar and asphaltene fractions. Carbon isotopic compositions (δ vs PDB) of free hydrocarbons and of S-bound hydrocarbons were also measured. Relationships between these carbon skeletons, precursor biolipids, and the organisms producing them could then be examined. Concentrations of S-bound lipids and free hydrocarbons and their δ values were plotted vs depth in the marl bed and the profiles were interpreted in terms of variations in source organisms, ^{13}C contents of the carbon source, and environmentally induced changes in isotopic fractionation. The overall range of δ values measured was 24.7‰, from −11.6‰ for a component derived from green sulphur bacteria (Chlorobiaceae) to −36.3‰ for a lipid derived from purple sulphur bacteria (Chromatiaceae). Deconvolution of mixtures of components deriving from multiple sources (green and purple sulphur bacteria, coccolithophorids, microalgae and higher plants) was sometimes possible because both quantitative and isotopic data were available and because either the free or S-bound pool sometimes appeared to contain material from a single source. Several free *n*-alkanes and S-bound lipids appeared to be specific products of upper-water-column primary producers (i.e. algae and cyanobacteria). Others derived from anaerobic photoautotrophs and from heterotrophic protozoa (ciliates), which apparently fed partly on Chlorobiaceae. Four groups of *n*-alkanes produced by algae or cyanobacteria were also recognized based on systematic variations of abundance and isotopic composition with depth. For hydrocarbons probably derived from microalgae, isotopic variations are well correlated with those of total organic carbon. A resistant aliphatic biomacromolecule produced by microalgae is, therefore, probably an important component of the kerogen. These variations reflect changes in the depositional environment and early diagenetic transformations. Changes in the concentrations of S-bound lipids induced by variations in conditions favourable for sulphurization were discriminated from those related to variations in primary producer assemblages. The water column of the lagoonal basin was stratified and photic zone anoxia occurred during the early and middle stages of marl deposition. During the last stage of the marl deposition the stratification collapsed due to a significant shallowing of the water column. Contributions from anaerobic photoautotrophs were apparently associated with variations in depth of the chemocline.

Key words—sulphurization, biomarkers, palaeoenvironment, photic zone anoxia, anaerobe photoautotrophs, stable carbon isotopes

INTRODUCTION

In the previous paper, Sinninghe Damsté *et al.* (1995b) described the variations in palaeodepositional conditions in the Vena del Gesso depositional environment as reflected by analysis of the marl beds of 10 of the 14 evaporitic cycles of the Vena del Gesso (Gessoso-solfifera Formation, Messinian, Italy). Their observations were based on lipid analysis of relatively large samples of each marl bed without separating free hydrocarbons and S-bound lipids and indicated that, in general, the palaeoenvironment during the time of sedimentation of the marls varied significantly in terms of depth of the chemocline in the water column, terrestrial input and composition of the primary producer community. Previous work by Kohnen *et al.* (1992a,b) has shown that large differences existed in the composition of free hydrocarbons and hydrocarbons released from the polar fraction by desulphurization in three sub-samples of one marl bed. Therefore, we decided to study one representative evaporation cycle in more detail to trace the extent of variability in the palaeoenvironments during that cycle. To this end the well-developed marl layer of cycle IV [see Vai and Ricci Lucchi (1977) and Sinninghe Damsté *et al.* (1995b) for detailed

*To whom all correspondence should be addressed. Present address: Department of Geology and Geophysics, SOEST, University of Hawaii, 2525 Correa Road, Honolulu, HI 96822, U.S.A.

†Present address: Koninklijke/Shell Exploratie en Produktie Laboratorium, P.O. Box 60, 2280 AB Rijswijk, The Netherlands.

descriptions of the stratigraphy] was subsampled and investigated in detail. Free hydrocarbons and S-bound lipids were identified and quantified in 10 sub-samples each representing *ca* 13 cm of the marl bed.

Recent developments in isotope geochemistry now enable the determination of the stable carbon isotopic compositions of individual compounds (Hayes *et al.*, 1990). The assessment of $\delta^{13}C$ values at the molecular level adds a new dimension to biomarker geochemistry since, apart from the carbon skeleton and functional group information of biological markers, their ^{13}C contents also provide clues to their origin (e.g. Freeman *et al.*, 1989; Collister *et al.*, 1992; Sinninghe Damsté *et al.*, 1993c; Schoell *et al.*, 1994b; Kenig *et al.*, 1994a,b; Schoell and Hayes, 1994). The $\delta^{13}C$ values of free and S-bound lipids in one sample of a marl layer of the Gessosso-solfifera Formation allowed for the assignment of source organisms to these specific, mainly isoprenoidal, components (Kohnen *et al.*, 1992a,b). Therefore, it was decided to determine also the ^{13}C contents of free hydrocarbons and those released by desulphurization of polar fractions of the 10 sub-samples of marl layer IV. These analyses not only provided clues to the origin of carbon skeletons occurring in these sediments but also allowed for the reconstruction of changes in profiles of $[CO_2(aq)]$ and $\delta^{13}C$ of dissolved inorganic carbon in the water column of the Messinian lagoonal system.

EXPERIMENTAL

Samples

Ten samples from the marl bed of cycle IV of the Messinian Vena del Gesso sediments (Vai and Ricci Lucchi, 1977; Sinninghe Damsté *et al.*, 1995b) were collected from a freshly exposed outcrop in the open gypsum mine of Riolo Terme (Sinninghe Damsté *et al.*, 1995b). Each sample represents approx. 13 cm of the marl bed. All samples together covered the entire marl bed (Fig. 1). The samples are numbered 1 to 10 from bottom to top, respectively. A sample of the stromatolitic, carbonate-rich bed overlaying the marl bed was also collected to enable a comparison of its bulk geochemical parameters with those of the underlying marls. After collection the samples were freeze-dried and stored.

Bulk geochemical data

Total organic carbon (TOC) of decarbonated rock-samples were determined using a LECO carbon analyser. The calcium carbonate content was obtained by subtraction of the TOC values from the total carbon values obtained by LECO analyses of whole rocks. The hydrogen index (HI, in mg of hydrocarbon per g of TOC obtained during pyrolysis) was determined by Rock-Eval pyrolysis following the method described by Espitalié *et al.* (1977). For isotope analyses of TOC ($\delta^{13}C_{TOC}$, ‰ vs PDB), 5–10 mg of powdered decalcified sample were combusted in a sealed quartz tube at 850°C for 4 h. The CO_2 produced was cryogenically distilled and analyzed for its stable carbon isotope composition using a Finnigan Mat 252 mass spectrometer.

Extraction

Powdered samples were Soxhlet-extracted for 24 h using a dichloromethane (DCM):methanol (MeOH)

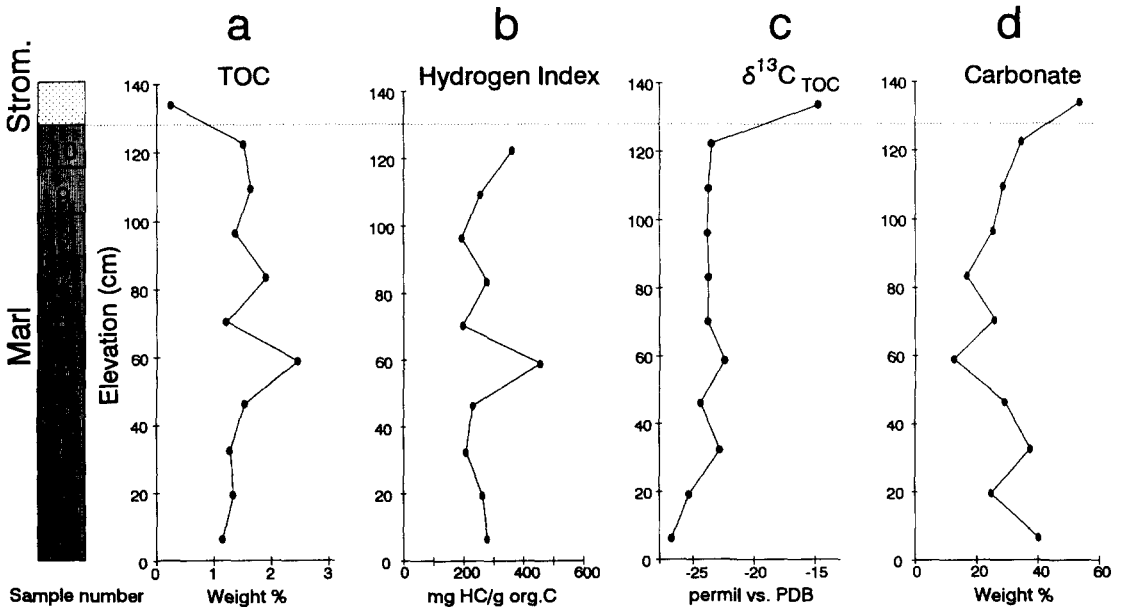

Fig. 1. Bulk geochemical data of the 10 samples of the marl bed of cycle IV and the overlaying stromatolitic bed plotted vs depth: (a) total organic carbon (TOC in wt %). (b) Hydrogen index (HI, in mg of hydrocarbon per g of TOC). (c) $\delta^{13}C_{TOC}$ in ‰ vs PDB. (d) Calcium carbonate content in wt %.

Table 1. Quantities of the major fractions analyzed

Samples	EOM* (mg/gTOC)	Maltene (mg/gTOC)	Asphaltenes† (mg/gTOC)	Polar (mg/gTOC)	Apolar‡ (mg/gTOC)
VDG IV-1-10	43.6	77.4	7.0	14.7	1.7
VDG IV-1-9	33.4	20.2	8.0	11.4	1.8
VDG IV-1-8	66.4	43.1	15.1	21.3	2.8
VDG IV-1-7	36.6	24.1	8.4	12.2	2.4
VDG IV-1-6	93.6	49.4	22.8	26.4	3.0
VDG IV-1-5	25.2	19.2	4.7	10.7	1.8
VDG IV-1-4	90.8	50.8	22.4	27.7	6.7
VDG IV-1-3	92.5	66.0	19.3	37.6	5.4
VDG IV-1-2	72.1	50.7	8.8	35.0	4.5
VDG IV-1-1	25.9	59.0	7.3	30.3	8.2

*Extractable organic matter (EOM).
†These values were obtained after removal of the salts. This explains the difference between EOM and the sum of the maltene and asphaltene fractions.
‡Apolar fraction: these values were obtained after removal of elemental sulphur. This explains the difference between the maltene and the sum of the polar and apolar fractions.

(7.5:1, v/v) solvent mixture. Extracted salts were removed by washing with water. The DCM layer was separated from the H_2O/MeOH layer in a separatory funnel. The H_2O/MeOH layer was re-extracted twice with DCM. The DCM layers were combined and dried over Na_2SO_4. The bitumens were obtained by removal of the DCM by a rotary evaporator operated under vacuum.

Separation

Bitumens were first separated into asphaltene and maltene fractions (Fig. 2). Bitumens were dissolved in a minimum amount of DCM and a 40-fold excess of *n*-heptane was added under stirring. These mixtures were kept refrigerated for 12 h during which the asphaltenes flocculated out. The asphaltenes and the supernatants were collected separately. The asphaltene fractions were purified by repeating the precipitation procedure once.

The maltenes were separated into an apolar and a polar fraction with column chromatography using a column (25 cm x 2 cm; $V_0 = 35$ ml) packed with activated (>2 h at 150°C) aluminium oxide (Al_2O_3) by elution of 150 ml of hexane/DCM (9:1 v/v) and 150 ml MeOH/DCM (1:1 v/v), respectively. Elemental sulphur was removed from the apolar fraction using a mini-column (2 cm x 0.4 cm) of activated (HCl, 6N) copper. After addition of known amounts of four internal standards (St1: 6,6-d_2-2-methylhenicosane; St2: 2,3-dimethyl-5-(1,1-d_2-hexadecyl)thiophene; St3: 2-methyl-2-(4,8,12-trimethyldecyl)chroman and St4: 2,3-dimethyl-5-(1,1-d_2-hexadecyl)thiolane), to an aliquot of the apolar fraction, it was further separated by argentation thin layer chromatography with hexane as a developer. Merck TLC plates (0.25 mm thick), precoated with silica-gel, were impregnated with a solution of $AgNO_3$ (1%) in MeOH/H_2O (4:1 v/v) for 45 s and dried at 120°C for 1 h. Three fractions (A1,

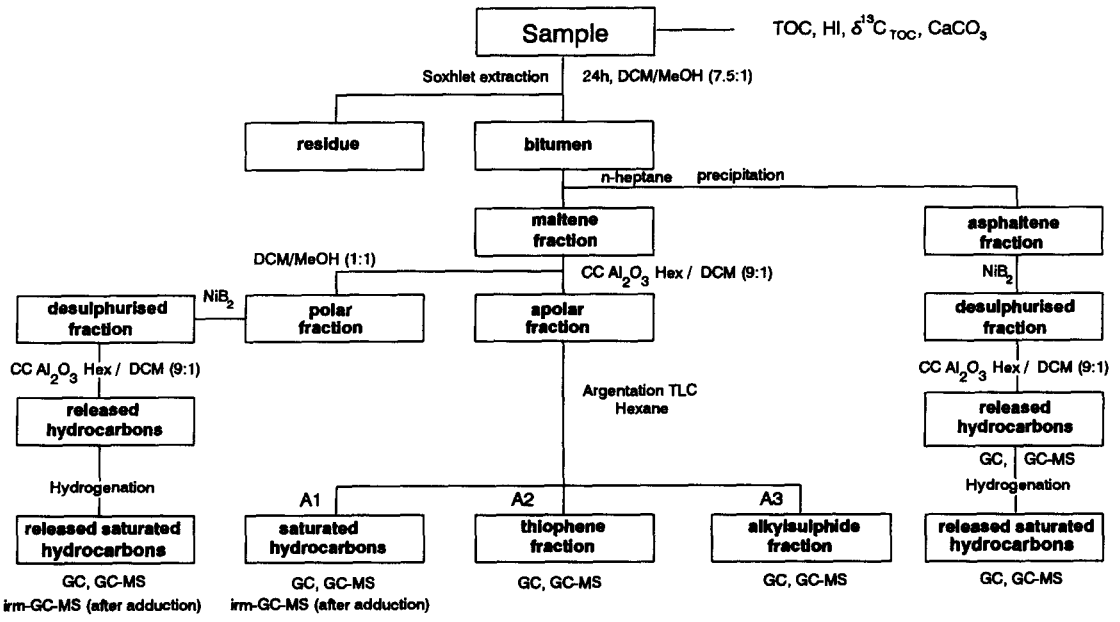

Fig. 2. Analytical flow diagram.

R_f = 0.85–1.00, hydrocarbon fraction which contains St1; A2, R_f = 0.06–0.6, thiophene fraction which contains St2 and St3; A3, R_f = 0.00–0.06, alkylsulphide fraction which contains St4) were scraped off and ultrasonically extracted with ethylacetate (× 3). The A1 and A2 fractions obtained were analyzed by gas chromatography (GC) and gas chromatography–mass spectrometry (GC–MS).

Some of the free hydrocarbon sub-fractions were further separated to yield *n*-alkyl and branched/cyclic components using molecular sieves (silicalite, PQ Corporation). Specifically, the hydrocarbons were deposited at the top of a Pasteur pipette filled with 4 cm of silicalite. The branched and cyclic compounds were recovered by elution with 4 ml of pentane. The *n*-alkanes were recovered by dissolution of the sieves with hydrofluoric acid followed by four successive rinses of the acid with 1 ml of hexane.

Desulphurization and hydrogenation

Approximately 20 mg aliquots of the polar fractions of the maltenes and of the asphaltene fractions were desulphurized with NiB_2 following the method described by Schouten *et al.* (1993a). Before desulphurization a known amount of a deuterated standard (St2) was added. The hydrocarbons released upon desulphurization were separated using column chromatography (Al_2O_3) as described above and then analyzed by GC and GC–MS. These hydrocarbons were then hydrogenated using PtO_2 as a catalyst and further analyzed by GC and GC–MS. The hydrocarbons obtained from the polar fraction were further separated into *n*-alkane and branched/ cyclic fractions using silica molecular sieves (Silicalite, PQ Corporation.

The A2 fraction of sample 5 was hydrogenated using PtO_2 as a catalyst. This resulted in the unexpected desulphurization of all thiophenes present in this fraction, i.e. *n*-alkyl, isoprenoid, and hopanoid thiophenes. The complete desulphurization of a polysulphide standard (dioctadecyl-hexasulphide, *n*-C_{18}–S_6–*n*-C_{18}) and of a thiophene standard (St2) using the same procedure confirms that PtO_2 can act as a desulphurization catalyst. The desulphurized thiophene fraction of sample 5 was further separated in three subfractions using silicalite: (i) a non-adduct fraction eluted with pentane, (ii) a non-adduct fraction eluted with benzene, and (iii) an adducted *n*-alkane fraction recovered by dissolution of the sieves. Fractions (ii) and (iii) were further analyzed by GC, GC–MS and irm–GC–MS.

Gas chromatography (GC)

GC was performed using a Carlo-Erba 5300 instrument equipped with an on-column injector and a fused silica capillary column (25m x 0.32 mm) coated with CP Sil-5 (film thickness 0.12 μm) and a flame ionization detector (FID). Helium was used as a carrier gas. The samples, dissolved in hexane, were injected at 70°C. The temperature of the oven was programmed from 70°C to 130°C at 20°C/min and at 4°C/min to 320°C at which it was held for 15 min.

Gas chromatography–mass spectrometry (GC–MS)

GC–MS was performed on a Hewlett–Packard 5890 Series II gas-chromatograph interfaced to a VG Autospec Ultima operated at 70 eV with a mass range *m/z* 50–800 and a cycle time of 1.8 s. The column and the temperature program used were identical to those described above for GC analyses. Helium was used as carrier gas.

Isotope ratio monitoring–gas chromatography–mass spectrometry (irm–GC–MS)

Carbon isotopic compositions of individual compounds were determined by irm–GC–MS analyses (Hayes *et al.*, 1990; Ricci *et al.*, 1994). The gas chromatograph was equipped with an on-column injector and a fused silica HP Ultra-1 column (50 m × 0.32 mm, 0.52 mm film thickness) and was coupled, via a combustion interface, to a Finnigan Delta S mass spectrometer. For *n*-alkane fractions, the temperature of the chromatographic column was programmed at 20°/min from 60 to 130°C and at 4°/min to 320°, at which it was held for 40 min. For branched/cyclic hydrocarbon fractions, the column temperature was programmed at 20°/min from 60 to 130°C; at 4°/min to 300°C, at which it was held for 45 min; and at 10°/min to 320°C, at which it was held for 40 min. Each δ value reported is an average of at least two independent analyses and uncertainties reported in the text are the standard deviations of these sets of replicates.

Quantitation

The concentrations (mg/g TOC) of selected compounds present in the hydrocarbon fractions (A1) were obtained by integration of their peak areas and that of the internal standard (St1) in a *m/z* 57 mass chromatogram. For quantitation purposes it has been assumed that the percentage of the *m/z* 57 ion of the total ion yield of the mass spectra is constant for the components studied. For cases where this is not true (i.e. 17(,21β(H)-homohopane and fernene), relative concentrations are reported. The concentrations of selected compounds of the thiophene fractions (A2) were obtained by integration of their peak areas in the FID-traces and that of the internal standard (St2). No quantitation of components present in the alkylsulphide fractions (A3) were attempted at this stage. The fractions are still under investigation. The concentrations of selected hydrocarbons released after desulphurization of the polar fractions of the maltenes and of the asphaltenes were obtained by integration of their peak areas in FID-traces and comparison of the resulting values with those of the desulphurized internal standard St2 (3-methyl-6,6-d_2-henicosane) which was added before desulphurization.

RESULTS AND DISCUSSION

The extracts of the 10 sub-samples of the marl bed of cycle IV of the Vena del Gesso sediments were fractionated into a saturated hydrocarbon fraction (A1), a thiophene fraction (A2), which also contains unsaturated and aromatic hydrocarbons, an alkylsulphide fraction (A3), a polar fraction, and an asphaltene fraction (Fig. 2). The polar and the asphaltene fractions contain macromolecularly S-bound lipids (Kohnen *et al.*, 1991a,b, 1992a,b) which were released upon desulphurization and analysed as hydrocarbons. Hydrocarbons were identified by comparison of their GC-retention times and mass spectra with those of standards and compounds described in the literature. The concentrations of selected components of each fraction were determined and are plotted vs depth in order to visualize the variability of biomarkers and to use these variations to trace changes in depositional conditions.

Absolute concentrations (mg/g TOC) could not be obtained for all components due to coelution problems or insufficient quantities. However, to exemplify variations of non-quantified components, appropriate mass chromatograms are shown for three representative samples. Polar fractions represented approximately 60% of the sum of the fractions analyzed, asphaltene fractions *ca* 30% and apolar fractions *ca* 10% (Table 1). The total amount of hydrocarbons released by desulphurization of the polar fraction (average yield of 10 samples: 86 mg HC/g polar fraction) dominates the amount of hydrocarbons released from other fractions (i.e. average yield of 10 asphaltene samples: 29 mg HC/g asphaltene). The data obtained for each fraction and subfraction will be described in order of decreasing abundance.

Twenty nine different samples were analyzed isotopically: (i) eight of the free hydrocarbon fractions, (ii) nine of the *n*-alkane fractions derived by desulphurization of the polar fractions, (iii) ten of the branched/cyclic-hydrocarbon fractions derived by desulphurization of the polar fractions, and (iv) the two subfractions obtained by molecular sieving of the desulphurized thiophene fraction from sample 5. Because of insufficient chromatographic resolution, δ values could be obtained for only a limited number of the branched and cyclic compounds identified and quantified. In contrast, examination of adducted materials allowed determination of δ values for all free *n*-alkanes except those present in very low concentrations and for all of the S-bound *n*-alkyl carbon skeletons.

In principle, since many of the compounds analyzed derive from S-bound fractions, isotopic offsets (preserved carbon skeletons vs precursor biolipids) due to the kinetic isotopic effect associated with sulphurization might be taken into account (Schouten *et al.*, 1995b). However, such offsets are probably consequential only when many of the carbon positions in the precursor biolipid are susceptible to sulphurization and when carbon skeletons derived from residual, unsulphurized lipids are analyzed (Hartgers *et al.*, 1994a,b). In the present case, attention is focused on the S-bound products and, since most of the branched and cyclic carbon skeletons do not have free-hydrocarbon equivalents, it is likely that sulphurization approached completion. Although some *n*-alkanes are found in both the free-hydrocarbon and S-bound fractions, the large isotopic differences (e.g. in sample 1: free *n*-C_{17},–36.3‰; S-bound *n*-C_{17},–27.3‰) strongly point to distinct sources for these carbon skeletons.

Bulk data

The TOC content (TOC) of the 10 marl samples investigated varies between 1.2% for sample 1 and 2.5% for sample 5 (Fig. 1). The TOC values do not vary significantly with depth and do not exhibit a particular trend. The stromatolitic bed contains a minor amount of organic carbon (0.2%).

The calcium carbonate contents of the marl samples vary between 17 and 40%. Two trends characterize the profile [Fig. 1(d)]: (i) a general decrease in carbonate content from the base toward the middle part of the bed and (ii) an increase from the middle part toward the top of the bed. The latter trend is enhanced by the increase in the carbonate content of the overlaying stromatolite bed. The depth profile is negatively correlated with that of TOC, indicating that the organic matter might be concentrated in the clay compartment of the marls.

The hydrogen index (HI in mg HC/g TOC) varies significantly between 194 (sample 8) and 454 (sample 5) and co-varies relatively well with the TOC [Fig. 1(b)]. It should be noted that a slight increase in HI for the upper samples of the bed does not seem to correlate with the TOC variations and might be related to changes in the source of the organic matter or conditions of preservation.

The stable carbon isotope contents of the TOC ($\delta^{13}C_{TOC}$) of the 10 marl samples vary between–26.7‰ (sample 1) and −22.4‰ (sample 5). The most ^{13}C depleted TOC-values are those found for the marls at the base of the bed [Fig. 1(c)]. The most ^{13}C enriched marl sample (sample 5) displays the highest TOC and the highest HI values. The marked difference between the stable carbon isotope value of the overlaying stromatolite (−14.7‰) and those of the marl samples probably reflects two totally different types of palaeoenvironments. The organic matter in the marls is mainly of algal origin and produced in the photic zone of the water column, whilst the organic matter in the stromatolite is probably reflecting cyanobacterial mats growing in very shallow water (Vai and Ricci Lucchi, 1977). This latter type of environments is characterized by ^{13}C-enriched organic matter because of a diffusion-limited assimilatory pathway of CO_2 (Schidlowski *et al.*, 1984) in cyanobacterial mats.

Desulphurized polar fractions

The FID traces of the hydrocarbons released from the polar fractions after desulphurization and subsequent hydrogenation of three representative samples (samples 1, 5 and 10) exemplify relative and absolute variations throughout the marl bed [Fig. 3(a–c)]. The compounds indicated in Fig. 3, *n*-alkanes, phytane, the C_{25} highly branched isoprenoid (HBI) alkane (**I**), regular steranes, 17β-trinorhopane, 17β,21β(H)-pentakishomohopane (**II**), gammacerane (**III**), 4,23,24-trimethylcholestane (dinosterane, **IV**), 4-methyl-24-ethylcholestane, isorenieratane (**V**) and compounds tentatively identified as 23,24-dimethylcholestane (4-desmethyldinosterane; **VI**) and a C_{33} diaryl isoprenoid hydrocarbon (**VII**), were quantified in all 10 samples.

The components released by desulphurization are dominated by *n*-alkanes, phytane and steranes (Fig. 3). The relative concentrations of steranes decrease from bottom to top. Isorenieratane (**V**) and the C_{33} diaryl isoprenoid hydrocarbon (**VII**) are clearly present at the base and in the center of the marl bed but are absent in the top sediment. The *n*-alkanes are dominated by octadecane and display, in the C_{16}–C_{26} carbon number range, an even-over-odd carbon number predominance as observed previously in many hydrocarbon fractions obtained after desulphurization of high-molecular-weight fractions of sedimentary organic compounds (Sinninghe Damsté *et al.*, 1988, 1990; Kohnen *et al.*, 1991a; Adam *et al.*, 1993). Variations in the relative and absolute concentrations of these compounds as well as their origin as determined by their δ values will be discussed in the following paragraphs.

Diaryl isoprenoid hydrocarbons. The compound reflected by the dominating peak in the mass chromatogram of *m/z* 133 obtained by GC–MS analysis of the hydrocarbons from the polar fraction of sample 5 (Fig. 4) was identified by a coelution experiment with an authentic standard as isorenieratane (**V**), or the partially saturated equivalent of the diaromatic carotenoid isorenieratene (**VIII**). This compound reveals the presence of sulphurized isorenieratene or partially hydrogenated isorenieratene moieties and not free isorenieratene, although this component has been reported in these sediments (Keely *et al.*, 1995). Examination of the apolar and polar fractions of a representative sample from this bed by HPLC revealed that free isorenieratene is not present in large quantities in either of these two fractions (less than 10% of the concentration of sulphurized isorenieratene) (Keely, unpublished results). This is probably due to the relatively apolar nature of the solvent system used for extraction in this study; full recovery of free isorenieratene from sediments requires extraction with acetone (Keely, personal communication) or methanol (Repeta, 1993). Since isorenieratene is a characteristic carotenoid of Chlorobiaceae (Liaaen-Jensen, 1978a, b), the presence of this compound or derivatives thereof clearly indicate the presence of this obligate anaerobic green sulphur bacteria in the palaeoenvironments represented by the samples in which these compounds were found. These photoautotrophic organisms fix carbon via the reverse tricarboxylic acid cycle, leading to biomass significantly enriched in ^{13}C (Quandt *et al.*, 1977; Sirevag *et al.*, 1977) relative to other phototrophic organisms using the Calvin–Benson cycle. The δ values measured here for isorenieratane (between -11.6 and -14.8‰, Fig. 5), by Kohnen *et al.* (1992b; -10.7‰) in another study of the Vena del Gesso sediments, and by Sinninghe Damsté *et al.* (1993c) and Hartgers *et al.* (1994a,b) in other sediments, confirm the relationship between isorenieratene produced by Chlorobiaceae and isorenieratane released from the polar fractions of these sedimentary extracts.

Other compounds revealed by mass chromatography of *m/z* 133 include the compound tentatively identified as the C_{33} diaryl isoprenoid hydrocarbon (**VII**) (Fig. 4). This compound is eluting just after another tentatively identified compound, the C_{32} diaryl isoprenoid hydrocarbon (**IX**) (Fig. 4). The mechanism explaining their diagenetic formation from isorenieratene may parallel mechanisms proposed for products produced from β-carotene (**X**) upon thermal stress. Vetter *et al.* (1971) proposed a mechanism for the formation of lexene (**XI**), a C_{33} pseudo-homologue of β-carotene, and toluene from β-carotene upon thermal stress. A similar mechanism has been proposed by Byers and Erdman (1983) to explain the formation of philene (**XII**), a C_{32} pseudo-homologue of β-carotene, and xylene from β-carotene. If these mechanisms are applied to isorenieratene (**VIII**), C_{32} and C_{33} "carotenoids" result. These unsaturated compounds have obviously become sulphurized. In four samples where all three could be analysed, δ values of isorenieratane and of the C_{33}-and C_{32}-diaryl isoprenoids do not deviate by more than 0.7‰ from the group averages (Fig. 5). The similarity of the depth profiles of the C_{40} and the C_{33} diaryl isoprenoids [Fig. 6(a–b)] as well as the identical $\delta^{13}C$ values obtained for C_{40}, C_{33} and C_{32} diaryl isoprenoids support a common origin of these three compounds, i.e. Chlorobiaceae-derived isorenieratene.

The presence of Chlorobiaceae in the palaeoenvironment indicates that an anoxic water mass reached into the photic zone. The depth profiles of isorenieratane (**V**) and the C_{33} diaryl isoprenoid (**VII**) show a maximum concentration of these compounds in sample 2 and then a decrease up section, though with a second maximum for sample 6 [Fig. 6(a–b)]. Sulphur-bound isorenieratane is absent in samples 9 and 10. This indicates that during the deposition of the lower part of the marl bed, the water column was stratified, and, that sufficient light could reach the anaerobic water column so that the development of an obligate anaerobic photosynthetic sulphur bacterial community was possible.

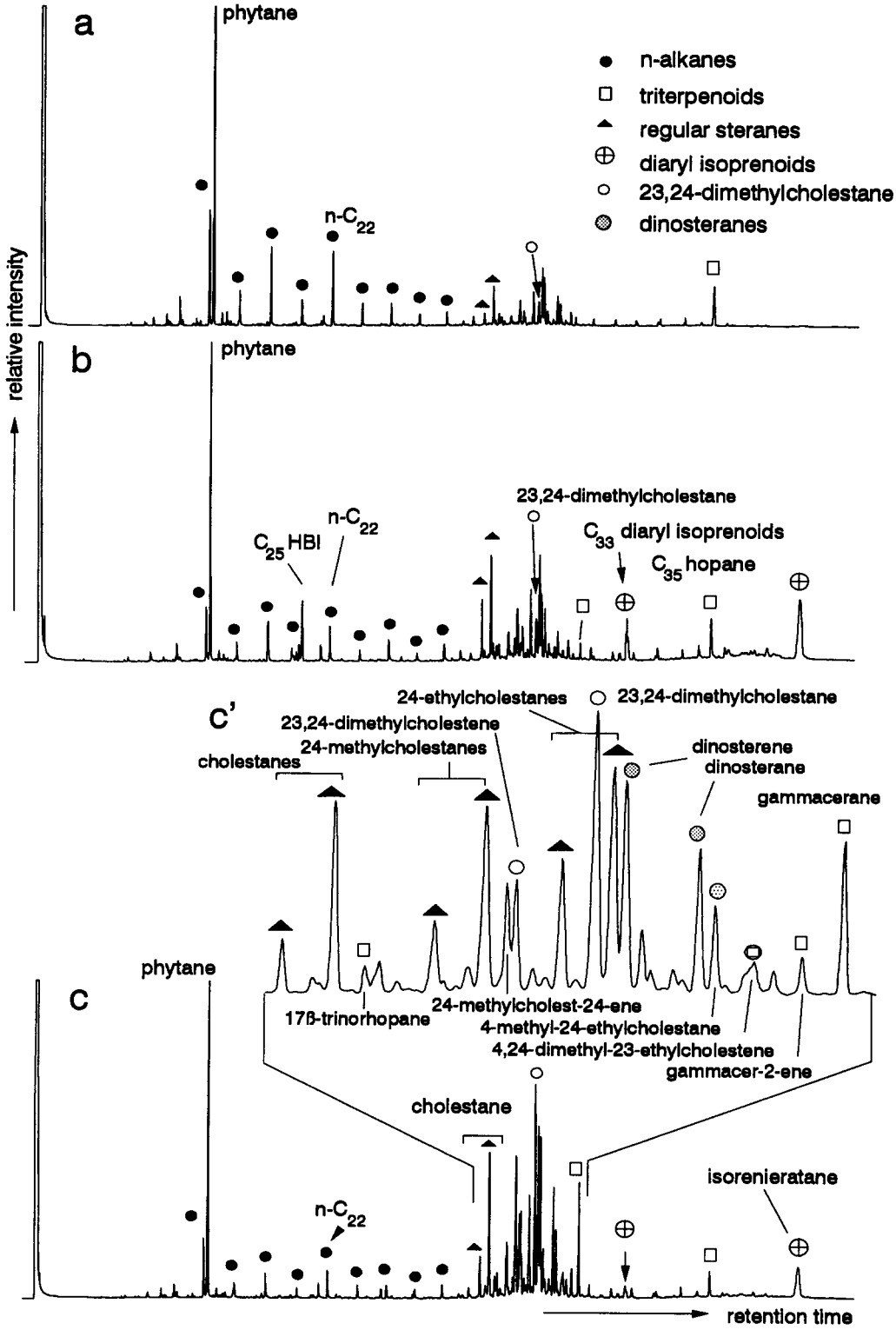

Fig. 3. FID chromatograms of the hydrogenated hydrocarbon fraction released with nickel boride desulphurization of the polar fraction of sample 10 (a), sample 5 (b) and sample 1 (c and c'). Location of the samples in the profile is given in Fig. 1. Inset (c') shows enlargement of sterane and triterpane region of the FID trace of sample 1.

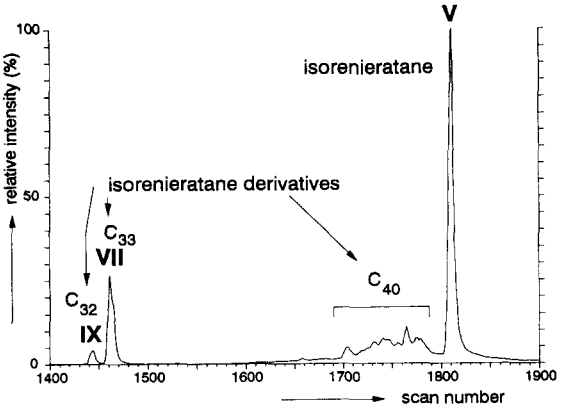

Fig. 4. Partial mass chromatogram of m/z 133 showing the distribution of diaryl-isoprenoids in the hydrogenated hydrocarbon fraction obtained after desulphurization of the polar fraction of sample 5. The structures of roman-numbered compounds are given in the Appendix.

Steroid hydrocarbons. The regular C_{27}, C_{28} and C_{29} steranes, 4,23,24-trimethylcholestane (dinosterane, **IV**), 4,23,24-trimethylcholest-22-ene (dinosterene), 4-methyl-24-ethylcholestane and compounds tentatively identified based on their mass spectra as 23,24-dimethylcholestane [**VI**, Fig. 7(a)] and 23,24-dimethylcholest-22-ene [Fig. 7(b)] are major components released from the polar fraction after desulphurization and hydrogenation. The relative concentrations of these steroids when compared with those of other compounds, notably phytane, decrease up section (Fig. 3).

A good correlation exists between the concentration profiles of 5α-and 5β-cholestane [Fig. 6(e)]. Similarly good correlations were also observed for 5α- and 5β-24-methylcholestane and -24-ethylcholestane. This clearly indicates that the 5α- and 5β-steranes are diagenetically related and originate from the same precursors, i.e. Δ^5-sterols (de Leeuw *et al.*, 1989). Figure 8(a–c), displaying mass chromatograms of m/z 217 for samples 1, 5 and 10, indicate a decrease in concentration of 24-methylcholestanes relative to the other steranes up section and that the relative proportion of the cholestanes and the 24-ethylcholestanes is not constant throughout the marl bed. The concentration of 23,24-dimethylcholestane (**VI**) decreases significantly relative to those of the regular steranes up the section. The presence of 5β- and 5α-27-nor-24-methylcholestane, which have similar mass spectra as that of cholestane (Schouten *et al.*, 1994), should be noted in samples 5 and 10 [Fig. 8(a–b)].

The relative intensities of 4,24-dimethylcholestane, dinosterane and 4-methyl-24-ethylcholestane are revealed by the mass chromatograms of m/z 231

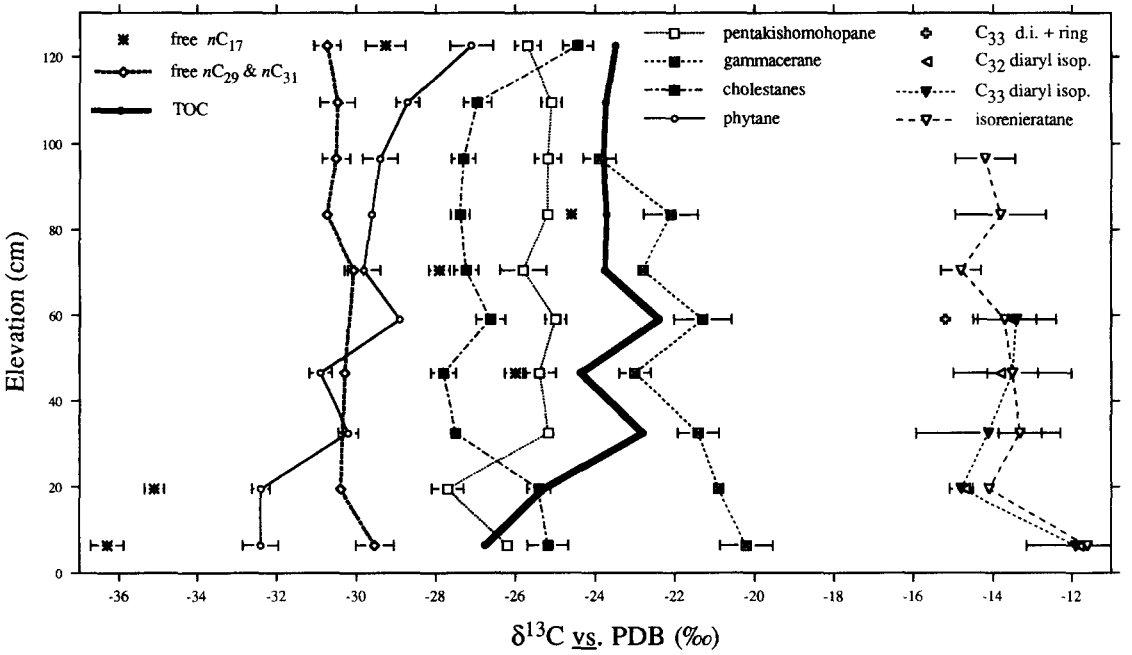

Fig. 5. δ vs PDB (‰) of total organic carbon (TOC) and of compounds released upon desulphurization of the polar fraction: 2,6,10,14-tetramethylhexadecane (phytane), 17β,21β(H)-pentakishomohopane (**II**), isorenieratane (**V**), C_{33} diaryl isoprenoid (**VII**), C_{32} diaryl isoprenoid (**IX**), quantitative average of 5β-and 5α-cholestane (cholestanes) and gammacerane (**III**) plotted vs elevation in the marl bed. The δ of free hydrocarbons, *n*-heptadecane (*n*-C_{17}), the average δ values of *n*-nonacosane (*n*-C_{29}) and *n*-heneitriacontane (*n*-C_{31}), and C_{33} diaryl isoprenoid with an additional ring (**XXII**) in sample 5 are plotted for comparison. The standard deviations based on a minimum of two measurements are indicated. When not shown, standard deviation is inferior to the width of the mark indicating the data point.

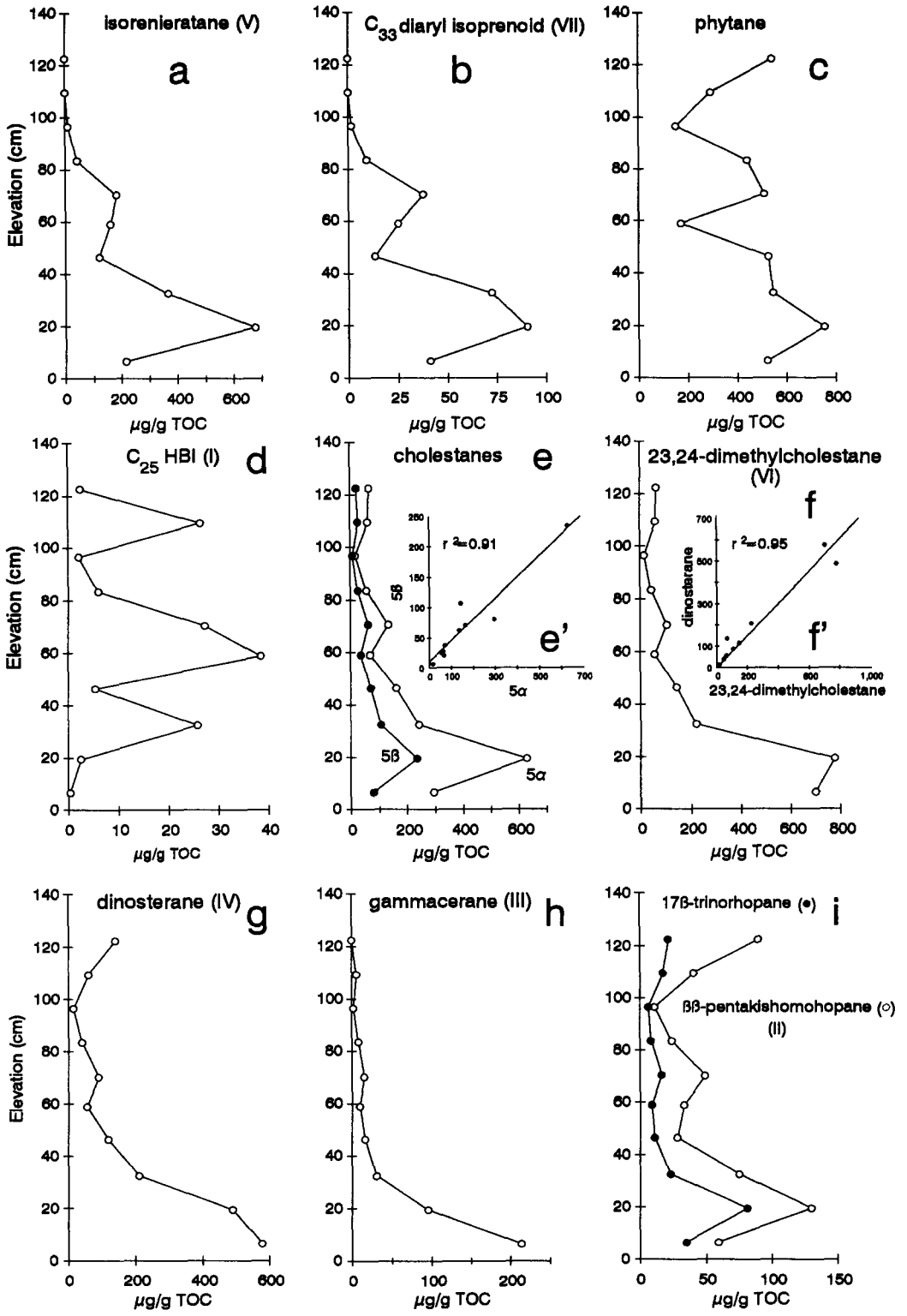

Fig. 6. Depth profiles of the concentrations of (a) isorenieratane (**V**), (b) C_{33} diaryl isoprenoid (**VII**), (c) phytane, (d) C_{25} HBI alkane (**I**), (e) 5α-and 5β-cholestane, (f) 23,24-dimethylcholestane (**VI**) + 23,24-dimethylcholestene, (g) dinosterane (**IV**) + dinosterene, (h) gammacerane (**III**), (i) 17β-trinorhopane and 17β,21β(H)-pentakishomohopane (**II**) obtained after desulphurization of the polar fraction. Insets (e' and f') are correlation plots of the steroid data indicated.

[Fig. 8(d–f)]. Dinosterol, the precursor of dinosterane, is exclusively synthesized by dinoflagellates (Boon *et al.*, 1979; Volkman, 1988). Therefore, the presence of S-bound dinosterane is indicative of the presence of dinoflagellates. Other 4-methyl-steroids may also derive from dinoflagellate species (Djerassi, 1981; Kokke *et al.*, 1981), but may also originate from prymnesiophyte microalgae of the genus Pavlova (Volkman *et al.*, 1990) or diatoms (Volkman *et al.*, 1992; Nichols *et al.*, 1990). 4,24-Dimethylcholestanol, the possible precursor of 4,24-dimethylcholestane, has been identified together with dinosterol in some dinoflagellate algae (Alam *et al.*, 1984; Robinson *et al.*, 1987). However, in contrast to what was observed in the Salt IV Formation of the Mulhouse basin (Sinninghe Damsté *et al.*, 1993a), there is no correlation between the relative intensities of regular 4-methylsteranes and dinosteranes in the Vena del Gesso marls. Hence, these compounds can be produced by species biosynthesizing different amounts of 4-methylsterols under varying conditions or can be biosynthesized independently by different algal species.

The depth profiles of the concentrations of 23,24-dimethylcholestane and dinosterane are similar [Fig. 5(f–g)] and their concentrations are well correlated [Fig. 5(f')]. At present, the source of 23,24–dimethylcholestane is unclear. However, traces of its potential precursors, 23,24-dimethyl-5α-cholest-22-en-3β-ol and 23,24*R*-dimethyl-4,22E-cholestadien-3-one were identified in cultures of dinoflagellates by Robinson *et al.* (1987) and Kokke *et al.* (1982),

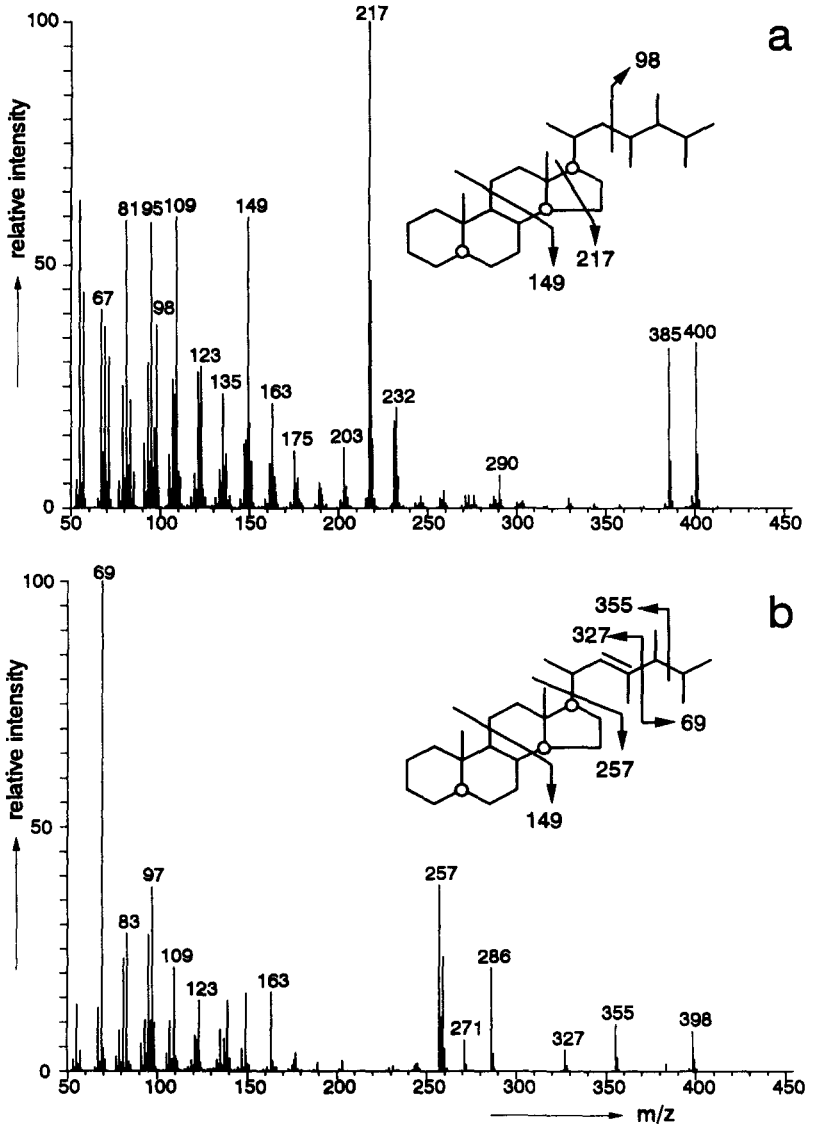

Fig. 7. Mass spectra, corrected for background, and tentative structures of (a) 23,24-dimethyl-5α-cholestane (VI) and (b) 23,24-dimethyl-5α-cholest-22-ene.

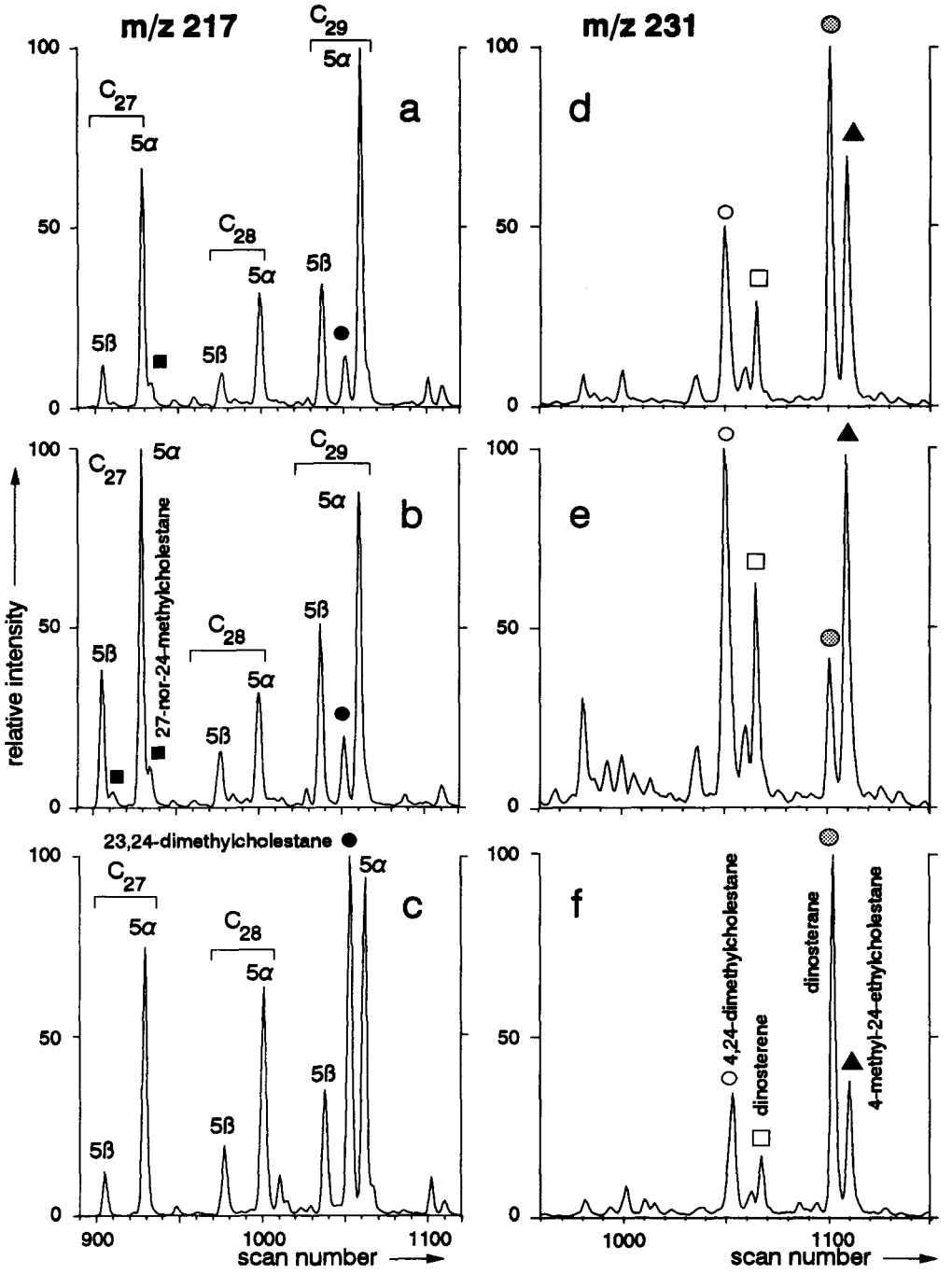

Fig. 8. Partial mass chromatograms of *m/z* 217 and *m/z* 231 of sample 10 (a and d), sample 5 (b and e) and sample 1 (c and f) revealing the distributions of regular steranes, 4-methyl-24-ethyl-5α-cholestane, 4,24-dimethyl-5α-cholestane, 23,24-dimethyl-5α-cholestane (**VI**) and 4,23,24-trimethyl-5α-cholestane (dinosterane, **IV**) in the hydrocarbon fractions obtained after desulphurization and hydrogenation of the polar fractions.

respectively. Another potential precursor for 23,24-dimethylcholestane, 23,24-dimethylcholesta-5,22E-dien-3β-ol was identified in trace amounts in *Biddulphia sinensis* by Volkman *et al.* (1980a). It may be speculated that the precursor of 23,24-dimethylcholestane is abundantly produced by one or several, partly unknown, species of dinoflagellates.

The differences in the relative intensities of the steranes, dinosterane, 4-methylsteranes and 23,24-dimethylcholestane as observed by mass chromatography, reveal variations in the composition of the algal

primary producers in the euphotic zone during the deposition of the marls. The absolute concentration depth profiles of cholestanes [Fig. 6(e)], 23,24-dimethylcholestane [Fig. 6(f)] and dinosterane [Fig. 6(g)] show maximum concentrations of these steranes in sample 2. A similar profile was also observed for 4-methyl-24-ethylcholestane (not shown). As these steranes were released upon desulphurization, it is likely that their absolute concentrations are mainly determined by their incorporation into sulphur-rich macromolecules, and are thus also dependent on the environmental and early diagenetic conditions prevailing during deposition and reflect only to some extent variations in compositions of algal sources.

The δ values of S-bound steranes from all 10 samples are summarized in Fig. 9. Limited chromatographic resolution prevented isotopic analysis of some products of desulphurization, namely dinosterane (**IV**), dinosterene, 23,24-dimethylcholestane, 4,24-dimethylcholestane and 4-methyl-24-ethylcholestane, but parts a, c, and d of the figure show that δ-values obtained for the C_{27} and C_{29} regular steranes were closely correlated and varied systematically through the section. As shown in Fig. 9(b), however, the isotopic compositions of 24-methylcholestanes differ

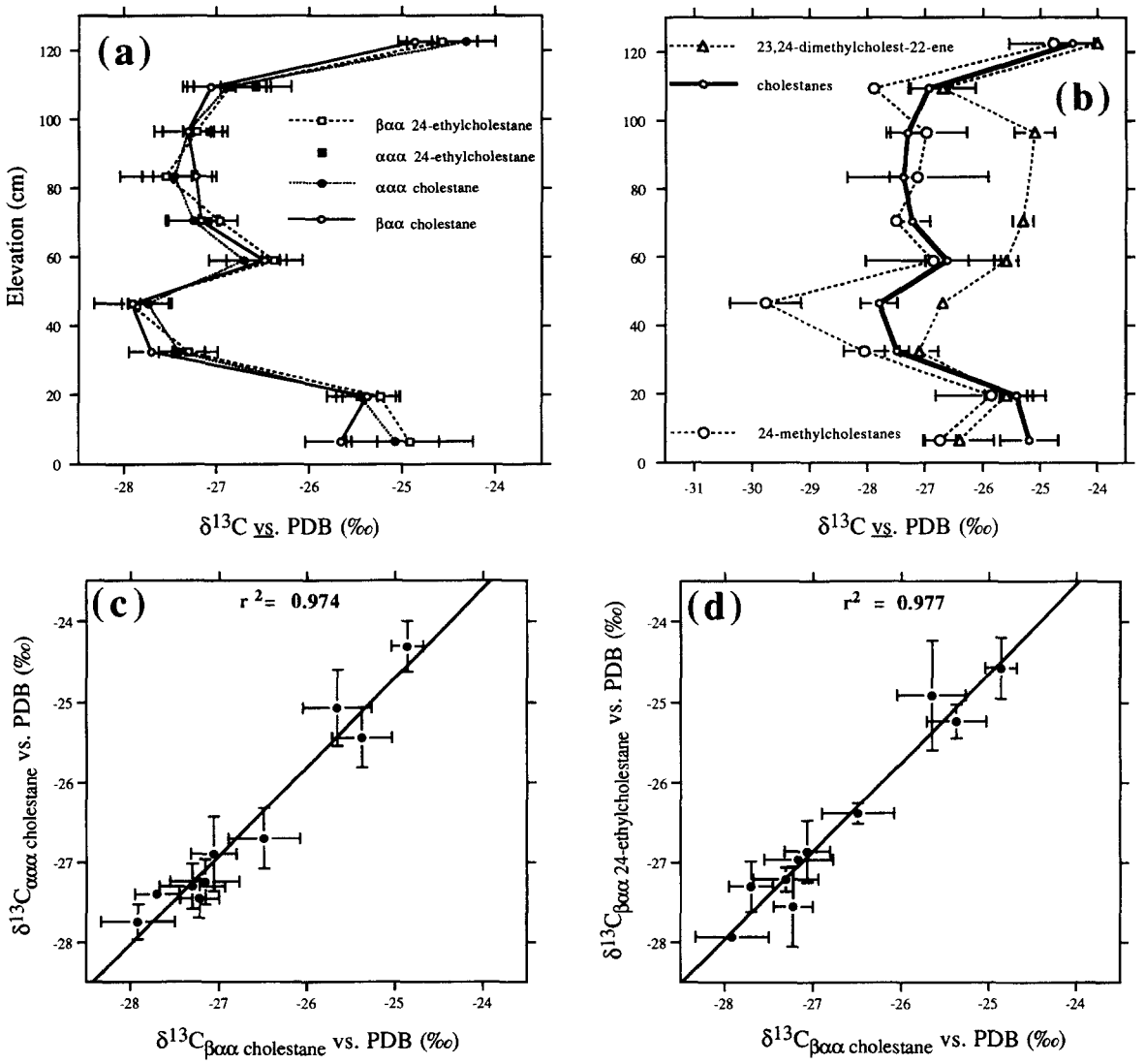

Fig. 9. (a) δ vs PDB (‰) of 5β-and 5α-cholestane and of 5β-and 5α-24-ethylcholestane and corresponding standard deviations plotted vs depth in the marl bed. (b) δ vs PDB (‰) of the average of 5β-and 5α-24-methylcholestane (24-methylcholestanes), the average of 5β-and 5α-cholestane (cholestanes) and 23,24-dimethylcholest-22-ene plotted vs elevation in the marl bed. (c) Plot of the δ vs PDB (‰) of 5β-vs 5α-cholestane. (d) Plot of the δ vs PDB (‰) of 5β-24-ethylcholestane vs 5β-cholestane. When not shown, standard deviation, based on a minimum of three measurements, is inferior to the width of the mark indicating the data point.

distinctly from those of the C_{27} and C_{29} regular steranes in samples 1 and 4 and the isotope profile of the S-bound 23,24-dimethylcholest-22-ene does not resemble that of the regular steranes. The first of these observations confirms the hypothesis based on concentration profiles that the 24-methylcholestanes derived, in part, from sources other than those of the other regular steranes, particularly in samples 1 and 4. The second may provide information on the isotopic compositions of dinoflagellates, but this can unfortunately not be checked against δ values for dinosterane and dinosterene.

Steroidal carbon skeletons can be produced by numerous species of eukaryotic algae (e.g. Volkman, 1988). The isotopic profile shown in Fig. 9(a) can therefore be taken as representative of isoprenoid lipids derived from eukaryotic primary producers. The best estimate is provided by the average obtained for 5α- and 5β-cholestane (heavy line in Fig. 9(b), also shown in Fig. 5), isomers for which particularly reliable isotopic analyses could be obtained.

Hopanes. Mass chromatograms of *m/z* 191 derived from the GC–MS data of the hydrocarbons released upon desulphurization of the polar fraction exemplify the variations in the distributions and relative concentrations of the pentacyclic triterpenoid hydrocarbons (Fig. 10). The extended hopanes are always dominated by 17β,21β(H)-pentakishomohopane. Non-extended hopanes are represented by 17β-trinorhopane and C_{30} hopanes, with the 17β,21β(H) isomer only present in minor amounts relative to its $\alpha\beta$ and $\beta\alpha$ counterparts.

Pentakishomohopane (**II**) derives from extended bacteriohopanoids (Ourisson *et al.*, 1982) which are biosynthesized exclusively by eubacteria, including cyanobacteria (Rohmer *et al.*, 1992). As shown in Fig. 5, values of δ for this compound are quite constant in samples 3–10. For almost all of this range (samples 3–9), this bacterial product is slightly enriched in ^{13}C relative to the cholestanes, noted above as representative of eukaryotic photoautotrophs. In other studies of the Vena del Gesso sediments (Kohnen *et al.*, 1992a,b) and in a study of the Monterey Formation (Schoell *et al.*, 1994b), it has been proposed that S-bound pentakishomohopanoids derive mainly from cyanobacteria. Here, significant contributions from methanotrophic bacteria can be excluded on the basis of the observed isotopic composition (−27.7 to −25.0‰). Exclusion of all sources other than cyanobacteria is, however, more difficult. In sample 10, the abundance of S-bound pentakishomohopane and the presence of the overlying stromatolite (Vai and Ricci Lucchi, 1977) raise the possibility of a benthic cyanobacterial mat and suggest a cyanobacterial origin for pentakishomohopane. In samples 1, 2, and 10, pentakishomohopane is depleted in ^{13}C relative to steranes (Fig. 5).

There have been no studies of the isotopic compositions of coexisting eukaryotic algae and cyanobacteria. On biosynthetic grounds, however, cyanobacterial isoprenoids would be expected to be enriched in ^{13}C relative to those of eukaryotic origin. This difference would reflect the differing origins of the carbon atoms in the respective C_5 biomonomers used to build up the isoprenoid carbon skeletons. In eukaryotes, three of the carbon atoms derive from the methyl and two from the carboxyl position of acetyl-CoA. The overall depletion in ^{13}C in isoprenoids apparently arises from a position-specific depletion at the latter position (for discussion and references, see Hayes, 1993). In eubacteria, however, it is now known (Rohmer *et al.*, 1993) that three of the carbon positions in the C_5 biomonomer do not derive from acetate but instead pass into lipid biosynthesis directly from carbohydrate metabolism. All of these are expected to be undepleted, leaving only a single, acetate-carboxyl-derived site of depletion in the eubacterial C_5 unit. Additionally, as pointed out by Schoell *et al.* (1994b), the C_5 side chain in extended hopanoids also derives from carbohydrate rather than lipid metabolism. Of the 30 carbon positions in eukaryotic squalene (the precursor of steroids), 12 are thus depleted relative to carbohydrate carbon. If, for example, that depletion were 8‰, the molecular-average depletion would be $(12 \times 8)/30 = 3.2$‰. Of the 35 carbon positions in an extended hopanoid, 6 would be depleted and the molecular-average depletion would be $(6 \times 8)/35 = 1.4$‰. Isotopic enrichment of hopanoids relative to steroids roughly equal to that observed in samples 3–9 is therefore consistent with derivation of the hopanoids from cyanobacteria occupying on average the same habitats as the eukaryotic algae.

The depth profiles of the hopanoids [Fig. 6(i)], like those of most steranes [Fig. 6(e–g)], maximize at sample 2. Similarly to what was speculated for the steroids the maximum at sample 2 is probably due to excellent conditions for sulphurization of organic matter during deposition of this sample. The hopanoid profiles and notably that of the pentakishomohopane, exhibit a submaximum at sample 10. This trend is hardly noticed in the steroid depth profiles and thus not likely reflects a change in the extent of sulphurization. Therefore, a significant increase in relative contributions of cyanobacterial primary producers is proposed in the depositional environment reflected by sample 10.

Gammacerane. The non-hopanoid compounds revealed by the *m/z* 191 mass chromatograms (Fig. 10) are gammacerane (**III**) and gammacer-2-ene. The depth profile of gammacerane is unique with a strong maximum at sample 1 and a progressive decrease towards sample 9 after which it is absent [Fig. 6(h)]. This profile is very different from those of the two hopanoids quantified, 17β-trinorhopane and 17β,21β(H)-pentakishomohopane [Fig. 6(i)]. Gammacerane and gammacer-2-ene have been proposed to derive from tetrahymanol (e.g. ten Haven *et al.*, 1989), a compound found in several species of the ciliate Tetrahymena (Mallory *et al.*, 1963; Holz and Conner, 1973). More recently, tetrahymanol has

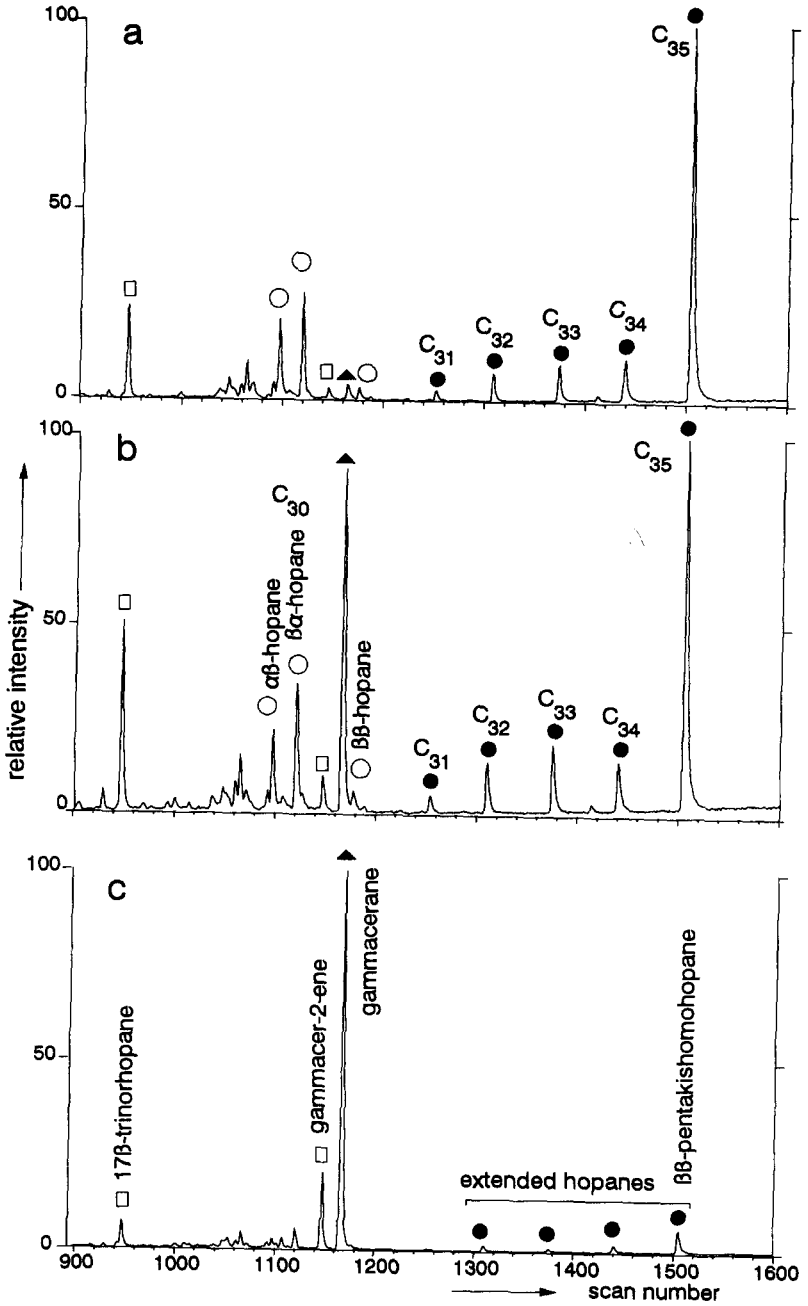

Fig. 10. Partial mass chromatograms of *m/z* 191 showing the distribution of pentacyclic triterpenoids in the hydrocarbon fraction obtained after desulphurization and hydrogenation of the polar fraction of three representative samples, sample 10 (a), sample 5 (b) and sample 1(c).

also been identified in the obligate anaerobic purple photosynthetic bacteria *Rhodopseudomonas palustris* (Kleemann *et al.*, 1990). These bacteria should be considered as an alternative source for gammacerane, especially in the Vena del Gesso palaeoenvironment, where obligate anaerobic photosynthetic green sulphur bacteria (Chlorobiaceae) were present (see above). It has been shown that purple sulphur bacteria can live above the layer of the brown strains of obligate anaerobic green sulphur bacteria (Montesinos *et al.*, 1983) which produce isorenieratene. However, the δ values of S-bound gammacerane range from -20.2 ± 0.7‰ in sample 1 to -23.9 ± 0.4‰ in sample 8, with ^{13}C contents decreasing from the bottom to the top of the section and following trends in δ_{TOC} between samples 3 and 6 (Fig. 5). These features do not suggest that the gammacerane precursors derive from purple sulphur bacteria. Values of δ for natural populations of those organisms commonly range from -26 to -36‰ (Schidlowski

et al., 1984). Here, the δ value for purple photosynthetic bacterial lipids in sample 1 will be estimated to be $-36.3‰$ based on the δ value obtained for free *n*-heptadecane (Fig. 5; see *n*-Alkanes section 3.4.1 below). The ^{13}C content of gammacerane, therefore, indicates that bacterivorous ciliates living at or below the chemocline and partially feeding on green sulphur bacteria are the origin of this component (*cf.* Sinninghe Damsté *et al.*, 1995a).

Acyclic isoprenoid hydrocarbons. Phytane (2,6,10,14-tetramethylhexadecane) is by far the most abundant compound among the hydrocarbons released by desulphurization (Fig. 3). The macromolecularly S-bound phytane carbon skeletons result from the incorporation of sulphur into phytol-derived phytadienes (Kohnen *et al.*, 1991a) or phytenal (Schouten *et al.*, 1993b). The sources of phytol can be diverse because cyanobacteria, eukaryotic algae, higher plants and purple sulphur bacteria are potential sources for these compounds in these palaeoenvironments. As shown in Fig. 5, δ values of S-bound phytane vary from $-32.4‰$ in sample 1 to $-27.1‰$ in sample 10, paralleling variations in δ_{TOC} between samples 3 and 8. The large range of δ values for S-bound phytane (5.3‰) and its depletion in ^{13}C relative to lipids from primary producers suggest a mixed origin for this compound and thus for phytol. The only potential source of ^{13}C-depleted phytol identified in these sediments is purple sulphur bacteria (Chromatiaceae), for which an *n*-alkyl lipid δ value has been estimated at $-36.3‰$ in sample 1 (see *n*-Alkanes section 3.4.1 below). If all S-bound phytane is assumed to derive from either Chromatiaceae or phytoplankton, their relative contributions, and thus the importance of anaerobic photosynthesis, can be estimated by comparison of the phytane and sterane δ profiles, which are separated by more than six permil at the bottom of the section but by less than three at the top (Fig. 5). The most important change occurs between samples 2 and 3, suggesting a marked decrease in production by purple photosynthetic bacteria above that interval. The depth profile of the S-bound phytane skeleton [Fig. 6(c)], exhibits a maximum at sample 2, and shows no clear trend. The scattered data may thus also reflect the diversity of the sources of this skeleton.

The S-bound C_{25} HBI alkane (2,6,10,14-tetramethyl-7-(3-methylpentyl)pentadecane; I) exhibits a unique depth profile [Fig. 6(d)]. Kohnen *et al.* (1992b) proved, on the basis of stable carbon isotope analyses, that in another Vena del Gesso sediment the macromolecularly S-bound C_{25} HBI carbon skeleton originates from algal compounds though probably not from specific diatoms (Nichols *et al.*, 1988; Volkman *et al.*, 1994) because the C_{25} HBI thiophenes reflecting the C_{25} HBI unsaturated compounds of these specific algae had significantly different stable carbon isotope values (Kohnen *et al.*, 1992b).

n-Alkanes. Large variations in the distributions of S-bound *n*-alkanes are noticed [Fig. 11(b–d)]. This immediately hints to the multiple origins for these S-bound compounds. In the distributions of all samples and also in the weighed averaged distribution for the total marl bed [Fig. 11(a)] a strong even-over-odd carbon number predominance in the C_{16}–C_{28} range is noticed, in agreement with data previously reported for hydrocarbon fractions obtained upon desulphurization of polar fractions of other sediments (Sinninghe Damsté *et al.*, 1988, 1990; Kohnen *et al.*, 1991a; Adam *et al.*, 1993). This feature disappears for the longer *n*-alkanes which are dominated by the C_{30} alkane and show a regular decrease in intensity between *n*-C_{31} and *n*-C_{36}. The C_{37} and C_{38} alkanes dominate over *n*-C_{36} and *n*-C_{39}.

As indicated in Figs 12(a) and (b), many of these *n*-alkanes exhibit similar concentration profiles. Moreover, these profiles do not differ much from those of S-bound branched and cyclic compounds (cf. Fig. 6). Together, these observations indicate that the quantities isolated have been controlled by the extent of sulphurization rather than the abundances of precursors. To minimize effects of this overprint, we have multiplied all yields of desulphurized hydrocarbons (mg/g TOC) by the factor required to make them equal to that in sample 2, where the highest yield was obtained (see discussion hereafter). The resulting "corrected concentration profiles" exhibit distinct trends [Fig. 12(c–d)], but the large differences between concentrations of different compounds make a comparison difficult. As a final step, therefore, the corrected concentration profiles were recast in terms of relative concentrations of each alkane. The profiles shown in Fig. 13(a) comprise "group I" and are those of S-bound *n*-alkanes for which the greatest concentration occurs in sample 10 (where relative concentration $\equiv 1$). Figure 13(b), "group II," collects the group maximizing in sample 8. Group III includes homologues maximizing in sample 5 and includes *n*-alkanes with 16, 35, 37 and 38 carbon atoms. The profiles for *n*-C_{37} and *n*-C_{38} are nearly congruent [Fig. 13(c)], strongly indicating similar origins. The remaining relative-concentration profiles are shown in Fig. 13(d), which includes C_{30}, the only *n*-alkane which maximizes at sample 2.

In each group, variations in relative concentrations with depth are at least roughly parallel. Group I includes all short-chain *n*-alkanes in the C_{17}–C_{25} range as well as *n*-C_{27}. The latter compound also exhibits a second maximum at sample 8, indicating association with group II. The relative concentration of the *n*-C_{24} homologue is notably enhanced at sample 5, suggesting association with group III. Group II includes all *n*-alkanes in the C_{26}–C_{36} range with the exception of *n*-C_{27}, *n*-C_{30}, and *n*-C_{35}. But some trends cut across all groups. All relative concentrations increase at sample 5 and most increase at sample 3. In the latter case, exceptions include C_{17}–C_{20} from group I, C_{28} from group II, and all three of the homologues shown in Fig. 13(d). The overall increases at samples 3 and 5 might be a reflection of environmental

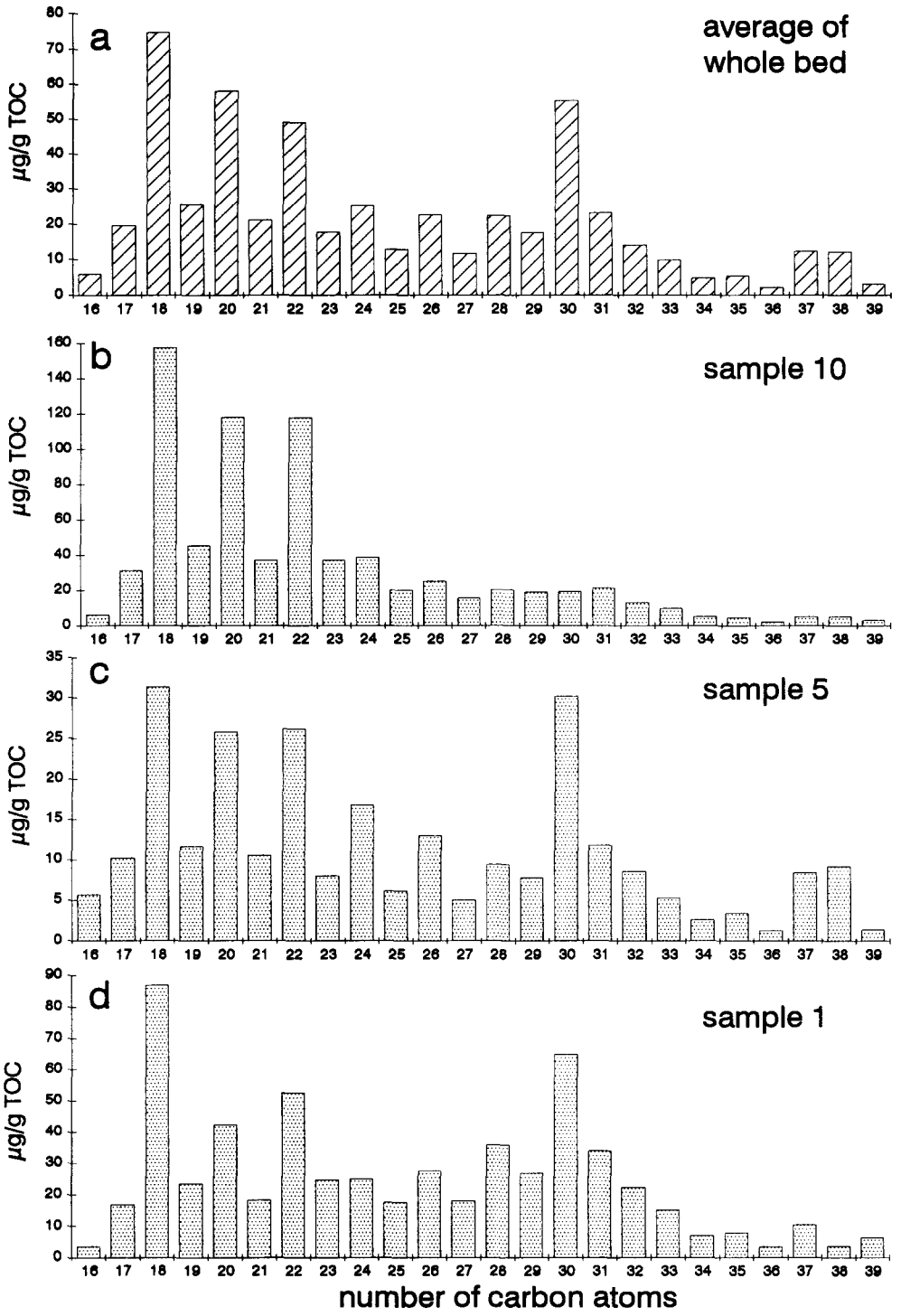

Fig. 11. Concentration of *n*-alkanes released upon desulphurization of the polar fraction. (a) Calculated averages for the whole bed using 9 samples. These averages take into account the thickness, the organic carbon content and *n*-alkane concentration of each sample. Sample 9 was not included as it was contaminated. These averages are similar to the concentrations obtained for sulphur-bound *n*-alkanes in a sample of the entire marl bed (Koopmans *et al.*, unpublished results). (b) Sample 10, (c) sample 5 and (d) sample 1.

changes affecting most of the organisms producing precursors of the S-bound *n*-alkanes. This observation provides a reminder that correlations between concentration profiles provide evidence for but not proof of commonality of sources. Whole groups of organisms can be affected by environmental changes. Isotopic analyses can assist in further dissection of this problem.

As shown in Fig. 14, the δ values of S-bound *n*-alkanes overlap considerably with those of upper water column primary-producer lipids (UWCPL), with 61% falling within the range defined by the S-bound cholestanes and pentakishomohopane (Fig. 5). The ^{13}C enrichments displayed by most *n*-alkanes at samples 3 and 5 are correlated with those in TOC and S-bound phytane in these same samples (Fig. 5). Not many of the δ values for S-bound *n*-alkanes fall into the range characteristic of terrestrial lipids (defined below), indicating that the precursors of S-bound *n*-alkanes are mainly of aquatic origin. A few S-bound *n*-alkyl carbon skeletons are consistently enriched in ^{13}C relative to the UWCPL range. These include *n*-C_{16}, *n*-C_{31}, *n*-C_{32} and, to a lesser extent, *n*-C_{17} and *n*-C_{19}. In sample 1, *n*-C_{36}, *n*-C_{38} and *n*-C_{37} are the most enriched in ^{13}C (Fig. 14).

The homogeneity of the groups defined on the basis of concentration profiles does not hold when isotopic data are considered. The C_{17}–C_{25} *n*-alkanes of group I have, between samples 1 and 8, similar trends in their δ profiles, as shown for some of them in Fig. 15(a), but the very large ranges of δ values, up to 4.8‰ in sample 7, do not point to derivation from a single source. Minimum spreads of 2.4, 1.7, and 2.6‰ occur in samples 1, 2, and 4, respectively. Between samples 8 and 10, the δ values in this group are much less smoothly covariant, indicating a change in the dominant source for some of them at sample 10. For this group, a marked oscillation occurs in all isotopic profiles between samples 2 and 6, with enrichments of ^{13}C maximizing at samples 3 and 5. The functionalized precursors of these shorter-chain *n*-alkanes can be multiple and identification of their source organisms is difficult. Many algae and cyanobacteria produce functionalized compounds with *n*-alkyl carbon skeletons of this size (e.g. Johns *et al.*, 1979; Volkman *et al.*, 1980a Volkman *et al.*, 1980b, 1989). Variations in assemblages of these primary producers, including microalgae, diatoms, and prymnesiophytes, are therefore probably responsible for the observed isotopic variations.

The *n*-alkanes of group II (C_{26}–C_{36}, excluding C_{27}, C_{30}, and C_{35}) display variable trends in their isotopic profiles. Values of δ for C_{31} and C_{32} are well correlated with each other and to some extent with δ_{TOC} [Fig. 15(b)] but do not resemble those of other components of group II [Fig. 15(c)]. The greatest depletions of ^{13}C among the S-bound *n*-alkanes occur for the even-carbon homologues with 26, 28, and 30 carbon atoms. Although placed in group II on the basis of concentration profiles, they do not display, between samples 2 and 6, the oscillations characteristic of C_{31}, C_{32}, and most other S-bound *n*-alkyl carbon skeletons and must, therefore, be produced by organisms not sensitive to the causes of that feature. The isotopic profile for S-bound *n*-C_{16} is similar to those of *n*-C_{31} and *n*-C_{32}, although the shorter chain is more enriched in ^{13}C in the upper part of the bed [Fig. 15(b)]. The concentration profiles for these compounds, however, are *not* similar, revealing the complexity of the situation.

The origins of the precursors of these S-bound *n*-alkanes are difficult to determine. However, those of C_{31} and C_{32} could be the C_{30}–C_{32} 1,15-alkyl diols (**XIII**) or the alkan-15-one-1-ols (**XIV**) commonly found in immature marine and lacustrine sediments (de Leeuw *et al.*, 1981; Morris and Brassell, 1988 and references cited therein; Zeng *et al.*, 1988). Indeed, Koopmans *et al.* (1995b) find in a composite sample of the marl of cycle IV, and in artificial maturation products of this marl bed, mid-chain thiophenes in the C_{28}–C_{32} range, structures which point to incorporation of sulphur mainly at position 15 of functionalized precursors with linear carbon skeletons. The C_{30}–C_{32} 1,15-alkyl diols are abundant bound lipids in microalgae of the class Eustigmatophyceae (Volkman *et al.*, 1992). Previously, C_{30}–C_{32} 1,15-alkyl diols were thought to derive from cyanobacteria since they were identified in plankton tows collected during a bloom of the cyanobacterium *Aphanizomenon flos aquae* in the Baltic Sea (Morris and Brassell, 1988). Subsequent investigation of axenic cultures of this cyanobacterium by de Leeuw *et al.* (1992) did not, however, show the presence of any of these compounds. Their identification in some microalgae by Volkman *et al.* (1992) strongly indicates that these organisms are sources of the S-bound C_{31} and C_{32} alkanes. There are, however, discrepancies between the distributions in microalgae, dominated by C_{32} homologues, the distributions in most sediments, dominated by C_{30} homologues and the relative amounts of S-bound *n*-C_{31} and *n*-C_{32} found here. In the Vena del Gesso marls, the isotopic and concentration profiles of the C_{30} *n*-alkane, one of the most abundant in the S-bound hydrocarbon fraction [Fig. 12(b)], are very different from those of S-bound *n*-C_{31} and *n*-C_{32}. The *n*-C_{30} carbon skeleton must therefore, at least in part, have an origin different from that of the S-bound *n*-C_{31} and *n*-C_{32}. To explain such discrepancies, Volkman *et al.* (1992) suggested that microalgae different from those analysed are the likely sources of the alkyl diols found in most sediments. C_{30}–C_{32} 1,15-alkyl diols were found in association with analogous alkan-15-one-1-ols by de Leeuw *et al.* (1981) in sediments from the Black Sea. As ketones react readily with reduced sulphur species (Schouten *et al.*, 1993b), these compounds are also likely precursors of the S-bound *n*-C_{31} and *n*-C_{32}. Moreover, Koopmans *et al.* (1995b) have suggested that sulphurization of these carbon skeletons can occur via dehydration of the diols. It should be noted that C_{16} functionalized lipids, which could act as the

precursor for S-bound n-C_{16}, are not reported by Volkman *et al.* (1992) to occur in microalgae of the class Eustigmatophyceae. On basis of the similar ^{13}C contents we, however, think that the S-bound n-C_{16}, n-C_{31} and n-C_{32} are related to each other.

The C_{37} and C_{38} n-alkanes of group III have similar and unique isotopic profiles [Fig. 15(d)], confirming the shared origin suggested by analysis of the concentration profiles. Their isotopic profiles do not display the oscillation observed between samples 2 and 6 for most of the other S-bound alkanes. The S-bound C_{37} and C_{38} n-alkanes probably derive from C_{37} and C_{38} unsaturated methyl and ethylketones (Sinninghe Damsté *et al.*, 1988; Schouten *et al.*, 1993b) which are biosynthesized by certain strains of prymnesiophytes (Volkman *et al.*, 1980b). However, in sample 1, the concentrations and ^{13}C contents of the compounds are not well correlated and a contribution from an additional source is likely [Fig. 13(c) and 15(d)].

Desulphurized asphaltene fraction

The compounds released upon desulphurization of the asphaltene fractions are for all samples similar to those obtained by desulphurization of the polar fractions. For example, isorenieratane (**V**) and the C_{33} diaryl isoprenoid (**VII**) are present in the lower and middle sediments but are absent in the top sediments. There is also an identical relative distribution of n-alkanes with predominance of short even-numbered n-alkanes. However, the relative intensities of classes of compounds vary when compared with the polar fractions. The regular sterane, dinosterane (**IV**) and 23,24-dimethylcholestane (**VI**) carbon skeletons are relatively more abundant than in the polar fractions.

The yield of hydrocarbons released upon desulphurization of the asphaltene fractions (average of 10 samples: 29 mg HC/g) is significantly smaller than that of the polar fractions (average of 10 samples: 86 mg HC/g). Moreover, the asphaltene fractions are significantly less abundant than the polar fraction (Table 1). Thus, the yields of hydrocarbons released from the asphaltene fractions upon desulphurization is inferior to those released from the polar fractions. The contribution of certain hydrocarbon skeletons released from the asphaltene fractions to the total amounts of compounds released upon desulphurization from both the asphaltene and polar fractions, is *ca* 8% for the three representative samples tested (1, 5 and 10; Table 2).

The limited amount of hydrocarbons released upon desulphurization of the asphaltene fractions, and the strong resemblance in the distributions of the hydrocarbons released from the asphaltenes with those released from the polar fractions, indicate that the biomarkers released from the asphaltene fractions do not contribute to a better understanding of the nature and changes of the palaeoenvironments reflected by these Vena del Gesso sediments. They will, therefore, not be discussed any further.

Free hydrocarbon fraction

Mass chromatograms of m/z 57 of the free hydrocarbons of three representative samples (samples 1, 6, 10) exemplify the relative variations between the various samples (Fig. 16). n-Alkanes, phytane, C_{20} (**XV**) and C_{21} (**XVI**) HBI alkanes, 2,6,10,15,19-pentamethylicosane (PME; **XVII**), fernene (**XVIII**), 17β,21β(H)-homohopane and 2,6,10,14,19,23,-27,31-octamethyldotriacontane (lycopane; **XIX**) are indicated as these are the compounds quantified (Fig. 17).

n-Alkanes. All samples are dominated by n-alkanes that exhibit a strong odd-over-even carbon number predominance with a maximum at n-C_{31} (Fig. 16). Their distributions, very different from those observed for the S-bound n-alkanes, suggest that these compounds are mainly derived from vascular plants (Eglinton *et al.*, 1962). The presence of fossils of leaves in the sediments also suggests some contribution from land plants. The concentrations of certain long-chain n-alkanes plotted vs depth are shown in Fig. 17(a). The scattered but generally decreasing concentration of long-chain odd n-alkanes from the bottom to the top of the marl bed suggests a progressive decrease of the contribution of vascular plant debris to the basin. There is a clear contrast between the concentrations of odd long-chain n-alkanes and even long-chain n-alkanes but their concentrations co-vary, indicating a common source. The δ values of n-C_{29} and n-C_{31} differ by less than 0.6‰ and their mean, which is nearly constant throughout the marl bed (Fig. 18), is consistent with a derivation from terrigenous C_3 plants (Popp *et al.*, 1989). The ^{13}C contents of C_{23}–C_{32} n-alkanes do not differ strongly from those of n-C_{29} and n-C_{31} (Fig. 18), and, together with similarities in concentration profiles, suggest a similar derivation from continental sources.

The concentration profile of heptadecane [n-C_{17}, Fig. 17(b)] is rather unique, possibly indicating that heptadecane derives at least partly from specific sources. Moreover, as shown in Fig. 18, δ values of free n-C_{17} range widely, from -36.3 ± 0.4‰ in sample 1 to -24.6 ± 0.1‰ in sample 7. Multiple sources are indicated. Purple sulphur bacteria, such as Chromatium, produce n-C_{17} as their most abundant hydrocarbon (Jones and Young, 1970). Values of δ reported for their biomass in natural populations range from -36 to -26‰ (Schidlowski *et al.*, 1984). Since the associated lipids will have more negative δ values (Wong *et al.*, 1975), the -36‰ hydrocarbons found here suggest biomass δ values near the middle of the natural range. Since such anaerobic phototrophs live just below the chemocline in natural environments, it is likely that the depletion of ^{13}C reflects both use of ^{13}C-depleted dissolved inorganic carbon and the presence of high concentrations of

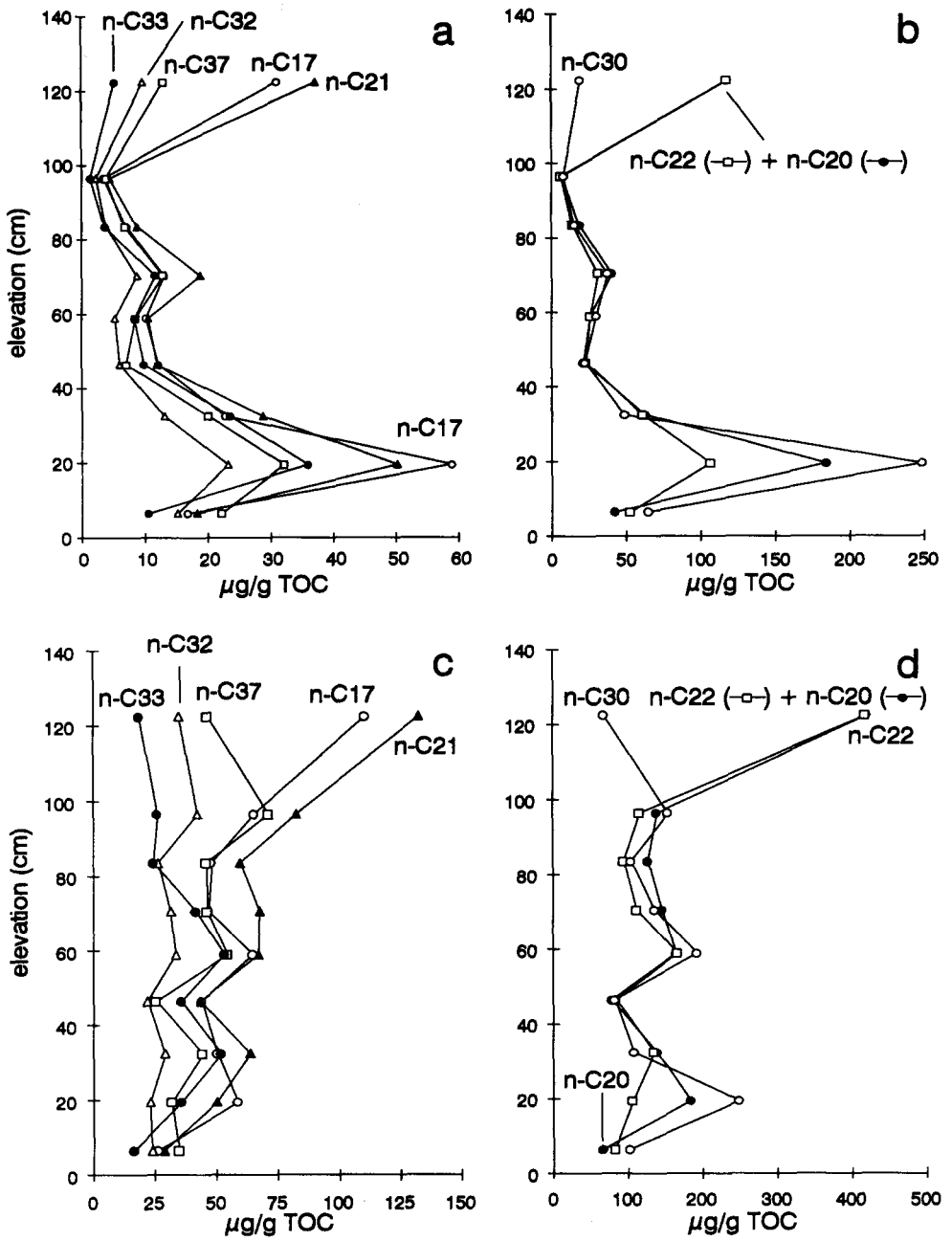

Fig. 12. Concentration profiles of *n*-alkanes released upon desulphurization of the polar fraction: *n*-C_{17}, *n*-C_{21}, *n*-C_{32}, C_{33} and *n*-C_{37} (a), *n*-C_{20}, *n*-C_{22} and *n*-C_{30} (b). Concentration profiles, corrected for the extent of sulphurization, for *n*-C_{17}, *n*-C_{21}, *n*-C_{32}, C_{33} and *n*-C_{37} (c), *n*-C_{20}, *n*-C_{22} and *n*-C_{30} (d). Corrections for the extent of sulphurization of organic matter were made by dividing the total hydrocarbon yield upon desulphurization of each sample by that of sample 2 (maximum yield) and correcting the concentrations by dividing them by the factor obtained.

dissolved CO_2 (*cf.* Freeman *et al.*, 1994). At the top of the marl bed, the free *n*-C_{17} is more enriched in ^{13}C. Values of δ approach those of the cholestanes and pentakishomohopane and are consistent with an origin from algae or cyanobacteria.

The concentration profiles of the other C_{16}–C_{22} *n*-alkanes also display diverse concentration profiles suggesting contributions from multiple sources [Fig. 17(b)]. Values of δ for these *n*-alkanes are also variable. That of *n*-C_{21}, for example, varies from $-23.6 \pm 0.2‰$ in sample 7 to $-29.4 \pm 0.2‰$ in sample 9, suggesting significant changes in the mixture

of sources for this compound. However, the diversity of potential sources, i.e. cyanobacteria (Parker *et al.*, 1967; Han and Calvin, 1969; Winters *et al.*, 1969; Gelpi *et al.*, 1970), bacteria (Han *et al.*, 1968, 1969; Collister *et al.*, 1994) and eukaryotic algae (Clark and Blumer, 1967; Gelpi *et al.*, 1970), the limited structural specificity, the mixtures indicated by the complexity of the concentration profiles and the variability of the δ values make the deconvolution of mixed sources difficult.

Acyclic isoprenoid hydrocarbons. 2,6,10,15,19-Pentamethyleicosane [PME; **XVII**, Fig. 17(d)], lycopane [**XIX**; Fig. 17(e)], and highly branched isoprenoids with 20 (**XV**) and 21 (**XVI**) carbon atoms [Fig. 17(f–g)] were only found as free hydrocarbons and not as sulphurized components. This indicates

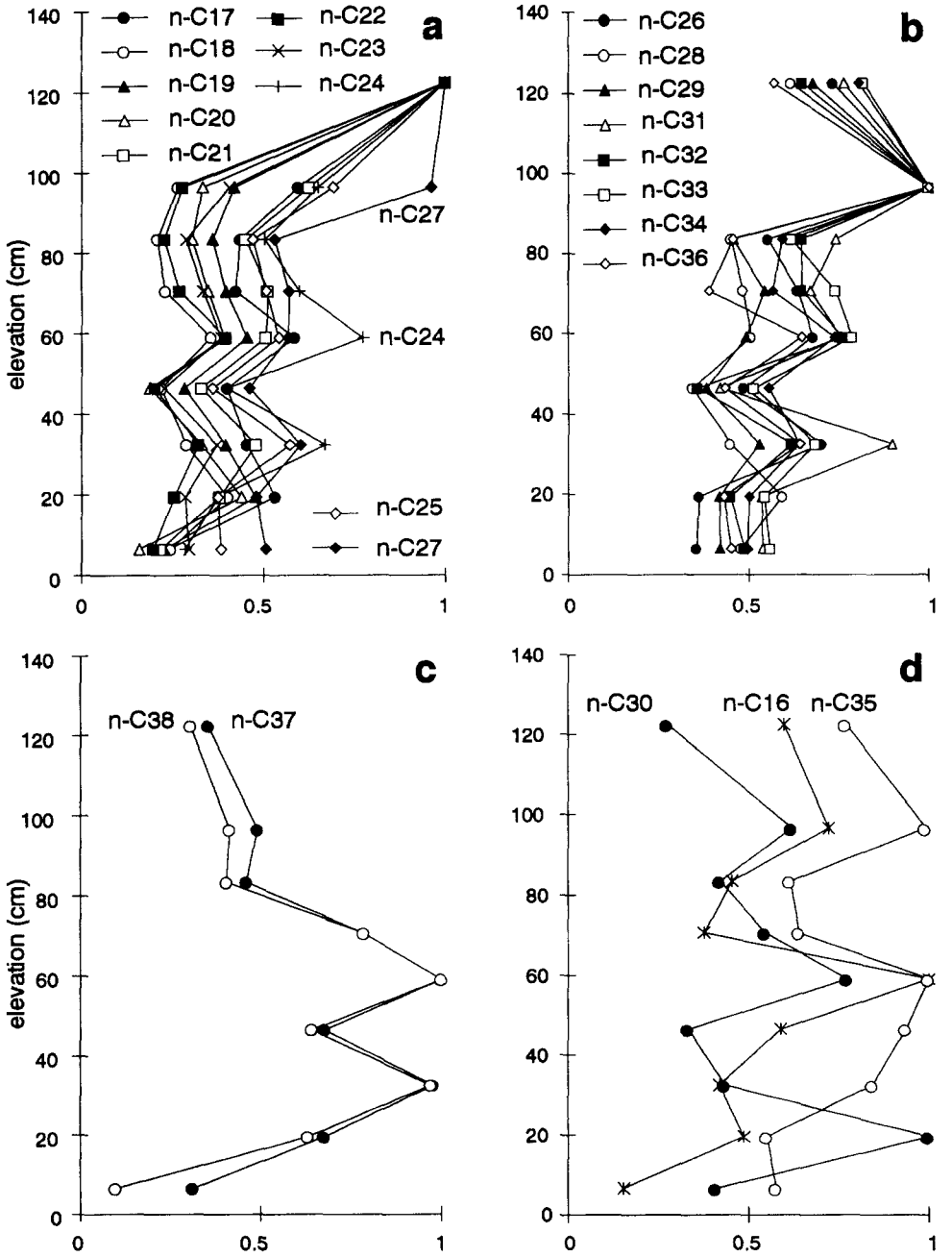

Fig. 13. Concentration profiles corrected for the extent of sulphurization and normalized to *n*-alkanes released upon desulphurization of the polar fraction. (a) Group 1, *n*-alkanes normalizing at sample 10, (b) group 2, *n*-alkanes normalizing at sample 8, (c) group 3, *n*-C_{37} and *n*-C_{38}, normalizing at sample 5, and (d) *n*-C_{16}, *n*-C_{30}, *n*-C_{35}.

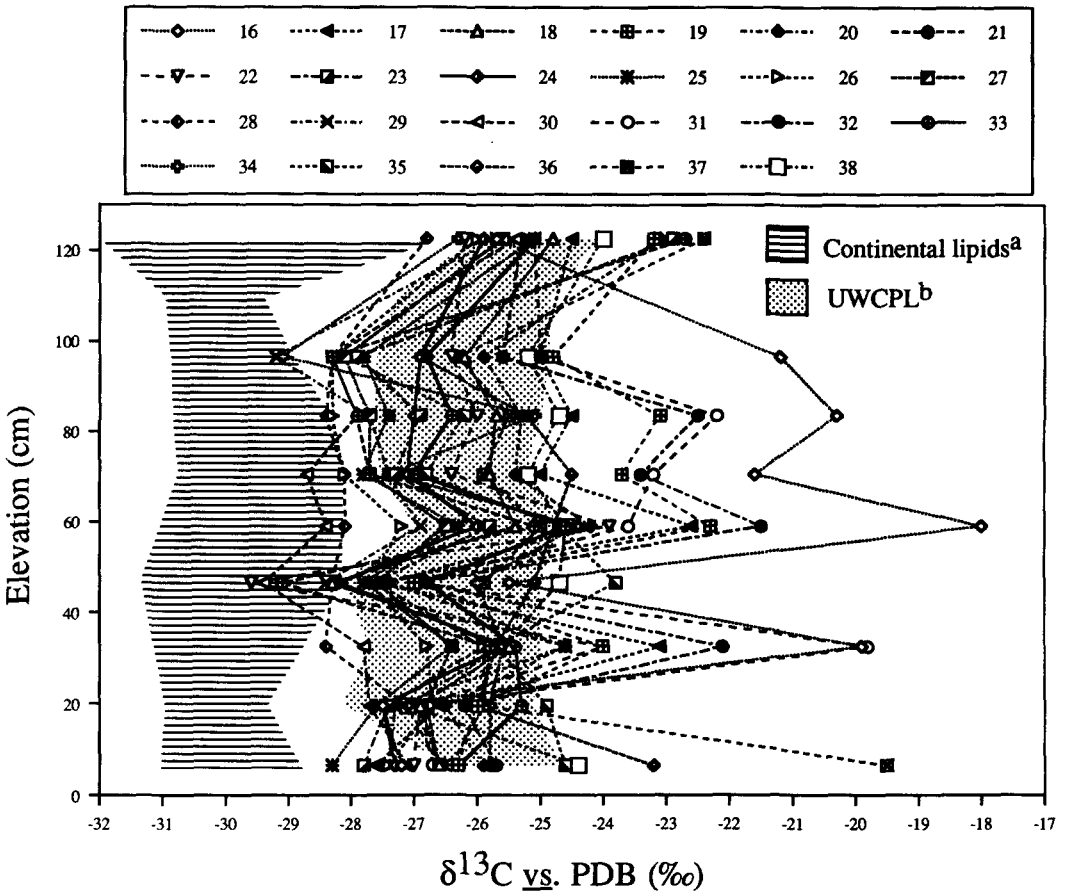

Fig. 14. δ vs PDB (‰) of all n-alkanes released upon desulphurization of the polar fractions plotted vs depth in the marl bed. [a]The striped area represents the range of continent derived lipids, free n-alkanes between C_{23} and C_{32} (see Figure 18). [b]The dashed area represents the upper water column primary producer lipids as defined by the total δ range of S-bound 5β-and 5α-cholestane and 17β,21β(H)-pentakishomohopane (**II**).

that the precursor biolipids lacked functional groups (Kohnen *et al.*, 1992a). In addition, free phytane was also encountered [Fig. 17(i)].

Lycopane is present in the upper eight samples of the marl bed [Fig. 17(e)]. In six of these, isotopic analyses were possible. Except in sample 10, where lycopane is relatively enriched in ^{13}C, the observed values of δ are similar to those of cholestanes (Fig. 18), supporting earlier suggestions that this compound derives from an algal source (Wakeham, 1990; McCaffrey *et al.*, 1991; Kohnen *et al.*, 1992a,b; Wakeham *et al.*, 1993; Freeman *et al.*, 1994).

As shown in Fig. 18, the δ values obtained for PME fall in the range associated here with primary producers, although sample 2, in which PME is significantly enriched in ^{13}C, is an exception. Kohnen *et al.* (1992a,b) and Freeman *et al.* (1994) suggested an algal origin for PME, an attribution consistent with the bulk of the present evidence. The higher δ value of PME in sample 2 falls within the range for archaebacterial biomarkers analysed in these sediments by Kohnen *et al.* (1992a,b). Production of PME has been reported in methanogenic and thermoacidophilic bacteria (Holzer *et al.*, 1979; Tornabene and Langworthy, 1979; Rissati *et al.*, 1984) and the compound has been considered as biomarker for methanogens (Brassell *et al.*, 1981). Hence, a contribution of PME from methanogenic bacteria may be considered for this particular sample.

The concentration profiles of the highly branched isoprenoid (HBI) alkane with 20 carbon atoms (2,6,10-trimethyl-7-(3-methylbutyl)dodecane; **XV**) and a compound tentatively identified as an HBI with 21 carbon atoms (3,7,11-trimethyl-6-(3-methylbutyl)tridecane; **XVI**) are both unique and congruent [Fig. 17(f–g)], indicating derivation from a distinct source. The C_{21} HBI alkane exhibits a similar mass spectrum to that of the compound tentatively identified by Kenig (1991) in Holocene sabkha sediments from Abu Dhabi. It is different from the C_{21} HBI alkane tentatively identified in Shark Bay (2,6,10-trimethyl-7-(3-methylpentyl)dodecane; **XX**) by Dunlop and Jefferies (1985), a compound also encountered in the Abu Dhabi sediments (Kenig *et al.*, 1990). Due to low concentrations, the ^{13}C content of

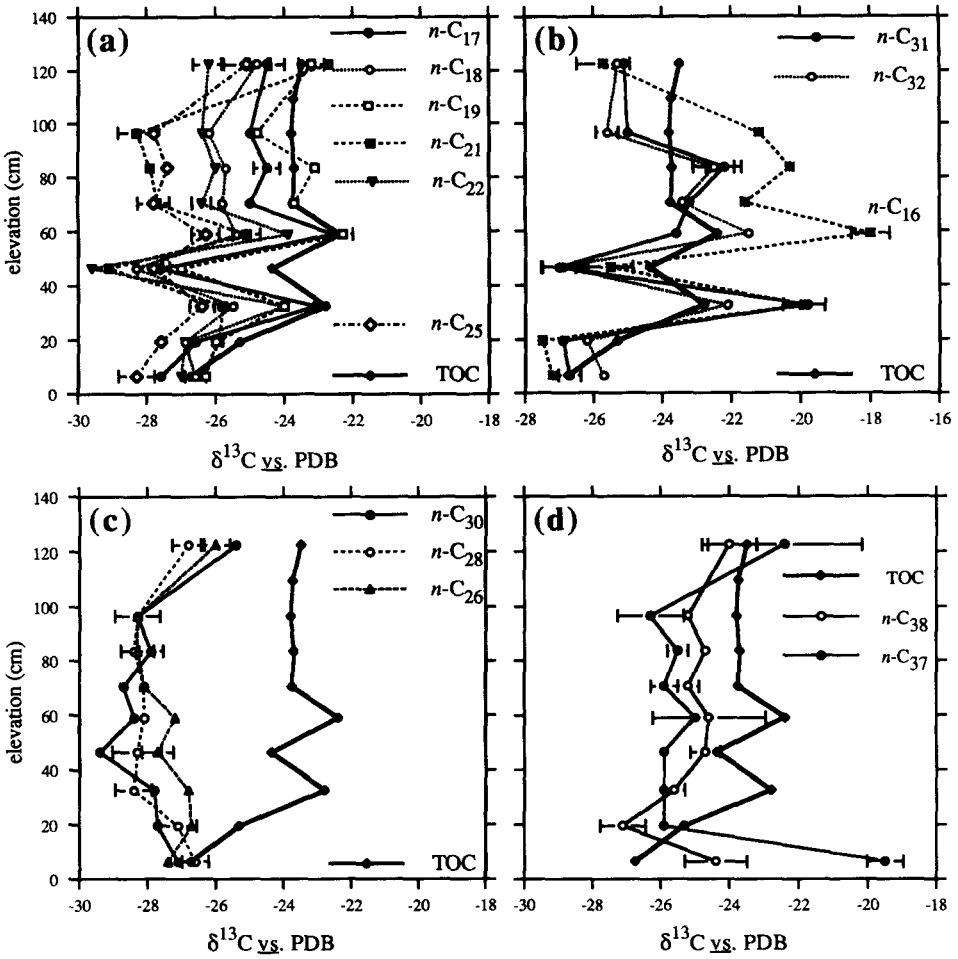

Fig. 15. δ vs PDB (‰) of *n*-alkanes released upon desulphurization of the polar fractions plotted vs depth in the marl bed: (a) *n*-C_{17}, *n*-C_{18}, *n*-C_{19}, *n*-C_{20} and *n*-C_{25}, (b) *n*-C_{16}, *n*-C_{30}, *n*-C_{31} and *n*-C_{32}, (c) *n*-C_{33} and *n*-C_{34} and (d) *n*-C_{37} and *n*-C_{38}.

the C_{20} compound could be measured reliably in only three samples and in only one of those could a δ value be obtained for the C_{21} compound (Fig. 18). In that sample (number 7, about 85 cm above the base of the section), the δ values of the C_{20} and C_{21} compounds differed by 1.3‰ (-17.9 ± 0.4 vs -19.2 ± 0.1‰). Assessed solely in terms of precision, this difference might appear significant. No other evidence indicates multiple sources for compounds with δ values near -18.5‰, however, and the unique distribution of these compounds within the section has already been noted. The isotopic difference is therefore best attributed to a precisely reproducible coelution. For the three samples in which it was analysed, the C_{20} HBI is the most ^{13}C-enriched compound apart from diagenetic products of isorenieratene. Kohnen *et al.* (1992b) observed that the HBI δ values in other Vena del Gesso marls were covariant with those of S-bound *n*-C_{31} and suggested an algal origin. Here, the S-bound, microalgal *n*-C_{16}, *n*-C_{31} and *n*-C_{32} are almost the only components that are unrelated to isorenieratene and nearly as enriched in ^{13}C as the HBIs.

Structural differences (at least for the C_{21} compound) notwithstanding, the C_{20} and C_{21} HBIs in at least one Holocene sediment (Abu Dhabi; Kenig and Hayes, unpublished results) are also enriched in ^{13}C relative to other lipids in the same facies. Free unsaturated and S-bound C_{25} HBIs are also enriched in ^{13}C relative to other lipids in recent sediments of the Black Sea and Cariaco Trench (-18 to -22‰; Freeman *et al.*, 1994) and Hamelin Pool, Western Australia (Summons *et al.*, 1993) and in Miocene sediments of the Monterey Formation (Schouten *et al.*, 1995a). The pervasive enrichment of HBIs biosynthesized by different types of organisms and of different structure must reflect association of the HBI biosynthetic pathway with either reduced photosynthetic fractionation of carbon isotopes or use of a carbon source (such as bicarbonate) enriched in ^{13}C.

The phytane depth profile is shown in Fig. 17(i). Considering the multiple origin possible for phytane it is not possible to assign specific sources for this compound. Its depth profile is different from that obtained for phytane released by desulphurization of

Table 2. Fraction of S-bound carbon skeletons bound in the asphaltene fraction*

Carbon skeleton	IV1-1 (%)	IV1-5 (%)	IV1-10 (%)
n-C18	3.7	3.7	3.9
2,6,10,14-Tetramethylhexadecane	4.0	3.5	3.4
n-C19	6.2	5.6	6.0
n-C20	5.4	6.2	5.7
n-C21	7.0	6.1	6.5
2,6,10,14-Tetramethyl-7-(3-methylbutyl)pentadecane (**I**)	n.a.†	2.2	n.a.†
n-C22	5.9	5.6	5.4
n-C23	13	6.7	7.9
n-C24	9.9	7.4	7.8
n-C25	11	11	9.7
n-C26	20	11	12
5β-Cholestane	6.0	6.8	7.5
5α-Cholestane	6.4	7.8	9.2
5β-24-Methylcholestane	6.7	11	9.1
5α-24-Methylcholestane	7.4	12	12
23,24-Dimethylcholest-22-ene	10	11	n.d.‡
5α-23,24-Dimethylcholestane(VI)	6.1	7.8	11
5β-24-Ethylcholestane	7.0	6.8	7.2
5α-24-Ethylcholestane	7.8	7.8	11
4,23,24-Trimethylcholest-22-ene	7.4	8.7	10
5α-4,23,24-Trimethylcholestane (**IV**)	6.9	8.3	9.8
5α-4-Methyl-24-ethylcholestane	7.6	9.5	9.2
Gammacerane (**III**)	8.5	9.7	n.a.†
17β,21β(H)-Pentakishomohopane (**II**)	4.4	4.0	2.7
Isorenieratane (**V**)	4.9	4.1	n.a.†

*Determined from absolute amounts released upon desulphurization of polar and asphaltene fractions.
†Not applicable.
‡Non determined.

the polar fraction [Fig. 6(c)], suggesting different origins. As shown in Fig. 18, the δ values of free phytane range between -32.7 and -31.2‰ and are distinctly lower than the range associated with primary lipids (dotted area). The free phytane is, therefore, apparently not derived from phytol; its origin in these sediments remains unclear.

Triterpanes. The concentration profile of fernene (**XVIII**), a higher plant marker, shows a scattered though generally decreasing trend from the bottom to the top of the marl bed [Fig. 17(h)]. This general trend is similar to that of the odd long-chain *n*-alkanes such as *n*-C_{31} [Fig. 17(a)] and confirms the progressive decrease in contributions of vascular plant debris to the basin.

The concentration profile of 17β,21β(H)-homohopane [Fig. 17(c)] is similar to that of PME, suggesting a similar source. This could not be confirmed by comparison of their δ values since these were not available for 17β,21β(H)-homohopane.

Thiophene fraction

The FID traces of the thiophene fractions (Fig. 2; fraction A2) of three representative samples (samples 1, 4 and 10) exemplify the relative variations between these samples (Fig. 19). The thiophene fractions are dominated by hop-17(21)-ene with the exception of sample 4 [Fig. 19(b)] where cholest-4-ene is the major component. Other sterenes also contribute significantly to this fraction of sample 4. Identifications of the steroid and hopanoid hydrocarbons are indicated in a partial FID trace of sample 4 (Fig. 20) and in Table 3. Isoprenoid and *n*-alkyl thiophenes represent most of the peaks eluting in the first part of the FID trace (Fig. 19). Their distributions and concentrations vary significantly and the results concerning these compounds are discussed in Kenig *et al.* (1995).

Sterenes, diasterenes and aromatic steroids. The covariation of the concentration of Δ^4-, Δ^5- and diasterenes as indicated for the cholestenes [Fig. 21(a)], the 24-methylcholestenes [Fig. 21(b)] and 20*R*-diacholestenes [Fig. 21(c)] is striking and clearly indicates that these compounds are diagenetically related and originate from their precursors, Δ^5-sterols (de Leeuw *et al.*, 1989). It is, however, noteworthy that the Δ^4- and Δ^5-cholestadienes have almost identical concentrations in most samples and that this is not the case for the 24-methylcholestenes. This may indicate that these early diagenetic conversions are substrate specific, pointing to enzymatically induced transformations. The concentration profile of a component tentatively identified from its mass spectrum as 23,24-dimethylcholestadiene (compound 10 in Fig. 20) has a similar concentration profile [Fig. 21(d)] as those of the sterenes.

Because of their low concentrations and coelution with other compounds it was not possible to determine the absolute concentrations of ring B-aromatic anthrasteroids. Mass chromatograms of *m/z* 211 (Hussler and Albrecht, 1983) revealed, however, that their carbon number distributions vary significantly along the marl bed and that their distributions followed those of the other steroids.

The covariance of sterenes, diasterenes, 23,24-dimethylcholestadiene and the anthrasteroids clearly suggest that the total algal populations varied considerably in the depositional environments reflected by this sediment sequence. However, the abundances of these steroids are one order of

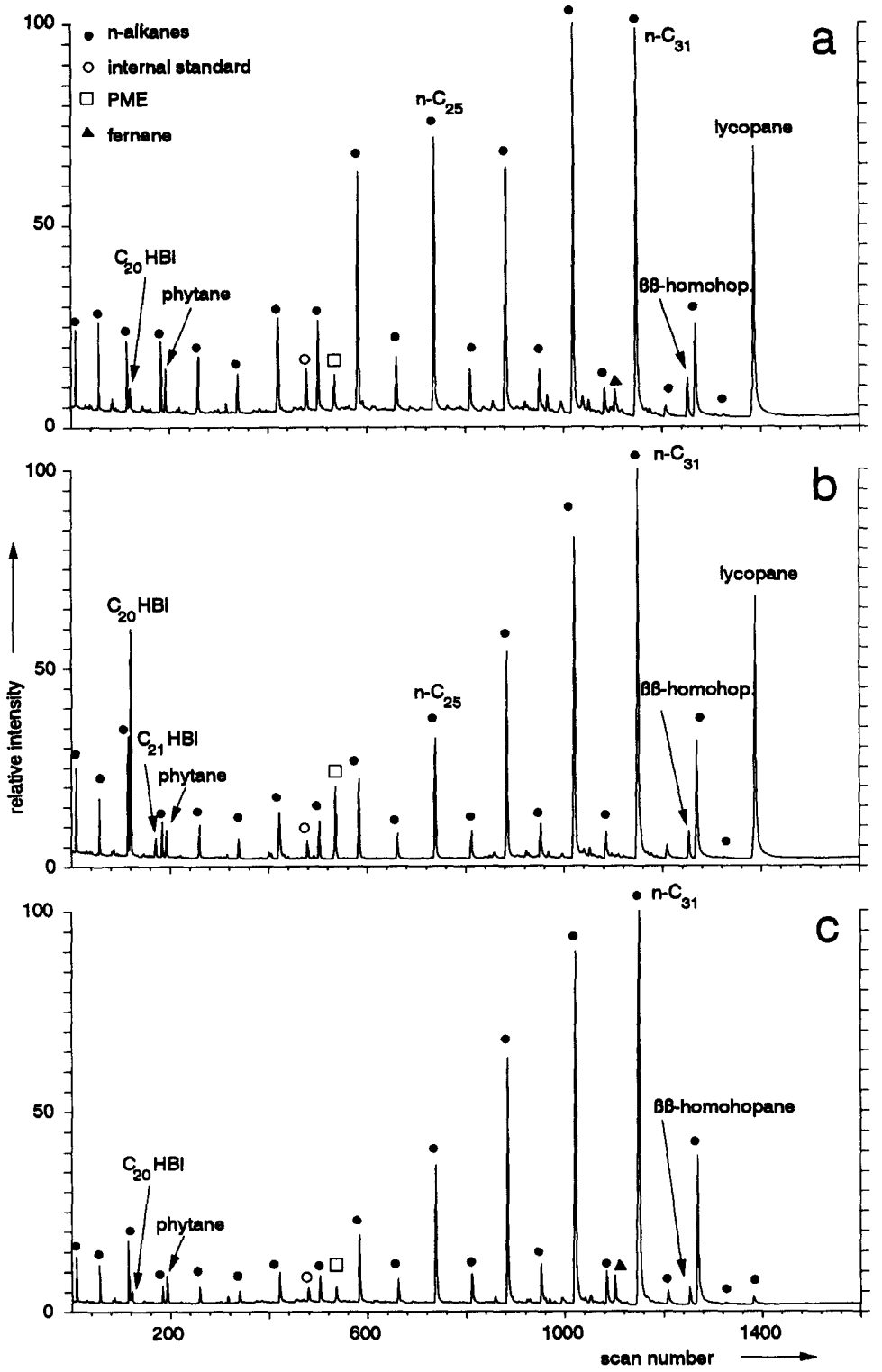

Fig. 16. Mass chromatograms of *m/z* 57 of the hydrocarbon fractions of sample 10 (a), sample 6 (b) and sample 1 (c).

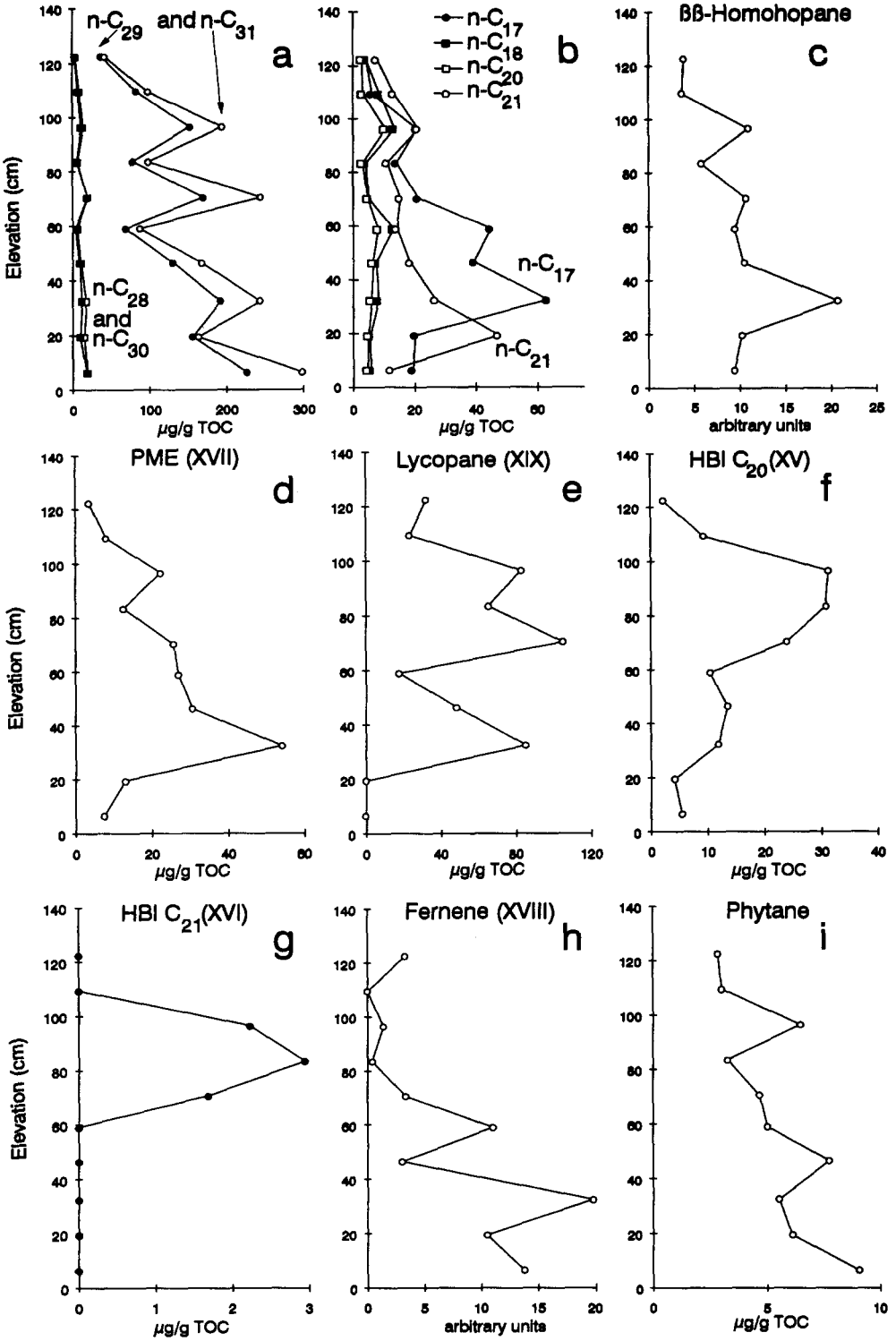

Fig. 17. Depth profiles of concentration of compounds in the hydrocarbon fractions. (a) Octacosane (n-C_{28}), nonacosane (n-C_{29}), triacontane (n-C_{30}) and hentriacontane (n-C_{31}), (b) heptadecane (n-C_{17}), octadecane (n-C_{18}), nonadecane (n-C_{19}), icosane (n-C_{20}) and henicosane (n-C_{21}), (c) 17β,21β(H)-homohopane, (d) PME (**XVII**), (e) 2,6,14,19,23,27,31-octamethyldotriacontane (lycopane; **XIX**), (f) 2,6,10-trimethyl-7-(3-methylbutyl)dodecane (C_{20} HBI; **XV**), (g) 3,7,11-trimethyl-6-(3-methylbutyl)-tridecane (C_{21} HBI; **XVI**), (h) fernene (**XVIII**), (i) 2,6,10,14-tetramethylhexadecane (phytane).

magnitude less than those of their S-bound counterparts so that the degree of sulphurization of Δ^5-sterols or their derivatives might be the major factor determining the intensities of the free steroids. In this respect, it is noteworthy that the concentrations of the free steroids are minimal in sample 2 whereas the S-bound steroids exhibit the highest concentrations in this sample [cf. Figure 6(e–g) and Figure 21(a–d)]. Relatively small differences in the ^{13}C contents of the free and S-bound steroids possibly due to kinetic isotope effects during sulphurization (Schouten *et al.*, 1995b) support this explanation for the variability of the concentration profiles of the free steroids.

Hopanoids. The concentration profiles of hop-17(21)-ene [Fig. 21(e)], 3-methylhop-17(21)-ene [Fig. 21(f)] and of the 30-(2′-methylenethienyl)-17β,21β(H)-hopane (C_{35} hopanoid thiophene **XXI**; Valisolalao *et al.*, 1984) exhibit dissimilar trends. The isotope value obtained for the desulphurized C_{35} hopanoid thiophene in sample 5 ($\delta^{13}C = -26.3 \pm 0.2$‰) is the same as reported for this component in another study of the Gessoso-solfifera Formation (Kohnen *et al.*, 1992b). These authors interpreted it as indicative of heterotrophic bacteria but because the δ value is similar to that of the C_{35} hopane released upon desulphurization of the polar fraction a cyanobacterial origin is assumed.

Based on its low ^{13}C content, 3-methylhopane in Green River shales was ascribed to an origin from methanotrophic bacteria (Collister *et al.*, 1992). The ^{13}C content obtained for 3-methylhopene in sample 5 ($\delta^{13}C = -24.3 \pm 0.2$‰) does, however, not support such an origin. Hop-17(21)-ene can derive from various prokaryotic sources. Its stable carbon isotope value, also obtained in sample 5 ($\delta^{13}C = -22.9 \pm 0.2$‰), could support heterotrophic bacteria as a potential source as it is enriched in ^{13}C relative to the primary algal photosynthate (Fig. 5). The differences in their concentration profiles and isotope contents imply that these three hopanoids are not derived from one common source.

Diaryl isoprenoid hydrocarbons and related compounds. No isorenieratane (**V**), nor its C_{33} (**VII**) and C_{32} (**IX**) diaryl isoprenoid pseudo-homologues are present in the thiophene fraction. The components reflected in the mass chromatogram of *m/z* 133, diagnostic for alkyltetramethylbenzenes, represent another family of diagenetic products of isorenieratene. Their molecular ions (M^+) are always 4 atomic mass units less than those of their diaryl isoprenoid counterparts despite two successive hydrogenations. These components are thought to result from cyclisation of isorenieratene and isorenieratene-derived C_{32} and C_{33} "carotenoids". The detailed structures and distributions of these compounds are described in

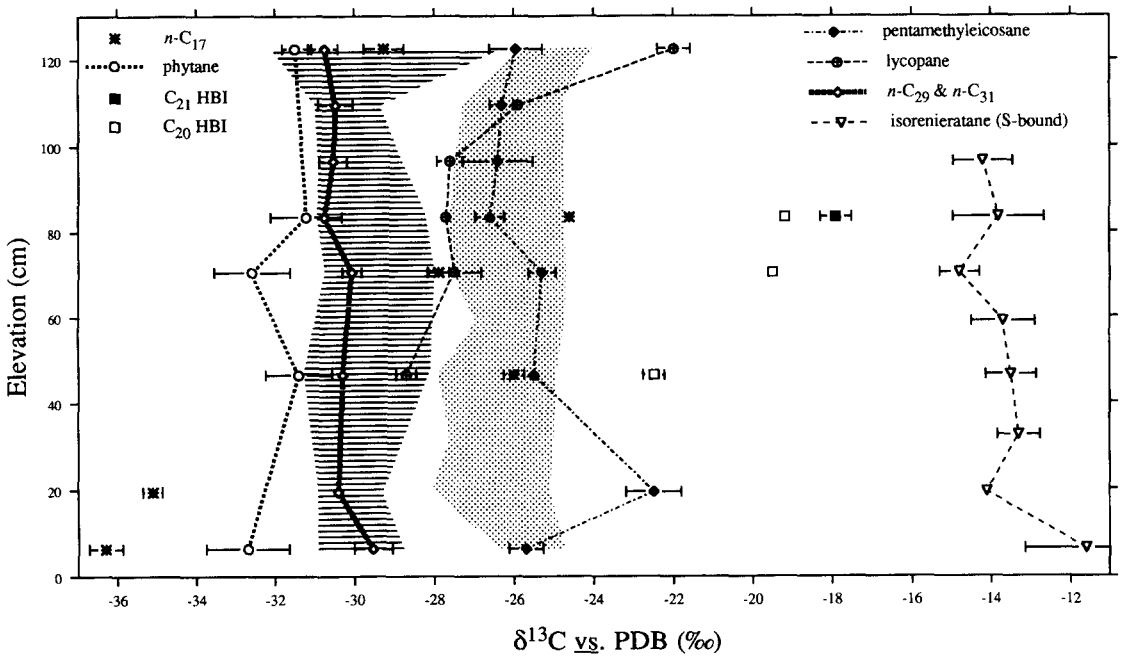

Fig. 18. δ vs PBD (‰) of free hydrocarbons, *n*-heptadecane (*n*-C_{17}), 2,6,10,14-tetramethylhexadecane (phytane), the average of δ values of *n*-nonacosane (*n*-C_{29}) and *n*-heneitriacontane (*n*-C_{31}), C_{20} (**XV**) and C_{21} (**XVI**) highly branched isoprenoids, 2,6,10,15,19-pentamethyleicosane (PME, **XVII**), 2,6,10,14,19,23,27,31-octamethyldotriacontane (lycopane, **XIX**) and corresponding standard deviations plotted vs depth in the marl bed. The striped area represents the range of δ values of free *n*-alkanes between C_{23} and C_{32}. The dashed area represents the δ values of upper water column primary producer lipids as defined by the total range of δ values of S-bound 5β-and 5α-cholestane and 17β,21β(H)-pentakishomohopane (**II**) (see Fig. 5). δ values of S-bound isorenieratane (**V**) are plotted for comparison.

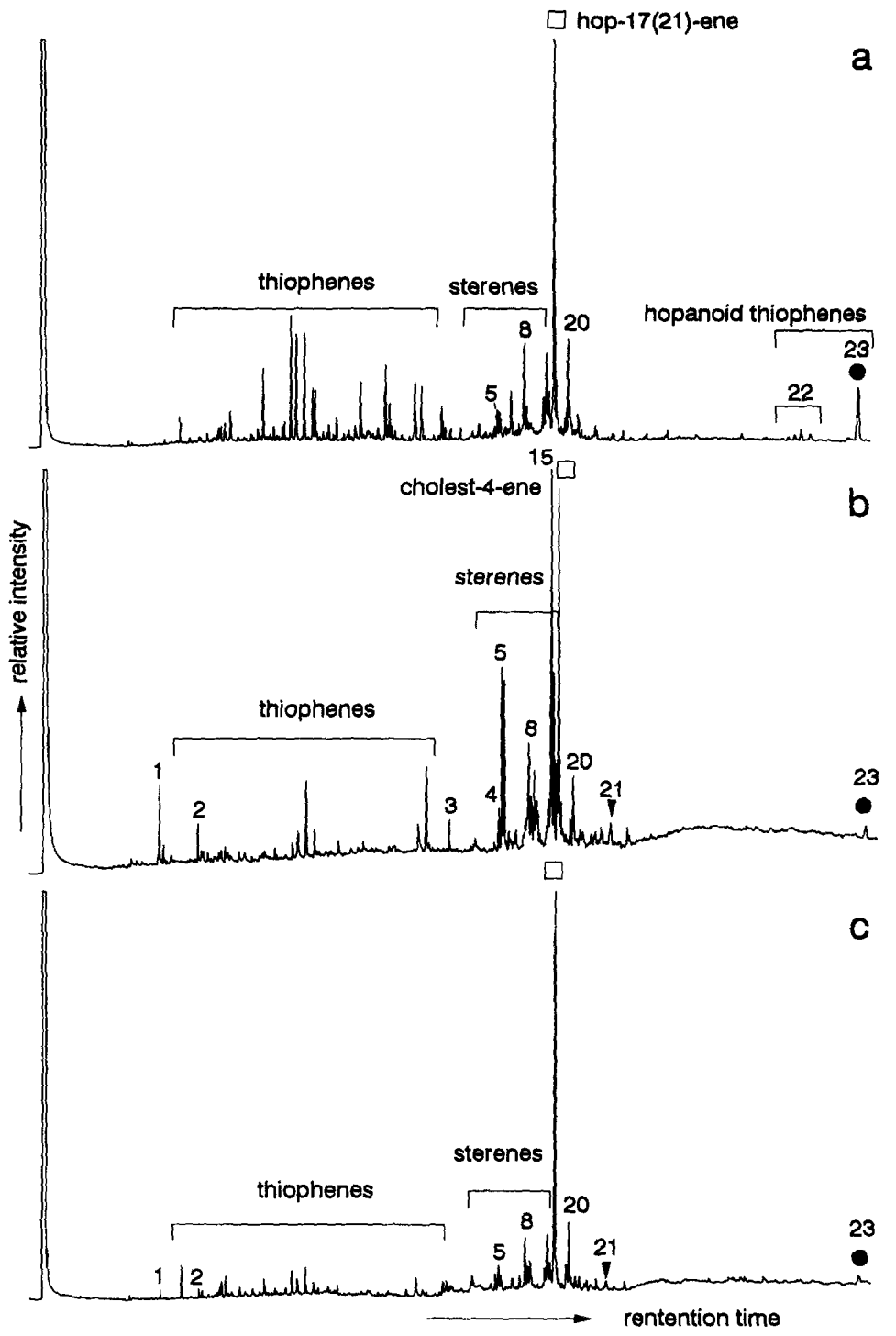

Fig. 19. FID chromatograms of the thiophene fraction of sample 10 (a), sample 4 (b) and sample 1 (c). Numbered compounds are listed in Table 3.

Koopmans *et al.* (1995a). The stable carbon isotope value measured for the C_{33} component (**XXII**) in sample 5 ($\delta^{13}C = -15.2 \pm 0.2‰$) confirms its relationship to isorenieratene (**VIII**) and its derivatives.

The concentration depth profile of the C_{33} diaryl isoprenoid (**XXII**) with an additional ring [Fig. 21(h)] has a common feature with those of isorenieratane and the C_{33} diaryl isoprenoid [Fig. 5(a–b)] in that these compounds are all absent in samples

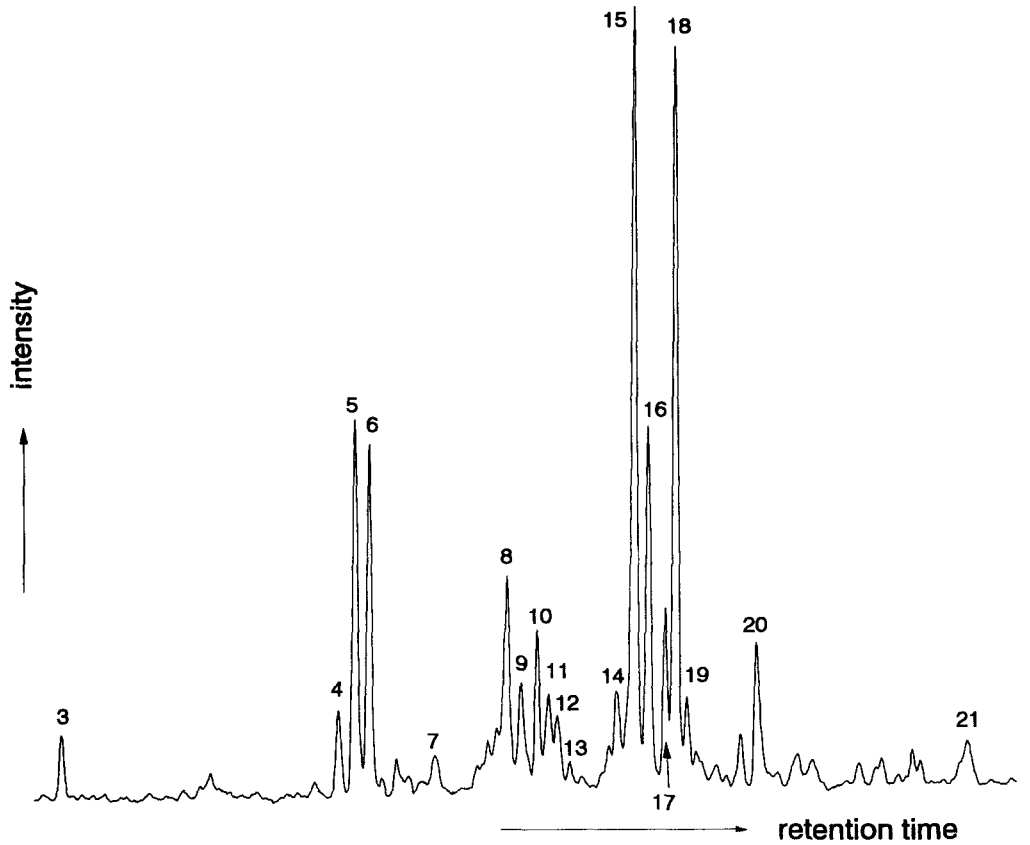

Fig. 20. Partial FID chromatograms of the thiophene fraction of sample 4 [Fig. 19(b)]. The compounds reflected by the numbered peaks are listed in Table 3.

9 and 10. Otherwise, the profiles are quite different with maxima at samples 3 and 5 for the C_{33} diaryl isoprenoid with an additional ring. These differences will be discussed later (see *Sources versus diagenetic effects* section).

Chromans. Only 2,5,7,8-tetramethyl-2-(4,8,12-trimethyltridecyl)chroman (5,7,8 - triMe - MTTC; **XXIII**; Sinninghe Damsté *et al.*, 1987) has been encountered in these sediments (Fig. 20, Table 3). The absence of other chromans suggests that the

Table 3. Compounds present in the thiophene fractions

Peak number	Identification
1	2,3,6,3′-Tetramethylbiphenyl
2	2-Isopropyl-5,2′,3′,6′-tetramethylbiphenyl
3	20*R* diacholestene
4	20*R* 24-ethyldiacholestene
5	Cholest-4-ene
6	Cholest-5-ene
7	2,5,7,8-Tetramethyl-2-(4,8,12-trimethyltridecyl)chroman(**XXIII**)
8	24-Methylcholest-4-ene
9	24-Methylcholeste-5-ene
10	4-Desmethyldinosteradiene
11	4-Desmethyldinosteradiene
12	24-Ethylcholesta-5,22-diene
13	24-Ethylcholestadience
14	Norhop-17(21)-ene
15	24-Ethylcholest-4-ene
16	24-Ethylcholest-5-ene
17	Dinosteradiene
18	Hop-17(21)-ene
19	3-Methylhop-17(21)-ene
20	Neogammacer-22(29)-ene
21	C_{33} Diaryl-isoprenoid with an additional ring (**XXII**)
22	Unsaturated hopanoid thiophenes
23	30-(2′-Methylenethienyl)-17β,21β(H)hopane (**XXI**)

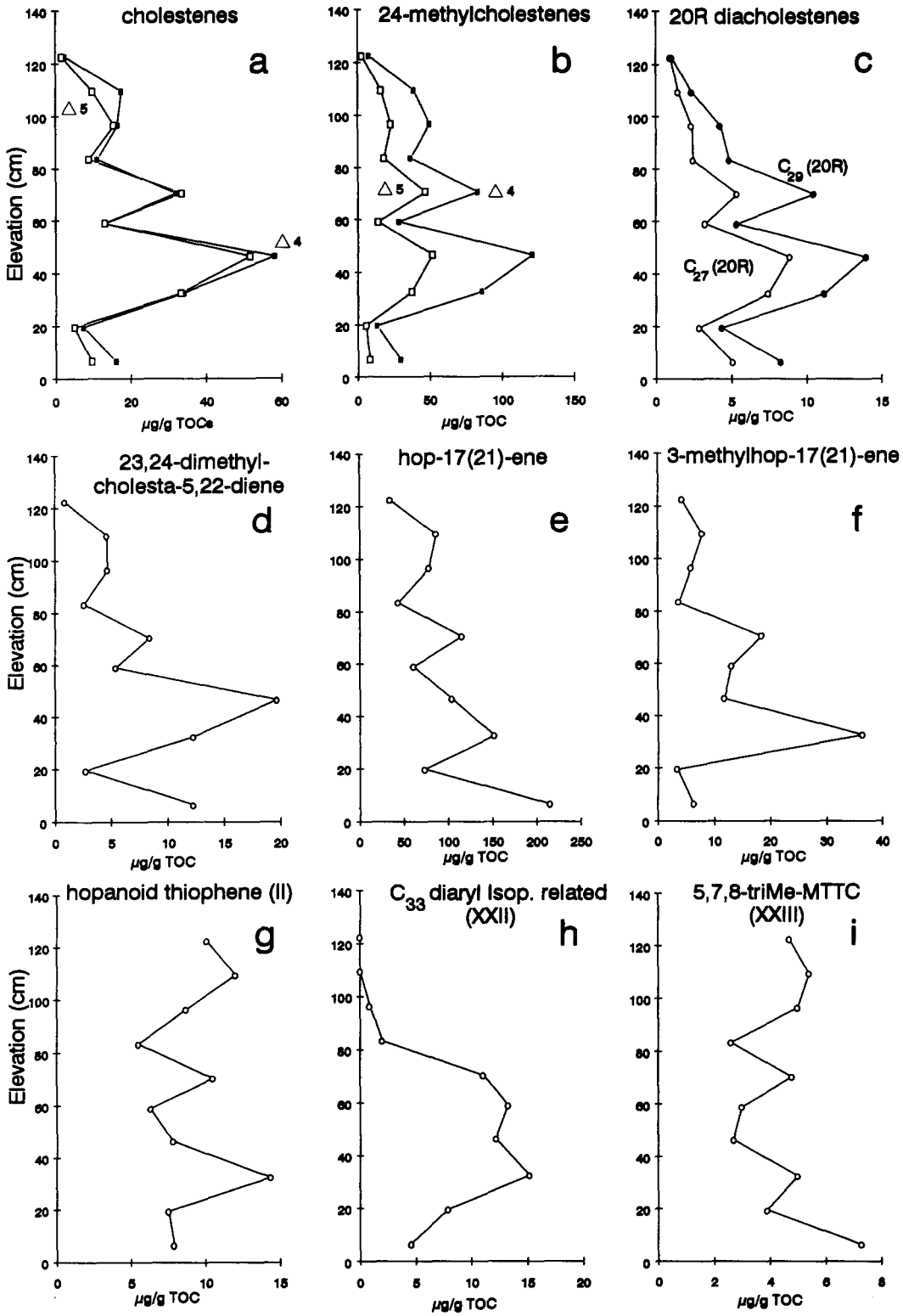

Fig. 21. Depth profiles of concentration of hydrocarbon components of the thiophene fraction (A2). (a) Cholest-4-ene (Δ^4) and cholest-5-ene (Δ^5), (b) 24-methylcholest-4-ene (Δ^4) and 24-methylcholest-5-ene (Δ^5), (c) 20*R*-diacholestene and 20*R*-24-ethyl-diacholestene, (d) 23,24-dimethylcholest-5,22-diene, (e) hop-17(21)-ene, (f) 3-methylhop-17(21)-ene, (g) 30-(2′-methylenethienyl)-17α,21β(H)hopane (C_{35} hopanoid thiophene; **XXI**), (h) C_{33} diaryl isoprenoid with an additional ring (**XXII**) and (i) 5,7,8-tetramethyl-2-(4,8,12-trimethytridecyl)chroman (**XXIII**).

photic zone of the water column was not hypersaline (Sinninghe Damsté *et al.*, 1987, 1993b). The exact origin of 5,7,8-triMe-MTTC is not clear. The stable carbon isotope value obtained for this compound in sample 5 ($\delta^{13}C = -26.3 \pm 0.2‰$), similar to that of S-bound regular steranes (Fig. 5), is consistent with an upper water column photoautotrophic organism as a source.

Sources versus diagenetic effects

The results, presented above, show variations in the concentrations of compounds with two modes of occurrence: compounds present as such in the saturated hydrocarbon and alkylthiophene fractions and macromolecularly S-bound compounds in the polar and the asphaltene fractions. For palaeoenvironmental reconstruction purposes, these differences in occurrence should be taken into account because free hydrocarbons and S-bound lipids, including the thiophenes, have been shown to originate from different sources (Kohnen *et al.*, 1992a,b and results presented here), since only the compounds with functional groups can react with reduced inorganic sulphur species (Kohnen *et al.*, 1992a,b). The concentrations of the free hydrocarbons can be considered as a measure for the abundance of the organisms by which they were produced, if it is assumed that they were degraded to the same extent. However, the formation of organic S-bound compounds requires the presence of reduced sulphur species (H_2S, HS_X^-, S°; for a review Sinninghe Damsté and de Leeuw, 1990). The degree of sulphurization is dependent on many factors such as the presence of iron, the activity of sulphate reducing bacteria, the sulphate concentration gradient in the upper sediments, etc. Presently, it is, however, not precisely known what environmental conditions determine the degree of sulphurization of organic compounds.

Sulphur-bound biomarkers released from the polar fraction are quantitatively much more important than alkylated thiophenes [0.5–7.3 mg/g C for polar fraction [Fig. 22(a)] vs 0.04–0.16 mg/g C for alkylthiophenes (Kenig *et al.*, 1995)] and are also much more important than biomarkers released from the asphaltene fraction. Comparison with the amounts of biomarkers released by desulphurization of the kerogens isolated from the same samples (Schaeffer *et al.*, 1995) indicates that the yields of hydrocarbons released from the kerogens (3–18 mg/g C) is within the same order of magnitude as the yields from the polar fractions. These data reveal that the polar fraction contains a significant part of the organically bound sulphur indicating that the concentration profiles of summed released compounds [Fig. 22(a)] can be interpreted in a palaeoenvironmental context. The conditions for sulphurization of organic matter were optimal during deposition of sample 2, but were progressively less favourable towards the top of the bed, with the exception of sample 10. Two hypotheses can be considered to explain the variation in the degree of sulphurization of the organic matter. (i) An enhanced input of iron in the basin after deposition of sample 2 since it is thought that reduced sulphur species react more readily with iron than with organic matter (Gransch and Posthuma, 1974; Berner, 1984, 1985). (ii) The depth of the chemocline did vary extensively. Enhanced sulphurization is expected with a shallow chemocline, as organic compounds reach the anoxic zone, where reduced sulphur species are available for sulphurization, faster and are thus less susceptible to oxidative degradation. Since the amount of clay in the samples does not show a systematic increase up-section (Fig. 1; carbonate content does not decrease) and the terrestrial input actually decreases up-section [Fig. 17(a)] hypothesis (i) seems implausible.

The large differences in extent of sulphurization pose the question whether TOC-normalized concentrations of S-bound biomarkers should be used for palaeoenvironmental interpretations. These concentrations depend on three factors: (i) the amounts and nature of appropriate precursors, (ii) the extent of sulphurization of these precursors, and (iii) the contribution to TOC of material inert to sulphurization (e.g. saturated hydrocarbons, vitrinite). The input of non-reactive organic matter into the basin is difficult to monitor. We will assume here that it is constant, even though markers for non-reactive continent-derived organic matter, such as long-chain odd *n*-alkanes show a progressive decrease in absolute concentration towards the top of the bed. To determine changes in the assemblages of primary producers the amounts of biomarkers released from the polar fractions should be corrected for the extent of sulphurization, because sulphurization leads to selective preservation of compounds which otherwise should undergo severe biodegradations and transformations.

In an attempt to perform such a correction, the yields of desulphurization of each sample were normalized to that of the sample with maximum yield (sample 2). A selection of these corrected concentration profiles are shown in Fig. 22. For example, the corrected concentration profiles of isorenieratene-derived compounds [Fig. 22(b)] are quite different from the profiles shown earlier [Fig. 5(a–b)] and show maxima at samples 3 and 5. The corrected profile is more similar to that obtained for the free isorenieratene-derived C_{33} diaryl isoprenoid with an additional ring identified in fraction A2 [Fig. 21(h)]. The resemblance between the depth profile of the free hydrocarbon with those, after correction for sulphurization, of the S-bound isorenieratane derivatives, all derived from the same precursor, is a strong indication that our approach is valid. It is thus possible to discriminate the differences in sulphurization from variations in abundances of source organisms.

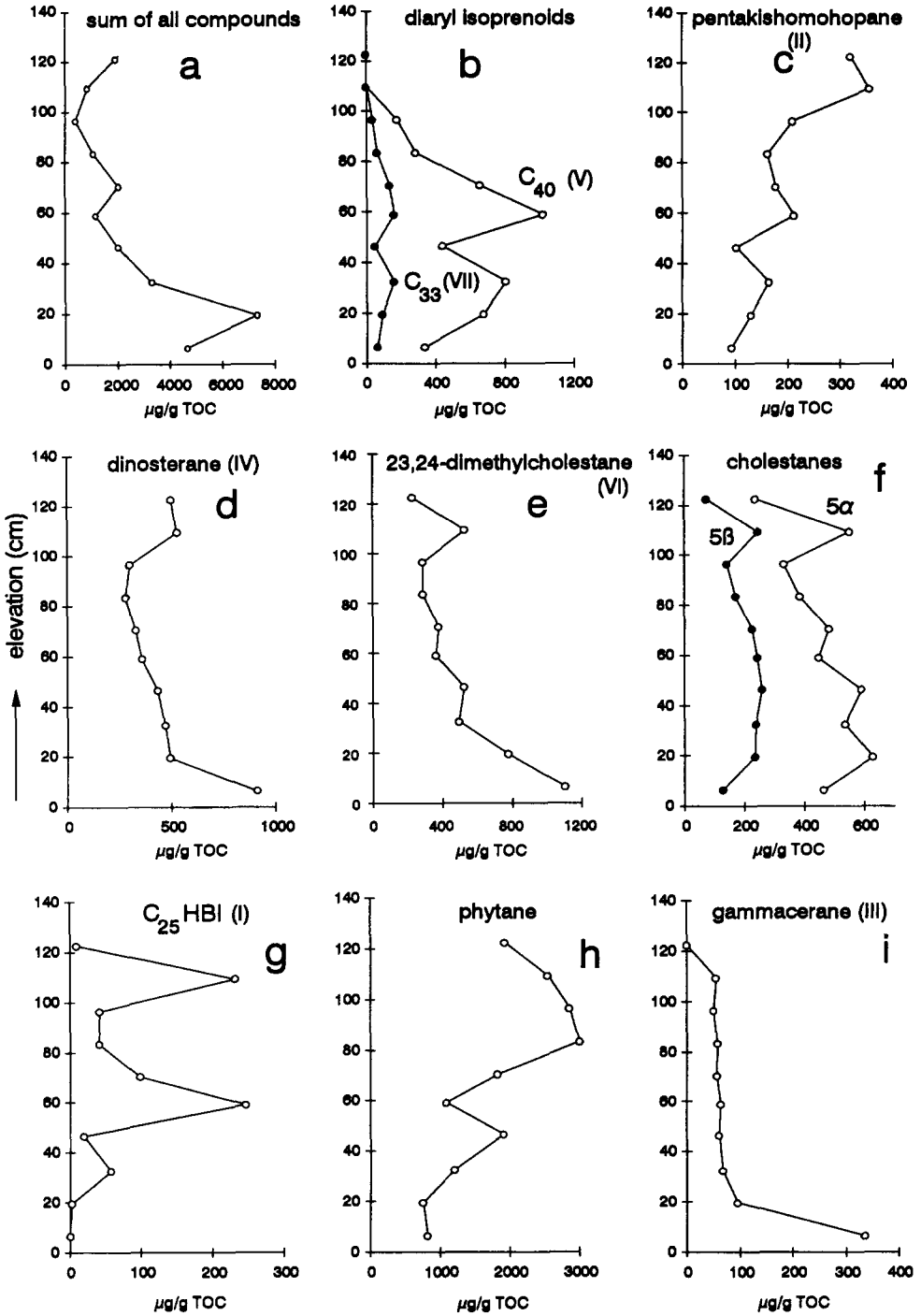

Fig. 22. (a) Summed concentrations of biomarkers released upon desulphurization of the polar fractions. Concentrations (corrected for the extent of sulphurization) of (b) isorenieratane (**V**) and C_{33} diaryl isoprenoid (**VII**), (c) 17β,21β(H)-pentakishomohopane (**II**), (d) dinosterane (**IV**) + dinosterene, (e) 23,24-dimethyl-5α-cholestane (VI) + 23,24-dimethylcholestene, (f) 5α-and 5β-cholestane, (g) C_{25} HBI alkane (**I**), (h) phytane and (i) gammacerane (**III**). Corrections for the extent of sulphurization of organic matter were made by using the data shown in (a): the yields of hydrocarbons released from the polar fractions of each sample were divided by that of sample 2.

PALAEOENVIRONMENTAL IMPLICATIONS

The significant changes in concentrations of biomarkers and the large range of their δ values observed reflects diversity. The interpretive problem is to reconstruct the particular types of palaeoenvironmental and biological diversity represented by these signals. How did conditions vary, and did differing habitats coexist or succeed each other? Which groups of organisms flourished in response to the environmental variations? The sources of organic matter will have included autochthonous primary producers and the full range of organisms involved in subsequent reworking of the primary inputs as well as allochthonous sources such as terrestrial plants. For all of these organisms, the isotopic compositions of biosynthetic products will depend on independently variable factors ranging from the isotopic composition of the carbon source to isotope effects associated with the assimilation of carbon and the assembly of carbon skeletons (Hayes, 1993).

Carbon sources and factors controlling isotopic fractionation

The nearly constant δ values observed for the free C_{29} and C_{31} *n*-alkanes (Fig. 5), presumably derived largely from terrigenous plant waxes, indicate that the isotopic composition of atmospheric CO_2, and thus of dissolved inorganic carbon in the open ocean, was essentially constant over the period of deposition. The evidence for isotopic constancy is not unexpected, since the time interval represented by the whole marl bed is probably less than 100 ka (Sinninghe Damsté *et al.*, 1995b) and the maximal rate of secular variation in the isotopic composition of marine carbonate during Messinian time was approximately 0.4‰/100 ka. More specifically, a shift of -0.8‰ in the δ value of marine carbonate occurred between approximately 6.3 and 6.1 Ma ago (the "magnetic-epoch-6 carbon shift"; Vincent *et al.*, 1980) and, apart from this, no secular trend in δ value is apparent during the Messinian. Deposition of the Cycle-IV beds may or may not have coincided with the Epoch-6 shift, so the expected total, bottom-to-top-of-section variation in the ^{13}C content of dissolved CO_2 in surface waters is between -0.4 and 0‰.

Aquatic products display varying degrees of isotopic variability. The S-bound *n*-alkanes with 16, 17, 19, 22, 31, and 32 carbon atoms have the widest range of δ values [Fig. 15(a–b)]. Values of δ for the cholestanes and hopanoids (Fig. 5) and S-bound *n*-alkanes with 26, 28, and 30 carbon atoms [Fig. 15(c)] are less variable. Apart from marked variations at the top and bottom of the cycle (which are discussed below), δ values of the C_{37} and C_{38} S-bound *n*-alkanes are nearly constant [Fig. 15(d)]. Such consistency is most logically interpreted in terms of a single producer not subjected to changes in any factors that would affect the isotopic composition of its biosynthetic products. These would include not only the concentration and isotopic composition of dissolved CO_2, but also availabilities of nutrients, which are important because variations can affect cellular carbon budgets and thus isotopic fractionation (Goericke *et al.*, 1994). The logical picture is one in which concentrations and isotopic compositions of CO_2 in surface waters, at or near equilibrium with the atmosphere and exchanging dissolved inorganic carbon and nutrients mainly with the ocean, were roughly constant, thus establishing the conditions indicated by the constant isotopic signals.

The varying isotopic signals must be linked to changes in the concentration and/or isotopic composition of dissolved CO_2, in nutrient levels, in the availability of electron donors and acceptors and in mixing of different, isotopically-distinct sources. Apart from the ^{13}C content of dissolved CO_2, which, as the ultimate carbon source, exerts a fundamental control, these factors will affect not only the isotopic fractionation accompanying fixation of carbon by autotrophs but also the identities and metabolic characteristics of the organisms comprising the community. The presence in all but the two uppermost samples of appreciable concentrations [Fig. 22(b)] of biomarkers characteristic of green sulphur bacteria (i.e. the diaryl isoprenoids) indicates not only that anaerobes flourished but even that—at least part of the time—the oxycline rose into the photic zone. Water columns in such environments often have significant gradients in concentrations of dissolved CO_2 (more abundant near depths where sulphate reducers as well as other respiring organisms have produced CO_2) and in δ (more negative wherever much of the dissolved inorganic carbon derives from oxidation of organic carbon) as well as in O_2 and HS^- (e.g. Freeman *et al.*, 1994). Moreover, balances among these factors can be affected sharply by variations in the depth of the oxycline. Extension of the logical picture, therefore, places the origin of the more highly variable isotopic signals in deeper waters just above the oxycline where isotopic consequences of environmental changes are expected to be amplified.

Isotopic compositions of CO_2 near the oxycline can be estimated from values of δ observed for the isorenieratane carbon skeleton. Sinninghe Damsté *et al.* (1993c) found that the Chlorobium-derived lipid, isorenieratane, in Black Sea surface sediments was depleted in ^{13}C by only 3.5‰ relative to dissolved CO_2 at the Black Sea chemocline. Similarly, in studies of laboratory cultures, Quandt *et al.* (1977) found that whole cells of Chlorobiaceae were depleted in ^{13}C relative to CO_2 dissolved in the medium by 2.5–5.2‰ (since carbon fixed by the reverse-TCA cycle can flow directly to lipid biosynthesis, the apparent lack of depletion in lipids relative to total biomass is not surprising). Based on the natural system examined by Sinninghe Damsté *et al.* (1993c), values of δ for dissolved CO_2 available to green sulphur bacteria in the Vena del Gesso palaeoenvironment were near -8.1‰ vs PDB ($= -11.6 + 3.5$‰) at the time of

deposition of sample 1 and $\approx -10.5‰$ thereafter. Values of δ for total dissolved inorganic carbon in open-marine surface waters were then approximately +2.5‰ vs PDB (Vincent *et al.*, 1980). At 20°C, the δ value of dissolved CO_2 in equilibrium with that pool would be $-6.5 \pm 0.5‰$ (the precise value being affected by possible variations in alkalinity). The observed δ values therefore reflect considerable additions to the deeper waters of CO_2 derived from the oxidation of organic material. These additions appear to have already affected the isotopic composition of the dissolved-CO_2 pool during the deposition of the sediments in sample 1, with an approximate steady state being maintained (CO_2 produced = CO_2 recycled to mixed layer) during deposition of samples 2–8. The latter point is of particular interest, since it provides indirect evidence of the delivery of ^{13}C-depleted CO_2 to the deeper waters of the oxic photic zone. In the modern Black Sea, this same phenomenon leads also to high concentrations of dissolved CO_2 in waters near the chemocline (Goyet *et al.*, 1991).

For heterotrophic organisms, notably the ciliates that produced the tetrahymanol that was the precursor of the S-bound gammacerane, the carbon source was organic and must have included the green sulphur bacteria. The heterotrophic enrichment in ^{13}C associated with respiratory isotope effects (De Niro and Epstein, 1978) maximizes at ~1.5‰ in vertebrates with low efficiencies of carbon conversion (food → biomass). It is probably much lower in invertebrates or protozoans, which retain much larger portions of assimilated carbon as biomass (Hayes *et al.*, 1990). Heterotrophic enrichment alone is therefore very unlikely to account for the isotopic differences between gammacerane and coexisting algal lipids, which are as large as 5‰. Inclusion of the ^{13}C-enriched green-sulphur-bacterial biomass would, however, readily explain the difference. Partial reliance on this prokaryotic source is also indicated by the presence of significant concentrations of gammacerane, since ciliates only biosynthesize significant quantities of tetrahymanol when feeding on carbon sources with low concentrations of sterols (Harvey and McManus, 1991). Indeed, ciliates have been found in abundance at and below the chemocline of the stratified Black Sea, where they are thought to feed mostly on sulphide-oxidising bacteria (Zubkov *et al.*, 1992). Marine ciliates able to biosynthesize tetrahymanol (Harvey and McManus, 1991) were identified in both the oxycline and the anoxic zone of the water column of Danish fjords (Fenchel *et al.*, 1990). There is thus potential for some species of ciliates biosynthesizing tetrahymanol to feed on green sulphur bacteria.

Temporal variations

To explore the "logical picture" in greater detail, we must examine specific variations, considering plausible relationships between environmental conditions, biomarker concentrations, and isotopic signals. In doing so, we must recall that each sample comprises sediments that accumulated over approximately 10^4 y and thus represents the condensed (or even collapsed) record of thousands of events involving a succession of biological communities in which diverse species have probably been dominant (e. g. Ignatiades, 1993 and references therein). For efficiency, we will consider the biomarker signals in order of specificity.

Higher plants. The concentration profiles [Fig. 17(a) and (h)] of higher plant markers such as long chain *n*-alkanes and fernene suggest a general decrease in terrestrial input from the base to the top of the bed.

Photosynthetic sulphur bacteria. The biological and environmental significance of the ^{13}C-enriched diaryl isoprenoids in samples 1–8 have already been noted. The disappearance of this signal in samples 9 and 10 [Fig. 22(b)] indicates the cessation of anaerobic photosynthesis. In principle, this could indicate either that light was no longer able to reach the anaerobic waters or that no part of the water column was anaerobic because stratification had been destroyed. The stratigraphic position of these samples—at the end of the cycle, just before a stromatolitic interval—clearly favours the latter alternative (Fig. 23).

In natural habitats, the spectrum and intensity of the light reaching the chemocline determines the species composition and the distribution of phototrophic bacteria (Parkin and Brock, 1980; Montesinos *et al.*, 1983; Abella and Garcia-Gil, 1988). It is controlled mostly by the biological activity in the upper water column (Parkin and Brock, 1980; Montesinos *et al.*, 1983) and by the depth of the chemocline. As there is no evidence that the biological productivity in the surface waters was enhanced during certain stages of deposition of the marl layer, variation of the depth of the chemocline is the more likely hypothesis to explain the variations in concentration of phototrophic bacterial products. Purple sulphur bacteria require higher light levels and wavelengths less capable of penetrating deeply in the water column than those used by the green sulphur bacteria and thus occupy the upper layer in the phototrophic bacterial community. Brown-coloured strains of Chlorobiaceae require less light because of their ability to biosynthesize the diaromatic carotenoid isorenieratene, which absorbs light with a relatively high wave length, and are usually found in deeper layers. Maximum occurrences of Chlorobiaceae occurred at samples 3 and 5 [Fig. 22(b)]. The importance in samples 1 and 2 of products of purple sulphur bacteria may therefore indicate that at this early stage of the cycle the chemocline was relatively high in the water column. In sample 1, the free n-C_{17} is depleted in ^{13}C by 28.2‰ relative to CO_2(aq), corresponding well with the sum of fractionations associated with fixation of CO_2 ($\leq$27‰; Farquhar *et al.*, 1982) and lipid biosynthesis ($\approx$4‰, Hayes, 1993). The smaller depletion in sample 2 (Fig. 5) indicates extensive dilution of the anaerobic product by algal or cyanobacterial *n*-heptadecane. Thus, it may be speculated that the

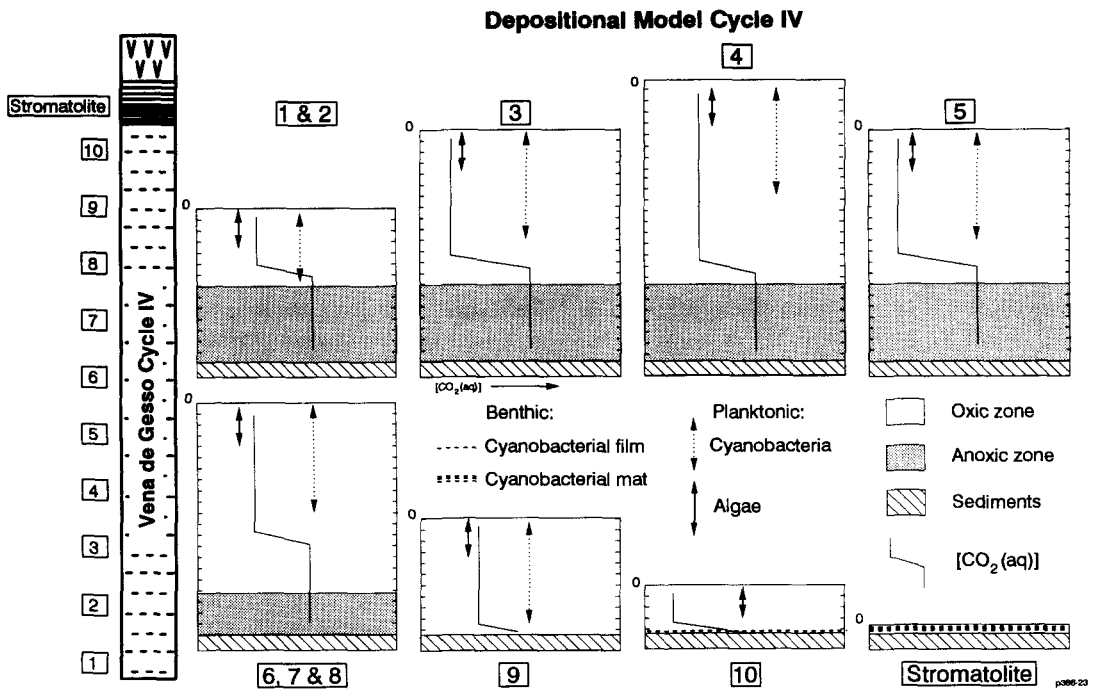

Fig. 23. Schematic reconstruction of the water column structure and its evolution during deposition of the marl bed of Cycle IV. The $[CO_2(aq)]$ curve indicates relative changes but cannot be related to firm values, and is thus displayed without scale.

amount of light reaching the chemocline, sufficient to support the growth of abundant Chromatiaceae during deposition of samples 1 and 2, reduced during deposition of sample 3, thus enhancing the production of isorenieratene by Chlorobiaceae and limiting the growth of Chromatiaceae (Fig. 23). The decrease in concentration of isorenieratane in samples 4 [Fig. 22(b)] is thought to result from a further deepening of the chemocline (Fig. 23).

Prymnesiophytes. As noted, the essentially constant δ values of the C_{37} and C_{38} S-bound *n*-alkyl carbon skeletons in samples 2–8 provide evidence of a consistent environment for their source organisms, the prymnesiophyte algae. The divergent isotopic compositions of the C_{37} species in samples 1 and 10 [Fig. 15(d)] are associated with significant variations in the C_{37}/C_{38} abundance ratio [Fig. 13(c)] and therefore suggest contributions from an additional source. The plausibility of this interpretation is enhanced by the observation of similar isotopic variations, associated with marked changes in the UK_{37}–T relationship which also indicate the presence of an additional species, in the surface waters of the Black Sea (Freeman and Wakeham, 1992). The isotopic differences are therefore not indicative of markedly different environmental conditions but of C_{37}-producing organisms with different isotopic characteristics. The concentration profile of the C_{37} and C_{38} S-bound *n*-alkyl carbon skeletons reveal maximum abundances of prymnesiophytes during deposition of samples 3 and 5 [Fig. 13(c)].

Eukaryotic microalgae. Isotopic signals representative of these organisms are carried most prominently by the S-bound C_{16}, C_{31}, and C_{32} *n*-alkanes [Fig. 15(b)]. The observed isotopic changes are extreme, approaching 10‰ for the C_{16} species. Relative abundances of the S-bound *n*-alkanes (which are certain to have multiple origins) also change. As shown in Fig. 13(b) the isotopic enrichments in the most important microalgal carbon skeletons in samples 3 and 5 are associated with two-fold increases in their relative abundances. The isotopic shifts are therefore logically interpreted not in terms of extreme environmental variations capable of producing large changes in fractionation but as due to the admixture of ^{13}C-enriched products to background levels of functionalized *n*-alkyl debris. In order to cause the observed changes in the net δ values of the S-bound *n*-alkanes, the δ value of the microalgal products must have been near −18‰ (or higher). At least one marine green microalga is known to biosynthesize a resistant outer wall (Derenne *et al.*, 1992) which is likely to be selectively preserved and to contribute to kerogen (Tegelaar *et al.*, 1989). This outer wall comprises a highly aliphatic biomacromolecule called algaenan (de Leeuw and Largeau, 1993 and references therein). Recently, Gelin *et al.* (1995a) reported that the marine eustigmatophyte *Nannochloropsis salina*, apart from the C_{30}–C_{32} diols (**XIII**) (Volkman *et al.*, 1992), biosynthesizes an algaenan probably based on ether-linked C_{30}–C_{32} linear chains. The pyrolysis products of both sulphurized C_{30}–C_{32} diols or keto-ols

and an eustigmatophyte algaenan were recognized by Gelin *et al.* (1995b, 1995c) upon Curie-point pyrolyses of the kerogens of the marls 3 and 5, both before and, after desulphurization. The peaks of microalgal production indicated by the isotopic signals at C_{16}, C_{31}, and C_{32}, therefore, probably explain the maximal values of δ_{TOC} in samples 3 and 5 [Fig. 15(b)].

The enrichment of ^{13}C in microalgal products could in principle be due either to (i) low concentrations of dissolved CO_2, expected either to minimize fractionation accompanying fixation of CO_2 or to provoke the assimilation with minimal fractionation of bicarbonate, which is isotopically enriched relative to CO_2 (Hayes, 1993); (ii) factors promoting rapid growth (Goericke *et al.*, 1994), particularly high nutrient levels, which affect cellular carbon budgets and lead to minimization of isotopic fractionation; or (iii) specific physiological characteristics of the producing organism, such as high resistance to mass transport of CO_2 or a particular affinity for assimilation of bicarbonate. If either of the first two factors were wholly responsible for the indicated enrichment of ^{13}C in the microalgae, at least some effect on other species would also be expected. For example, if there were some portion of the water column—the hypothetical microalgal habitat—in which depletion of CO_2 were sufficiently extreme to provoke an 8‰ shift in lipid δ values, correlated shifts of at least a few permil would be expected in other signals. Instead, the changes which are visible—in the δ values of some other S-bound *n*-alkanes, of phytane, and of the cholestanes—can be ascribed at least as readily to spillover of microalgal products as to changes in the major sources of those signals. Moreover, δ values of biomarkers representative of other organisms, the S-bound C_{26}, C_{28}, C_{30}, C_{37} and C_{38} *n*-alkanes, are largely unchanged. It is, therefore, most logical to view the isotopic signals as representative not of large environmental changes but of the distinct characteristics of the source organisms. It was recently reported by Boreham *et al.* (1994) that fossilized material of the freshwater alga *Botryoccocus braunii* is significantly enriched in ^{13}C, probably due to its thick outer cell wall causing slow diffusion of CO_2 into the cell. A similar explanation may hold for the microalgae of the class Eustigmatophyceae, since they probably also contain a thick aliphatic cell wall (see also Gelin *et al.*, 1995b).

Of course, some environmental change must have triggered the dominance of the microalgae during deposition of sample 3, their decreased importance during the interval represented by sample 4, and their reappearance at times represented by sample 5. The geochemical evidence does not allow recognition of the controlling factors but does give some indication that a typical biological phenomenon, namely competitive displacement of one producer by another, was involved. As could be expected given the cyclic nature of this deposit, changes recorded by the 3→4 transition were apparently reversed and the importance of the microalgae was reestablished during deposition of the sediments in sample 5. This is also evident from the position of the chemocline as recorded by the input of markers from Chlorobiaceae [Figs 22(b) and 23].

Cyanobacteria. Cyanobacteria are mostly represented by the S-bound pentakishomohopane. This compound exhibits a depth profile that indicates an increased contribution of cyanobacteria from the bottom to the top of the bed [Fig. 22(c)]. It can be speculated that the strong increase in concentration after sample 8 is related to the progressive formation of benthic cyanobacterial films after the disappearance of anoxic conditions in the water column and reduction of the basin depth of the water column.

Throughout most of the cycle (samples 3–9) δ values of pentakishomohopane are slightly higher than those of coexisting cholestanes and ethyl cholestanes (Fig. 5). As noted, this relationship would be expected if these organisms shared habitats and had equivalent metabolic and isotopic characteristics. That required physiological equivalence is by no means guaranteed, so the consistency of the observed signals is possibly coincidental. If, however, it is taken as significant, the depletion of ^{13}C in pentakishomohopane relative to the steranes in samples 1, 2, and 10 suggests that the cyanobacteria utilized a carbon source depleted in ^{13}C relative to that available to the eukaryotic algae or occupied a habitat with higher concentrations of dissolved CO_2. In samples 1 and 2, the change in hopanoidal δ values roughly tracks the estimated change in the isotopic composition of deep-water CO_2 (i.e. that based on the δ values of the diarylisoprenoids), suggesting that at least some of the cyanobacteria were dwelling deeper in the water column than the eukaryotic algae and that changes in their isotopic composition are due to changes in the δ value of the carbon source. In that case, the change in hopanoidal δ values between samples 2 and 3 would represent exclusion of the cyanobacteria from the deepest waters, possibly due to the deepening of the chemocline (Fig. 23). In the depositional environments reflected by samples 9 and 10, the water column was of limited depth and, as a result of sea-level draw down, no longer stratified. The photic zone reached the sediment–water interface and permitted the development of a cyanobacterial film. The isotopic depletion of pentakishomohopane in sample 10 probably reflects both higher concentrations of CO_2 and depletion of ^{13}C in the CO_2 (as a result of mineralization of organic matter at the sediment–water interface).

Eukaryotic algae. The cyclic nature of the depositional system is well represented by the variation in isotopic composition of eukaryotic algae in general, represented by the cholestanes [Fig. 9(a)]. Except for a perturbation in sample 5, probably due to the abundance of microalgal products in that interval, lower δ values are associated with deeper water columns. At the initiation of the cycle, time would have been required for the buildup of

^{13}C-depleted inorganic carbon in the deeper waters. The persistence of relatively high δ values in sample 2 quite possibly reflects this lag. Subsequently, however, the return of significant quantities of ^{13}C-depleted CO_2 from beneath the chemocline would have resulted, as it does in the modern Black Sea (Fry *et al.*, 1991; Freeman *et al.*, 1994), in higher concentrations of CO_2 and in some depletion of ^{13}C in dissolved CO_2. As observed in the isotopic record of cholestanes, both of those factors would lead to depletion of ^{13}C in algal products.

The *n*-alkyl carbon skeletons associated with the cholestanes (and, for that matter, with the hopanoids) in samples 3–9 would be expected to have δ values around −28‰. Apart from the homologues with 26, 28, and 30 carbon atoms, most of the S-bound *n*-alkanes have higher δ values except in sample 4. Since it has been postulated that the microalgae happened not to flourish in that interval, the otherwise-pervasive enrichment of ^{13}C among S-bound *n*-alkanes probably indicates the breadth of microalgal contributions to that carbon pool.

All phototrophs. Consideration of isotopic signals carried by phytane is of interest in the present context, not because this highly non-specific biomarker can add information to that already available, but because (i) examination of phytane relationships in this deposit can provide information useful in other settings, since δ values of phytane are usually among those available in even the most rudimentary studies of individual compounds and (ii) phytane presents some particular problems in the Vena del Gesso sediments.

With the idea that the phytane carbon skeleton is produced by almost all phototrophic organisms and that, therefore, its isotopic composition provides information about "average" primary products in any given environment, it is common to compare isotopic compositions of phytane with those of TOC (e.g. Hayes *et al.*, 1990; Kenig *et al.*, 1994a). Observed isotopic differences are then interpreted in terms of the nature of secondary processes, i.e. those involved in the reworking and preservation of organic material. In making such comparisons, the true diversity of the biological community is often ignored. Reassuringly, in spite of the diversity revealed by the detailed analyses, the parallel isotopic variations between phytane and TOC noticed repeatedly in prior investigations are found again here. In samples 1–8, however, the average S-bound phytane–TOC difference is unusually large: 6.3‰. Without any further information, one might say, "The isotopic difference is substantially larger than 4‰. Not even the burial of unaltered primary biomass would lead to so large a difference [and any preferential preservation of lipidic material would decrease it]. We have, therefore, evidence of secondary isotopic fractionation associated with heterotrophic reworking." Figure 5 shows, however, that the δ values of S-bound phytane are significantly lower than those of S-bound pentakishomohopane and the S-bound cholestanes and that, if the primary product-vs-TOC comparison were based on those compounds, a quite different interpretation would result. Moreover, serious problems would arise for sample 1, where the δ value of TOC is less than that of either of the cyclic primary biomarkers. On the one hand, it appears that phytane is well chosen in terms of its universality. Because it includes contributions from the Chromatiaceae, it provides an "explanation" for the low δ_{TOC} in sample 1. On the other hand, interpretation of phytane–TOC differences purely in terms of reworking of primary products is dangerous, since selective preservation of phytane from a single, ^{13}C-depleted producer can lead to an exaggerated isotopic contrast.

The opportunity to compare δ values for a variety of primary isoprenoids exposes an additional problem not previously encountered in compound-specific isotopic analyses. In samples 1–8, the phytane is depleted in ^{13}C relative to both of the cyclic biomarkers. For samples 1 and 2, there is evidence in the form of ^{13}C-depleted *n*-heptadecane that this arises because a significant portion of the S-bound phytane derives from photosynthetic purple sulphur bacteria. But when the *n*-heptadecyl signal becomes "normal" (e.g. in sample 4, see Fig. 5) and contributions to phytane from purple photosynthetic bacteria are therefore expected to be absent, the depletion of ^{13}C in S-bound phytane continues. Since the S-bound phytyl carbon skeleton then derives from either cyanobacteria or eukaryotic algae, should not its δ value fall somewhere between those of the cyanobacterial and eukaryotic isoprenoids, pentakishomohopane and cholestane? If this relationship is not observed in samples 3–8, it might be ascribed to the continued presence of *Chromatiaceae*, albeit a species which produced no significant quantities of *n*-heptadecane. But that explanation is far less attractive in samples 9 and 10, where all other evidence indicates a complete cessation of anaerobic photosynthesis. How is the isotopic depletion of phytane relative to both the cholestanes and pentakishomohopane to be explained in those samples?

It is, in fact, quite possible for phytane to derive only from cyanobacteria and eukaryotic algae and still to display a δ value lower than either the cholestanes or pentakishomohopane. For simplicity, consider a system in which only two primary producers, both eukaryotes, are present. Imagine that one produces isoprenoids (phytol and steroids) with $\delta = -22$‰ and the other produces isoprenoids with $\delta = -32$‰. It then follows that the δ values of sedimentary phytane and steranes must fall between −22 and −32 but not that they must be equal. If, for example, the organism with isoprenoids at −22‰ produced 10 × more sterol than phytol whereas this abundance ratio was reversed in the −32‰ organism, the bulk of sedimentary steranes would derive from the heavy organism and would have a δ value near −22‰ and most sedimentary phytane would derive from the light organism and have a δ value near −32‰. The record

would accurately reflect the compositions of primary products and no "internally conflicting evidence" would be involved in spite of the isotopic difference between the two preserved isoprenoid hydrocarbon pools. If, in fact, organisms living deeper in the water column were led by low light intensities to produce more pigments and thus more phytol, sedimentary phytane would tend to reflect more strongly the isotopic composition of deep dwelling organisms. And, since deep CO_2 is often depleted in ^{13}C or higher in concentration, it might generally be expected that pigment-derived biomarkers would be depleted in ^{13}C relative to other biomarkers. This provides a possible explanation for isotopic relationships in samples 9 and 10 in this section and should be recalled in future investigations.

Heterotrophic ciliates. Some ciliates are capable of completing their lifecycle under anoxic conditions and feed on bacteria living at or below the chemocline (see for a detailed discussion Sinninghe Damsté *et al.*, 1995a). In this cycle, isotopic compositions of gammacerane (Fig. 5) indicate that ciliates relied much more strongly on green photosynthetic bacterial carbon during deposition of sample 1 and, to a lesser extent (note the declining δ values of the diaryl isoprenoids) during deposition of sample 2. Notably, however, continued assimilation of green photosynthetic bacterial carbon by protozoans is indicated up to sample 8, the point in the cycle at which sedimentary concentrations of diaryl isoprenoids drop almost to zero. The high abundance of gammacerane in these sediments deposited under a stratified water column supports the suggestion of Schoell *et al.* (1994a) that high abundances of gammacerane might be a palaeoenvironmental marker for stratified water columns rather than hypersaline conditions *per se* (e.g. Peters and Moldowan, 1993).

Total organic carbon

Two features sieze attention in the record of δ values of TOC (Fig. 5): (i) the depletion of ^{13}C in samples 1 and 2 and (ii) the enrichments in samples 3 and 5. Based on the forgoing discussion, the latter can be securely associated with temporary dominance—interrupted in sample 4—of microalgae which are both enriched in ^{13}C and capable of producing resistant biopolymeric debris. The depletion of ^{13}C in the TOC of samples 1 and 2, however, may be surprising if compared to the δ values of the algal steranes, which are relatively high in those samples (Fig. 5), and it is certainly notable that the δ values of gammacerane and of the diaryl isoprenoids maximize in sample 1. The failure of δ_{TOC} to follow those trends indicates that organic carbon associated with average eukaryotic algae, with green sulphur bacteria, and with the ciliates that produced the gammacerane is not a major component of the TOC. Isotopic depletion is evident in the products of purple photosynthetic bacteria, and it may be that these are responsible for the overall depletion observed in the TOC. If so, there is a notable contrast with the consistently poor preservation of products of green sulphur bacteria, apart from the readily recognized and apparently refractory diaryl isoprenoids, which has recently been documented by Hartgers *et al.* (1994a,b). Alternatively, the precusor organisms of the majority of the S-bound *n*-alkanes in samples 1 and 2 (which are also relatively light) may also be responsible for the depleted δ_{TOC} in these samples.

CONCLUSIONS

The water column of the basin of deposition was stratified and, because the photic zone was reaching the anoxic zone, communities of phototrophic sulphur bacteria, Chromatiaceae and Chlorobiaceae could develop during the deposition of the basal to middle part of the bed. Their disappearance in the upper part of the marl bed is associated with a relative sea-level draw down, water column mixing and the photic zone reaching the water–sediment interface. The enriched ^{13}C content of S-bound isorenieratane and its derivatives confirms their origin from isorenieratene biosynthesized by green sulphur bacteria. Since the signal of purple sulphur bacteria is the strongest at the base of the section, and because these bacteria require a higher light intensity than the green sulphur bacteria, it is thought that during that time the chemocline was the highest. Our data confirm and detail the conclusions of Vai and Ricci Lucchi (1977), who suggested that these finely laminated silty marls, with an almost complete absence of megabenthos and bioturbation, were deposited under a density-stratified water mass and anoxic bottom conditions.

S-bound gammacerane is derived from tetrahymanol biosynthesized by anaerobic bacterivorous ciliates. Its ^{13}C content indicates that these ciliates were partially feeding on green sulphur bacteria. High abundances of gammacerane seem to indicate stratified water columns rather than hypersaline conditions *per se*. The abundance of gammacerane corroborates the conclusion based on photosynthetic bacterial lipids that during deposition of the basal to middle part of the bed the oxycline was located in the water column.

The conditions for sulphurization of organic matter were optimal during deposition of sample 2. This coincides with the situation with the highest chemocline suggesting that this situation promotes organic matter sulphurization since organic compounds will reach the anoxic zone—where reduced sulphur species are available for sulphurization—faster and are thus less susceptible for oxidative degradation.

The relatively constant $\delta^{13}C$ values of higher plant-derived free C_{25+} *n*-alkanes and aquatic photoautotroph-derived S-bound steranes, C_{35} hopane, C_{26}, C_{28}, C_{30}, C_{37} and C_{38} *n*-alkanes in the section studied provides evidence for a constant concentration and ^{13}C content of CO_2 in the atmosphere and surface

waters during deposition of the marl layer in Cycle IV. The concentration of higher plant markers suggest a decrease of terrestrial input up-section.

The isotopic compositions of CO_2 in surface waters and near the oxycline are estimated to be −6.5‰ and −10.5‰, respectively, indicating the delivery of ^{13}C-depleted CO_2 to the deeper waters of the photic zone by mineralization of organic matter. This situation is comparable to that of the present-day Black Sea, the world largest euxinic basin.

S-bound C_{16}, C_{31} and C_{32} *n*-alkanes in samples 3 and 5 are probably mainly derived from microalgae of the class Eustigmatophyceae. Their enriched ^{13}C content is explained by specific physiological characteristics. The corresponding enrichment in δ_{TOC} in samples 3 and 5 is explained by a significant input of algaenan from these algae, a conclusion corroborated by the molecular characterization of the kerogens (Gelin *et al.*, 1995b, c).

Though heterotrophic bacteria must have been present, it is assumed that most of prokaryotic biomarkers (i.e. hopanoids) present in these sediments are derived from cyanobacteria. The increase in input from cyanobacteria in the top of the section is related to the shallow water conditions, where light reached the bottom leading to the development of a cyanobacterial film (Fig. 23), announcing the presence of the subtidal to intertidal stromatolitic bed overlaying the marl. The relatively constant difference of *ca* 2‰ between the S-bound steranes and S-bound C_{35} hopane in samples 3–9 may be due to subtle differences in isoprenoid biosynthetic pathways between algae and cyanobacteria.

The complexity of the populations of photic zone primary producers is underlined by the diversity in concentration profiles of algal biomarkers along the marl bed. The specificity of certain of those biomarkers combined with their carbon isotope values permitted to trace several changes in the phototrophic populations of the upper waters. The contributions from prymnesiophytes, diatoms, and dinoflagellates were recognized.

Based on the compound specific carbon isotope data and the molecular structure data changes in the palaeoenvironment during deposition of the marl bed of Cycle IV were reconstructed; after a relatively fast filling of the basin a gradual shallowing is observed (Fig. 23). Ultimately the water column was so shallow that a cyanobacterial mat at the sediment/water interface developed.

Acknowledgements—This work was performed under the auspices of ENOG (European Network of Organic Geochemists) and has benefitted from scientific discussions within the group. ENOG comprises Laboratoire de Géochemie, IFP, Rueil Malmaison, France; Institute of Petroleum and Organic Geochemistry, KFA, Jülich, Germany; Laboratoire de Chimie Organiques de Substances Naturelles associé au CNRS, Université Louis Pasteur, Strasbourg, France; Netherlands Institute for Sea Research, Department of Marine Biogeochemistry Texel, The Netherlands; Department of Environmental Chemistry, CID-CSIC, Barcelona, Spain; Organic Geochemistry Unit, University of Bristol, U.K. and receives funding from the European Community (EC contract #ERBSC1*CT91-0736). This work was partly supported by a PIONIER grant to JSSD from the Netherlands Organisation for Scientific Research (NWO). Work at Indiana University was supported by the National Aeronautics and Space Administration (NGW-1940a) and the Indiana University Foundation (Friends of Biogeochemistry). We acknowledge Dr P. Hofmann (KFA Jlich) for TOC, carbonate and Rock Eval determinations. We thank Ion Peleanu for analytical assistance during his stay at NIOZ. Wim Pool and Marlèn Dekker from NIOZ assisted with the GC–MS analyses. We thank Julie Primack and Jon Fong for their assistance to FK during isotope analyses at Indiana University. We thank Gian Batista Vai, B.C. Schreiber, Brendan Keely, Peter Hofmann, Jan Ebbing, Stefan Schouten, other members of the ENOG group and the management of the gypsum mine for advice and assistance during sampling. Drs P. Adam, P. Albrecht, J. Connan and M.E.L. Kohnen provided constructive reviews on an earlier draft of this manuscript.

REFERENCES

Abella C. A. and Garcia-Gil J. (1988) Diel migration as a mechanism for enrichment of natural populations of branching species of pelodictyon. In *Green Photosynthetic Bacteria* (Edited by Olson J. M. and Trüper H. G.), pp. 269–285. Plenum Press, New York.

Adam P., Schmid J. C., Mycke B., Strazielle C., Connan J., Huc A., Riva A. and Albrecht P. (1993) Structural investigation of nonpolar sulfur cross-linked macromolecules in petroleum. *Geochim. Cosmochim. Acta* **57,** 3395–3419.

Alam M., Sandjura R., Watson D. A. and Loeblich A. R. III (1984) Sterol distribution in the genus Heterocapsa (Pyrrhophyta). *J. Phycol.* **20,** 331–335.

Berner R. A. (1984) Sedimentary pyrite formation: an update. *Geochim. Cosmochim. Acta* **48,** 605–615.

Berner, R. A. (1985) Sulphate reduction, organic matter decomposition and pyrite formation. *Phil. Trans. R. Soc. London Ser. A* **315,** 25–38.

Boon J. J., Rijpstra W. I. C., de Lange F., de Leeuw J. W. and Yoshioka (1979) Black sea sterol—a molecular fossil for dinoflagellate blooms. *Nature* **277,** 125–127.

Boreham C. J., Summons R. E., Roksandic Z., Dowling L. M. and Hutton A. C. (1994) Chemical, molecular and isotopic differentiation of organic facies in the Tertiary lacustrine Duaringa oil shale deposit, Queensland, Australia. *Org. Geochem.* **21,** 685–712.

Brassell S. C., Wardroper A. M. K., Thomson J. D., Maxwell J. R. and Eglinton G. (1981) Specific acyclic isoprenoids as biological markers of methanogenic bacteria in marine. *Nature* **290,** 693–696.

Byers J. D. and Erdman J. G. (1983) Low temperature degradation of carotenoids as a model for early diagenesis in recent sediments. In *Advances in Organic Geochemistry* 1981 (Edited by Bjorøy M. *et al.*), pp. 725–732. Wiley, Chichester.

Clark R. C. Jr and Blumer M. (1967) Distribution of *n*-parafins in marine organisms and sediment. *Limnol. Oceanogr.* **12,** 79–87.

Collister J. W., Summons R. E., Lichtfouse E. and Hayes J. M. (1992) An isotopic biogeochemical study of the Green River oil shale. In *Advances in Organic Geochemistry* 1991 (Edited by C. B. Eckhardt *et al.*). *Org. Geochem.* **19,** 265–276. Pergamon Press, Oxford.

Collister J. W., Lichtfouse E., Hieshima G. and Hayes J. M. (1994) Partial resolution of sources of *n*-alkanes in the saline portion of the Parachute Creek Member, Green River Formation (Piceance Creek Basin, Colorado). *Org. Geochem.* **21,** 645–659.

De Niro M. J. and Epstein S. (1978) Influence of diet on the distribution of nitrogen isotopes in animals. *Geochim. Cosmochim. Acta* **42,** 495–406.

Derenne S., Largeau C., Roussaeu B., Wilhem C and Hatcher P. G. (1992) Non hydrolysable macromolecular constituents from outer walls of Chlorella fusca and Nanochlorum eucaryotum. *Phytochemistry* **31,** 1923–1929.

Djerassi C. (1981) Recent studies in the marine steroid field. *Pure Appl. Chem.* **53,** 873–890.

Dunlop R. W. and Jefferies P. R. (1985) Hydrocarbons of the hypersaline basins of Shark Bay, Western Australia. *Org. Geochem.* **8,** 313–320.

Eglinton G., Gonzales A. G., Hamilton R. J. and Raphael R. A. (1962) Hydrocarbons constituents of wax coatings of plant leaves: a taxonomic survey. *Phytochemistry* **1,** 89–102.

Espitalié J., Laporte J. L., Madec M., Marquis F., Leplat P. and Paulet J. (1977) Méthode rapide de charactérisation des roches meres de leur potentiel pétrolier et de de leur degré d'évolution. *Rev. Inst. Fr. Petr.* **32,** 23–45.

Farquhar G. D., Ball M. C., Von Caemmerer S. and Roksandic Z. (1982) Effect of salinity and humidity on δ value of halophytes—evidences for diffusional isotope fractionation determined by the ratio of intercellular/atmospheric partial pressure of CO_2 under different environmental conditions. *Oceanologia* **52,** 121–124.

Fenchel T., Kristensen L. D. and Rasmussen L. (1990) Water column anoxia: vertical zonation of planktonic protozoa. *Mar. Ecol. Prog. Ser.* **62,** 1–10.

Freeman K. H. and Wakeham S. G. (1992) Variations in the distributions and isotopic compositions of alkenones in Black Sea particles and sediments. In *Advances in Organic Geochemistry* 1991 (Edited by C. B. Eckhardt *et al.*). *Org. Geochem.* **19,** 277–285. Pergamon Press, Oxford.

Freeman K. H., Hayes J. M., Trendel J. -M. and Albrecht P. (1989) Evidence from GC–MS carbon isotopic measurements for multiple origins of sedimentary hydrocarbons. *Nature* **353,** 254–256.

Freeman K. H., Wakeham S. G. and Hayes J. M. (1994) Predictive organic biogeochemistry: Hydrocarbons from anoxic marine basins. *Org. Geochem.* **21,** 629–644.

Fry B., Jannasch H., Molyneaux S. J., Wirsen C., Muramoto J. and King S. (1991) Stable isotope studies of the carbon, nitrogen and sulfur cycles in the Black Sea and Cariaco Trench. *Deep-Sea Res.* **38** (Suppl. 2), S1003–S1020.

Gelin F., Boogers I., Noordeloos A. A. M., Sinninghe Damsté J. S. and de Leeuw J. W. (1995a) Novel resistant microalgal polyethers as a major sink of organic carbon in the marine environment. *Nature* Submitted.

Gelin F., Sinninghe Damsté J. S., Harrison W. N., Maxwell J. R. and de Leeuw J. W. (1995b) Molecular indicators of palaeoenvironmental change in a Messinian evaporitic sequence (Vena del Gesso, Italy): III. Changes in the molecular structure of kerogen in a single marl bed. *Org. Geochem.* **23,** 555–566.

Gelin F., Sinninghe Damsté J. S., Harrison W. N., Maxwell J. R. and de Leeuw J. W. (1995c) Variations in origin and composition of kerogen constituents as revealed by analytical pyrolysis of immature kerogens before and after desulphurization. In *Abstract Book, EAOG Meeting*, San Sebastian, In press.

Gelpi E., Schneider H., Mann J. and Oro J. (1970) Hydrocarbons of geochemical significance in microspic algae. *Phytochemistry* **9,** 603-612.

Goericke R., Montoya J. P. and Fry B. (1994) Physiology of isotope fractionation in algae and cyanobacteria. In *Stable Isotopes in Ecology* (Edited by Lajtha K. and Michener B.), pp. 187–221. Academic Press, New York.

Goyet C., Bradshaw A. L. and Brewer P. G. (1991) The carbonate system in the Black Sea. *Deep-Sea Res.* **38** (Suppl. 2), S1049–S1068.

Gransch J. A. and Posthuma J. (1974) On the origin of sulphur in crudes. In *Advances in Organic Geochemistry* 1973 (Edited by Tissot B. and Bienner F.), pp. 727–739. Editions Technip, Paris.

Han J. and Calvin M. (1969) Hydrocarbon distribution of algae and bacteria and microbiological activity in sediments. *Proc. Natl. Acad. Sci.* **64,** 436–443.

Han J., McCarthy E. D., Calvin M. and Benn M. H. (1968) Hydrocarbon constituents of the Blue–green algae. *Nostoc muscorum, Anacystic nidulans, Phormidium luridum* and *Chlorogloea fritschii. J. Chem. Soc. C.* 2785–2791.

Han J., Chan H. W. S. and Calvin P. (1969) Biosynthesis of alkanes in *Nostoc muscorum. J. Am. Chem. Soc.* **91,** 5156–5159.

Hartgers W. A., Sinninghe Damsté J. S., Requejo A. G., Allan J., Hayes J. M., Long Y., Xie T.-M., Primack J. and de Leeuw J. W. (1994a) A molecular and carbon isotopic study towards the origin and diagenetic fate of diaromatic carotenoids. In *Advances in Organic Geochemistry* 1993 (Edited by N. Telnæs *et al.*). *Org. Geochem.* **22,** 703–725.

Hartgers W. A., Sinninghe Damsté J. S., Requejo A. G., Allan J., Hayes J. M., Long Y., Xie T.-M., Primack J. and de Leeuw J. W. (1994b) Evidence for only minor contributions from bacteria to sedimentary organic carbon. *Nature* **369,** 224–227.

Harvey H. R. and McManus G. B. (1991) Marine ciliates as a widespread source of tetrahymenol and hopan-3β-ol in sediments. *Geochim. Cosmochim. Acta* **55,** 3387–3390.

ten Haven H. L., Rohmer M., Rullkötter J. and Bisseret P. (1989) Tetrahymanol the most likely precursor of gammacerane, occurs ubiquitously in marine sediments. *Geochim. Cosmochim. Acta* **53,** 3073–3079.

Hayes J. M. (1993) Factors controling ^{13}C contents of sedimentary organic compounds: principle and evidence. *Mar. Geol.* **113,** 111–125.

Hayes J. M., Freeman K. H., Popp B. N. and Hoham C. H. (1990) Compound-specific isotopic analyses: A novel tool for reconstruction of ancient biogeochemical processes. In *Advances in Organic Geochemistry* 1989 (Edited by B. Durand and F. Behar). *Org. Geochem.* **16,** 735–747. Pergamon Press, Oxford.

Holz G. G. and Conner N. L. (1973) The composition, metabolism and roles of lipids in Tetrahymana. In *Biology of Tetrahymana* (Edited by A. M. Elliott), pp 99–122. Dowen, Hutchinson and Ross, Stroudburg.

Holzer G., Oro J. and Tornabene T. G. (1979) Gas chromatographic–mass spectrometric analysis of neutral lipids from methanogenic and thermoacidophylic bacteria. *J. Chromatogr.* **186,** 795–809.

Hussler G. and Albrecht P. (1983) C27–C29 Monoaromatic anthrasteroid hydrocarbons in Cretaceous black shales. *Nature* **304,** 262–263.

Ignatiades L. (1993) Species dominance and niche breadth in "bloom" and "non bloom" phytoplankton populations. *Oceanol. Acta* **17,** 89–96.

Jones J. G. and Young B. V. (1970) Major paraffin constituents of microbial cells with particular reference to Chromatium sp. *Arch. Mikrobiol.* **70,** 82–88.

Johns R. B., Nichols P. D. and Perry G. J. (1979) Fatty acid composition of ten marine algae from Australian waters. *Phytochemistry* **18,** 799–802.

Keely B. J., Blake S. R. and Maxwell J. R. (1995) Distributions of pigments in the organic matter of marls from the Vena del Gesso evaporitic sequence. *Org. Geochem.* **23,** 527–539.

Kenig F. (1991) Sédimentation, distribution et diagenèse de la matière organique dans un environnement carbonaté hypersalin: le système lagune sabkha d'Abu Dhabi (E.A.U.). Thèse de l'Université d'Orléans, France.

Kenig, F., Huc A. Y., Purser B. H. and Oudin J. L. (1990) Sedimentation, distribution and diagenesis of organic matter in a recent carbonate environment, Abu Dhabi, U.A.E. In *Advances in Organic Geochemistry* 1989 (Edited by B. Durand and F. Behar). *Org. Geochem.* **16,** 735–747. Pergamon Press, Oxford.

Kenig F., Hayes J. M., Popp B. N. and Summons R. E. (1994a) Isotopic biogeochemistry of the Oxford Clay Formation (Jurassic), UK. *J. Geol. Soc., London* **151,** 139–152.

Kenig F., Sinninghe Damsté J. S., de Leeuw J. W. and Hayes J. M. (1994b) Molecular palaeontological evidence for food web relationships. *Naturwissenschaften* **81,** 128–130.

Kenig F., Sinninghe Damsté J. S and de Leeuw J. W. (1995) Variability and significance of the thiophene record in a marl bed of one evaporitic cycle of the Gessoso-solfifera Formation (Messinian, Italy). In preparation.

Kleemann G., Poralla K., Englert G., Kjosen H., Liaaen-Jansen N., Neunlist S. and Rohmer M. (1990) Tetrahymanol from the phototrophic bacterium Rhodopseudomonas palustris: First report of a gammacerane triterpene from a prokaryote. *J. Gen. Microbiol.* **136,** 2551–2553.

Kohnen M. E. L., Sinninghe Damsté J. S., Kock-van Dalen A. C. and de Leeuw J. W. (1991a) Di-or polysulphide-bound biomarkers in sulphur-rich geomacromolecules as revealed by selective chemolysis. *Geochim. Cosmochim. Acta* **55,** 1375–1394.

Kohnen M. E. L., Sinninghe Damsté J. S. and de Leeuw J. W. (1991b) Biases from natural sulphurisation in paleoenvironmental reconstruction based on hydrocarbon biomarker distributions. *Nature* **349,** 775–778.

Kohnen M. E. L., Schouten S., Sinninghe Damsté J. S., de Leeuw J. W., Meritt D. and Hayes J. M. (1992a) The combined application of organic sulfur and isotope geochemistry to assess multiple source of palaeobiochemicals with identical carbon skeleton. In *Advances in Organic Geochemistry* 1991 (Edited by C. B. Eckardt *et al.*). *Org. Geochem.* **19,** 403–419. Pergamon Press, Oxford.

Kohnen M. E. L., Schouten S., Sinninghe Damsté J. S., de Leeuw J. W., Meritt D. and Hayes J. M. (1992b) Recognition of palaeobiochemicals by a combined molecular sulfur and isotope geochemical approach. *Science* **256,** 358–362.

Kokke W. C. M. C., Fenical W. and Djerassi C. (1981) Sterols with unusual nuclear unsaturation from three cultured marine dinoflagellates. *Phytochemistry* **20,** 127–134.

Kokke W. C. M. C., Fenical W. and Djerassi C. (1982) Sterols of the cultured dinoflagellate Pyrocystis lunula. *Steroids* **40,** 307–313.

Koopmans M. P., Köster J., van Kaam-Peters H. M. E., Kenig F. Schouten, S. Hartgers, W. A. de Leeuw J. W. and Sinninghe Damsté J. S. (1995a) Dia-and catagenetic products of isorenieratene: Molecular indicators of photic zone anoxia. *Geochim. Cosmochim. Acta* Submitted.

Koopmans M. P., Sinninghe Damsté J. S., Lewan M. D. and de Leeuw J. W. (1995b) Thermal stability of thiophene biomarkers as studied by hydrous pyrolysis. *Org. Geochem.* **23,** 583–596.

de Leeuw J. W. and Largeau C. (1993) A review of macromolecular organic compounds that comprise living organisms and their role in kerogen, coal, and petroleum formation. In *Organic Geochemistry, Principles and Application* (Edited by Engel M. H. and Macko S. A.), pp. 23–72. Plenum Press, New York.

de Leeuw J. W., Rijpstra W. I. C and Schenck P. A. (1981) The occurrence of C_{30}, C_{31} and C_{32} alkan-1,15-diols and alkan-15-one-1-ols in Unit I and Unit II of Black Sea sediments. *Geochim. Cosmochim. Acta* **45,** 2281–2285.

de Leeuw J. W., Cox H. C., van Graas G., van de Meer F. W., Peakman T. M., Baas J. M. A. and van de Graaf B. (1989) Limited double bound isomerization and selective hydrogenation of sterenes during early diagenesis. *Geochim. Cosmochim. Acta* **53,** 903–909.

de Leeuw J. W., Rijpstra W. I. C and Mur L. R. (1992) The absence of long-chain alkyl diols and alkyl keto-1-ols in cultures of the cynaobacterium Aphanizomenon flos-aquae. *Org. Geochem.* **18,** 575–578.

Liaaen-Jensen S. (1978a) Chemistry of carotenoid pigments. In *Photosynthetic Bacteria* (Edited by R. K. Clayton and W. R. Sistrom), pp. 233–247. Plenum Press, New York.

Liaaen-Jensen S. (1978b) Marine carotenoids. In *Marine Natural Products* (Edited by D. J. Falkner and W. H. Fenical), pp. 1–73. Academic Press, New York.

Mallory F. B., Gordon J. T. and Conner R. L. (1963) The isolation of a pentacyclic triterpenoid alcohol from a protozoan. *J. Am. Chem. Soc.* **85,** 1462–1363.

McCaffrey M. A., Farrington J. W. and Repeta D. J. (1991) The organic geochemistry of Peru margin surface sediments: II. Palaeoenvironmental implications of hydrocarbon and alcohol profiles. *Geochim. Cosmochim. Acta* **55,** 483–498.

Montesinos E., Guerrero R., Abella C. and Esteve I. (1983) Ecology and physiology of the competition for light between *Chlorobium limicola* and *Chlorobium phaeobacteroides* in natural habitats. *Appl. Envir. Microbiol.* **46,** 1007–1016.

Morris R. J. and Brassell S. C. (1988) Long-chain alkanediols: biological markers for cyanobacterial contributions to sediments. *Lipids* **23,** 256–258.

Nichols P. D., Volkman J. K., Palmisano A. C., Smith G. A. and White D. C. (1988) Occurrence of a C_{25} diunsaturated alkene and high neutral lipid content in Antarctic Sea-Ice diatom communities. *J. Phycol.* **24,** 90–96.

Nichols P. D., Palmisano A. C., Rayner M. S., Smith G. A. and White D. C. (1990) Occurrence of novel C_{30} sterols in Antartic sea-ice diatom communities during a spring bloom. *Org. Geochem.* **15,** 503–508.

Ourisson G., Albrecht P. and Rohmer M. (1982) Predictive microbial biogeo-chemistry and biochemistry of a group of natural products. *Pure Appl. Chem.* **51,** 709–729.

Parker P. L., van Balen C. and Maurer L. (1967) Fatty acids in eleven species of blue green algae: Geochimical significance. *Science* **155,** 707–708.

Parkin T. B. and Brock T. D. (1980) The effects of light quality on the growth of phototrophic bacteria in lakes. *Arch. Microbiol.* **125,** 19–27.

Peters K. E. and Moldowan J. M (1993) *The Biomarker Guide*, 363 pp. Prentice-Hall, London.

Popp B. N., Takigiku R., Hayes J. M., Louda J. W. and Baker E. W. (1989) The post-Paleozoic chronology and mechanisms of ^{13}C depletion in primary organic matter. *Am. J. Sci.* **289,** 436–454.

Quandt I., Gottshalk G., Ziegler H. and Stichler W. (1977) Isotope descrimination by photosynthetic bacteria. *FEMS Microbiol. Lett.* **1,** 125–128.

Repeta D. J. (1993) A high resolution historical record of Holocene anoxygenic primary production in the Black Sea. *Geochim. Cosmochim. Acta* **57,** 4337–4342.

Ricci M. P., Merritt D. A., Freeman K. H. and Hayes J. M. (1994) Acquisition and processing of data for isotope-ratio-monitoring mass spectrometry. *Org. Geochem.* **21,** 561–571.

Rissati J. B., Rowland S. J., Yon D. A. and Maxwell J. R. (1984) Stereochemical studies of acyclic isoprenoid—XII. Lipids of methanogenic bacteria and possible contributions to sediments. In *Advances in Organic Geochemistry* 1983 (Edited by P. A. Schenck *et al.*). *Org. Geochem.* **6,** 93–104. Pergamon Press, Oxford.

Robinson N., Cranwell P. A., Eglinton G. H. and Jaworski G. H. M. (1987) Lipids of four species of freshwater dinoflagellates. *Phytochemistry* **26,** 411–421.

Rohmer M., Bisseret P. and Neunlist S. (1992) The hopanoids, prokaryotic triterpenoids and precursors of ubiquitous molecular fossils. In *Biological Markers in Sediments and Petroleum* (Edited by Moldowan J. M. *et al.*), pp. 1–17. Prentice Hall, Englewood Cliffs, NJ.

Rohmer M., Knani M., Simonin P., Sutter B. and Sahm H. (1993) Isoprenoid biosynthesis in bacteria: A novel pathway for the early steps leading to isopentenyl diphosphate. *Biochem. J.* **295,** 517–524.

Schaeffer P., Harrison W. N., Keely B. J. and Maxwell J. R. (1995) Product distributions from chemical degradation of kerogens from a marl from a Miocene evaporitic sequence (Vena del Gesso, N. Italy). *Org. Geochem.* **23,** 541–554.

Schidlowski M., Matzigkeit U., Krumbein W. E. (1984) Superheavy organic carbon from hypersaline microbial mats, assimilitory pathways and geochemical implications. *Naturwissenschaften* **71,** 303–308.

Schoell M. and Hayes J. M. (Eds) (1994) *Compound-Specific analysis in Biogeochemistry and Petroleum Research. Org. Geochem.* **21,** 561–822.

Schoell M., Hwang R. J., Carlson R. M. K. and Welton J. E. (1994a) Carbon isotopic composition of individual biomarkers in gilsonites (Utah). *Org. Geochem.* **21,** 673–683.

Schoell M., Schouten S., Sinninghe Damsté J. S., de Leeuw J. W. and Summons R. E. (1994b) A molecular organic carbon isotope record of Miocene climate changes. *Science* **263,** 1122–1125.

Schouten S., Pavlovic D., Sinnninghe Damsté J. S. and de Leeuw J.W. (1993a) Nickel boride: an improved desulphurization agent for sulphur-rich geomacromolecule in polar and asphaltene fractions. *Org. Geochem.* **20,** 901–909.

Schouten S., van Driel G., Sinnninghe Damsté J. S. and de Leeuw J. W. (1993b) Natural sulphurization of ketones and aldehydes: A key reaction in the formation of organic sulphur compounds. *Geochim. Cosmochim. Acta* **57,** 5111–5116.

Schouten S., Sinninghe Damsté J. S., Schoell M. and de Leeuw J. W. (1994) A novel sterane, 27-nor-24-methyl-5(-cholestane, in sediments. *Geochim Cosmochim. Acta* **58,** 3741–3745.

Schouten S., Schoell M., Sinninghe Damsté J. S., Summons R. E. and de Leeuw J. W. (1995a) Molecular biogechemistry of Montery sediments (Naples Beach, USA) II: Stable carbon isotopic composition of free and sulphur bound carbon skeletons. In *AAPG Studies in Geology* (Edited by C. M. Isaacs and J. Rullkötter). In press.

Schouten S., Sinninghe Damste J. S., Kohnen M. E. L. and de Leeuw J. W. (1995b) The effect of hydrosulphurization on the carbon isotopic compositions of free and sulphur-bound lipids. *Geochim. Cosmochim. Acta* **59**(8), 1605–1609..

Sinninghe Damsté J. S. and de Leeuw J. W (1990) Analysis, structure and geochemical significance of organically bound sulphur in the geosphere: State of the art and future research. In *Advances in Organic Geochemistry* 1989 (Edited by B. Durand and F. Behar). *Org. Geochem.* **16,** 1077–1101. Pergamon Press, Oxford.

Sinninghe Damsté J. S., Kock-van Dalen A. C., de Leeuw J. W., Schenck P. A., Guoying S. and Brassell S. C. (1987) The identification of mono-, di-and trimethyl-2-methyl-(4,8,12-trimethyltridecyl)chromans and their occurrence in the geosphere. *Geochim. Cosmochim. Acta* **51,** 2393–2400.

Sinninghe Damsté J. S., Rijpstra W. I. C., Leeuw J. W. de and Schenck P. A. (1988) Origin of organic sulphur compounds and sulphur-containing high molecular weight substances in sediments and immature crude oils. In *Advances in Organic Geochemistry* 1987 (Edited by L. Mattavelli and L. Novelli). *Org. Geochem.* **13,** 593606. Pergamon Press, Oxford.

Sinninghe Damsté J. S., Eglinton T. I., Rijpstra W. I. C. and Leeuw J. W. de (1990) Characterisation of organically-bound sulfur in high-molecular-weight sedimentary organic matter using flash-pyrolysis and Raney Ni desulfurisation. In *Geochemistry of Sulfur in Fossil Fuels* (Edited by W. L. Orr and C. M. White) *ACS Symp. Ser.* **429,** 486–528. Am. Chem. Soc., Washington, DC.

Sinninghe Damsté J. S., Betts S., Ling Y., Hofmann P. and de Leeuw J. W (1993a) Hydrocarbon biomarkers of different lithofacies of the Salt IV formation of the Mulhouse basin, France. *Org. Geochem.* **20,** 1187–1200.

Sinninghe Damsté J. S., Keely B. J., Betts S. E., Baas M., Maxwell J. R. and de Leeuw J. W. (1993b) Variations in abundances and distributions of isoprenoid chromans and long chain alkylbenzenes in sediments of the Mulhouse Basin: A molecular sedimentary record of palaeosalinity. *Org. Geochem.* **20,** 1201–1215.

Sinninghe Damsté J. S., Wakeham S. G., Kohnen M. E. L., Hayes J. M. and de Leeuw J. W (1993c) A 6,000-year sedimentary molecular record of chemocline excursions in the Black Sea. *Nature* **362,** 827–829.

Sinninghe Damsté J. S., Kenig F., Koopmans M. L., Köster J., Hayes J. M. and de Leeuw J. W. (1995a) Evidence for gammacerane as an indicator of water column stratification. *Geochim. Cosmochim. Acta* **59**(9), 1895–1900.

Sinninghe Damsté J. S., Frewin N. L., Kenig F. and de Leeuw J. W. (1995b) Molecular indicators of palaeoenvironmental change in a Messinian evaporitic sequence (Vena del Gesso, Italy): I. Cyclic variations in extractable organic matter in eleven marl beds. *Org. Geochem.* **23,** 471–483.

Sirevag R., Buchanan B. B., Berry J. A. and Throughton J. H. (1977) Mechanisms of CO2 fixation in bacterial photosynthetis studied by the carbon isotope technique. *Arch. Microbiol.* **112,** 35–38.

Summons R. E., Barrow R. A., Capon R. J., Hope J. M. and Stranger C. (1993) The structure of a new C_{25} isoprenoid alkene biomarker from diatomaceous microbial communities. *Aust. J. Chem.* **46,** 907–915.

Tegelaar E. W., de Leeuw J. W., Derenne S. and Largeau C. (1989) A reappraisal of kerogen formation. *Geochim. Cosmochim. Acta* **53,** 3103–3106.

Tornabene T. G. and Langworthy T. A. (1979) Biphytanyl and diphytanyl glycerol ether lipids of methanogenic Archaebacteria. *Science* **203,** 51–53.

Vai G. B. and Ricci Lucchi F. (1977) Algal crust, autotochnous and clastic gypsum in a cannibalistic evaporite basin: a case histroy from the Messinian of Northern Apennines. *Sedimentology* **24,** 211–244.

Valisolalao J., Perakis N., Chappe B. and Albrecht P. (1984) A novel sulphur containing C_{35} hopane in sediments. *Tetrahedron Lett.* **25,** 1183–1186.

Vetter W., Englert G., Rigassi N. and Schwieter U. (1971) Spectroscopic Methods. In *Carotenoids* (Edited by O. Isler), pp. 189–266. Birkhauser, Basel.

Vincent E., Killingly K. S. and Berger W. H. (1980) The magnetic epoch-6 carbon shift: A change in the ocean $^{13}C/^{12}C$ ratio 6.2 million years ago. *Mar. Micropaleontol.* **5,** 185–203.

Volkman J. K. (1988) Biological marker compounds as indicators of the depositional environments of petroleum source rocks. In *Lacustrine Petroleum Source Rocks* (Edited by Fleet A. J. *et al.*), pp. 103–122. Blackwell, Oxford.

Volkman J. K., Eglinton G. and Corner E. D. S. (1980a) Sterols and fatty acids of the marine diatom *Biddulphia sinensis*. *Phytochemistry* **19,** 1809–1813.

Volkman J. K., Eglinton G., Corner E. D. S. and Forsberg T. E. V. (1980b) Long chain alkenes and alkenones in marine coccolithophorid *Emiliania Huxleyi*. *Phytochemistry* **10,** 2619–2622.

Volkman J. K., Jeffrey S. W., Nichols P. D., Rogers G. I. and Garland C. D. (1989) Fatty acid and lipid composition of 10 species of microalgae used in mariculture. *J. Exp. Biol. Ecol.* **128,** 219–240.

Volkman J. K., Kearney P. and Jeffrey S. W. (1990) A new source of 4-methyl sterols and 5((H)-stanols in sediments: prymnesiophyte microalgae of the genus Pavlova. *Org. Geochem.* **15,** 489–497.

Volkman J. K., Barrett S. M., Dunstan G. A. and Jeffrey S. W. (1992) C_{30}–C_{32} alkyl-diols and unsaturated alcohols in microalgae of the class Eustigmatophyceae. *Org. Geochem.* **18,** 131–138.

Volkman J. K., Barrett S. M., Dunstan G. A. and Jeffrey S. W. (1994) C_{25} and C_{30} highly branched isoprenoid alkenes in laboratory cultures of two marine diatoms. *Org. Geochem.* **21,** 407–413.

Wakeham S. G. (1990) Alagal and bacterial hydrocarbons in particulate organic matter and interfacial sediments of the Cariaco trench. *Geochim. Cosmochim. Acta* **54,** 1325–1336.

Wakeham S. G., Freeman K. H., Pease T. K. and Hayes J. M. (1993) A photoautrophic source for lycopane in marine water column. *Geochim. Cosmochim. Acta* **57,** 159–165.

Winters K., Parker P. L. and van Baalen C. (1969) Hydrocarbons of blue green algae: geochemical significance. *Science* **163,** 467–468.

Wong W., Sackett W. M. and Benedict C. R. (1975) Isotope fractionation in photosynthetic bacteria during carbon dioxide assimilation. *Plant Physiol.* **55,** 475–479.

Zeng Y. B., Eglinton G., Robinson N. and Cassani F. M. (1988) Long-chain alkane-diol and alkan-keto-1-ol components of the Messel kerogen. *Cour. Forsch.-Inst. Senckenberg* **107,** 53–71.

Zubkov M. V., Sazhin A. F. and Flint M. V. (1992) The microplankton organisms at the oxic–anoxic interface in the pelagial of the Black-Sea. *FEMS Microbiol. Ecol.* **101,** 245–250.

APPENDIX